

Conditional Predictive Inference for General Structured Data with Group Symmetries

Yichen Shen* Mengxin Yu†

May 19, 2026

Abstract

We study distribution-free predictive inference for data with group symmetries, aiming to establish *near-conditional coverage guarantees beyond exchangeability* for structured data. While many predictive inference methods have been developed to achieve a target coverage level, most existing methods primarily provide marginal coverage guarantees (Vovk et al., 2005; Angelopoulos et al., 2024). In practice, conditional predictive inference is often preferred, as it presents uncertainty quantification for black-box predictions given observed attributes, thereby accommodating heterogeneity. Although many efforts have been made to achieve efficient conditional coverage guarantees, existing methods rely on the i.i.d. (or exchangeable) assumption (Gibbs et al., 2025), which is often violated in structured settings such as networks, clustered data, and imaging data. Recently, the SymmPI framework (Dobriban and Yu, 2024) introduced a unified approach to predictive inference under general group symmetries beyond exchangeability; nevertheless, its guarantees remain marginal and do not account for population heterogeneity.

To bridge this gap, we introduce **C-SymmPI**, a framework that achieves near-conditional coverage under *general data structures with group symmetries*, extending beyond the exchangeability assumption to allow the conditional coverage for a variety of data structures such as networks, cluster-level data, etc. Inspired by the relaxed multi-accuracy perspective, our approach reformulates the conditional coverage as miscoverage error over a user-specified function class. We establish general theoretical guarantees under both distributional invariance and distribution-shift settings, and derive convergence rates for linear and RKHS function classes, recovering state-of-the-art results in the exchangeable setting as special cases. To ensure computational efficiency, we additionally develop two variants: a projection-based algorithm for high-dimensional observations, and a sampling-based algorithm for large or infinite groups. We further demonstrate the effectiveness of our approach on hierarchical and network-structured data. Empirical results show that **C-SymmPI** delivers more informative and stable conditional coverage with improved accuracy compared to existing methods.

Contents

1	Introduction	3
1.1	Our Contributions	4
1.2	Related Work	5
1.3	Outline	6
2	Preliminaries	6
2.1	Conformal Prediction and Group-Theoretic Predictive Inference	7
2.2	Multi-Accuracy	9

*Data Science Institute, University of Chicago. Email: ycshen@uchicago.edu

†Department of Statistics and Data Science, Washington University in St. Louis. Email: myu@wustl.edu

3	Methodology: C-SymmPI	10
3.1	Constructing Prediction Set	10
3.2	Theoretical Results	12
3.2.1	Near-Conditional Coverage under Distributional Invariance	12
3.2.2	Near-Conditional Coverage under Distributional Shift	12
3.3	Specifying Function Classes	13
3.3.1	Linear Function Class	13
3.3.2	RKHS Function Class	14
3.4	Computationally Efficient Variants	14
4	Examples	15
4.1	Exchangeable Data	15
4.2	Two-Layer Hierarchical Models	17
4.2.1	Setup: Data with Hierarchical Symmetries	18
4.2.2	Example: Supervised Learning with Two-Layer Hierarchical Data	18
4.2.3	Example: Cluster Randomized Trials	19
4.3	Network-Structured Data	21
5	Experiments	21
5.1	Numerical Simulation	21
5.2	Real Data Applications	23
5.2.1	PPACT Cluster Randomized Trial	23
5.2.2	Network-Assisted Classification on Cora Dataset	25
6	Discussion	26
A	Review of Group Theory	30
B	Examples of the SymmPI Framework	32
C	Real-World Example of Network Data	33
C.1	Network-Structured Data	33
C.2	Network-Assisted Classification on Cora Dataset	34
C.3	Network Data Beyond Joint Exchangeability	35
D	Reproducing Kernel Hilbert Space	36
E	Sampled C-SymmPI Algorithm	37
F	Dual Formulation for Efficient Computation	39
G	Proofs	41
G.1	Proof of Proposition 2.1	41
G.2	Proof of Theorem 3.1	41
G.3	Proof of Theorem 3.2	43
G.4	Proof of Theorem 3.3	45
G.5	Proof of Theorem D.1	46
G.6	Proof of Theorem E.1	47
G.7	Proof of Corollary E.1	48
G.8	Proof of Proposition F.1	49
G.9	Proof of Proposition F.2	50
G.10	Proof of Proposition F.3	51

1 Introduction

In distribution-free predictive inference, we observe a partially observed version Z_{obs} of an underlying complete data object Z . The goal is to construct a prediction set $\widehat{C}(Z_{\text{obs}})$ that contains the target Z , without making strong distributional assumptions. A widely used approach is conformal prediction (Vovk et al., 2005; Angelopoulos and Bates, 2021), which guarantees *marginal coverage* under the exchangeability assumption:

$$\mathbb{P}\left(Z \in \widehat{C}(Z_{\text{obs}})\right) \geq 1 - \alpha,$$

where $\alpha \in (0, 1)$ is a user-specified miscoverage level. This guarantee is marginal in the sense that it averages over the randomness in the training, calibration, and test data. As a result, it may exhibit local miscoverage when the data distribution is heterogeneous across different realizations of Z_{obs} . In other words, for some realizations of Z_{obs} , the prediction set $\widehat{C}(Z_{\text{obs}})$ may exhibit under- or over-coverage. Therefore, one may seek a stronger guarantee that holds conditionally on each realization of Z_{obs} , known as *conditional coverage*:

$$\mathbb{P}\left(Z \in \widehat{C}(Z_{\text{obs}}) \mid Z_{\text{obs}}\right) \geq 1 - \alpha.$$

While existing works provide counterexamples showing that exact conditional coverage cannot be achieved without distributional assumptions in general (Vovk et al., 2005; Foygel Barber et al., 2021), several recent papers address this limitation by pursuing *near-conditional coverage* (Hore and Barber, 2024; Gibbs et al., 2025; Lee and Ren, 2025). Nevertheless, these methods for achieving near-conditional coverage typically rely on the global exchangeability of the data (Romano et al., 2019; Hore and Barber, 2024; Zhang and Candès, 2024; Gibbs et al., 2025; Lee and Ren, 2025), an assumption that is frequently violated in practice for various complex structured data e.g., graph-, cluster-, or tree-structured data.

Recently, Dobriban and Yu (2024) proposed SymmPI, a unified predictive inference framework for constructing valid prediction sets under group-symmetry assumptions that extend beyond classical exchangeability (see Section 2.1). For example, SymmPI applies to graph-structured data and accommodates hierarchical data structures arising in cluster randomized trials. While SymmPI extends validity beyond global exchangeability, it *mainly guarantees marginal coverage*. In heterogeneous settings, marginal coverage may be insufficient, motivating the need for stronger conditional guarantees. This need arises naturally in several real-world scenarios:

- (i) In cluster randomized trials, heterogeneity arises at multiple levels (both across and within clusters). Different clusters may serve distinct patient populations or follow different protocols, inducing cluster-specific effects. Individuals within each cluster also differ in their characteristics and responses. A marginal predictive inference guarantee in the setting of (Dobriban and Yu, 2024; Wang et al., 2024) averages the randomness over all clusters and individuals, potentially masking the fact that prediction sets are too narrow for a high-risk cluster and too wide for low-risk ones. For clinical decision-making, conditional coverage that provides cluster- or individual-level validity is often preferred.
- (ii) Networks are often heterogeneous in their connectivity structure, with dense communities and sparse bridging regions. A marginal guarantee may fail to provide reliable coverage for structurally distinct nodes. For example, it may exhibit undercoverage for nodes in sparse regions, while exhibiting over-coverage for nodes in dense communities. This motivates guarantees conditioned on a node’s local topology in order to make robust inferences about structurally distinct node types.

In both scenarios, the marginal coverage provided by existing works (Dobriban and Yu, 2024; Wang et al., 2024) may not adequately capture the heterogeneity inherent in the data. Motivated by this limitation, we aim to address the following question:

Can we achieve near-conditional predictive inference guarantees for broader classes of data structures that go beyond exchangeability?

To address this challenge, we develop a novel framework **C-SymmPI** for near-conditional predictive inference for general structured data with group symmetries, thereby generalizing coverage guarantees beyond classical i.i.d. or exchangeable assumptions. We establish general theoretical guarantees under both distributional invariance and distribution shift settings, deriving convergence rates for linear and RKHS function classes and recovering the existing state-of-the-art i.i.d. results (Gibbs et al., 2025) as special cases. To ensure computational scalability, we further develop two algorithmic variants: a projection-based method for high-dimensional observations and a sampling-based method for large or infinite group sizes. Below, we summarize our key contributions:

1.1 Our Contributions

(i). A unified framework for achieving near-conditional guarantees for general data structures.

We present **C-SymmPI**, a novel unified framework for near-conditional predictive inference applicable to a broad class of data structures exhibiting group symmetries, including networks and clustered data and so on. These guarantees hold conditional on all observed data Z_{obs} (or arbitrary lower-dimensional embeddings $\eta(Z_{\text{obs}})$, mentioned in the next point), which may constitute any subset of the full data object Z . In the canonical setting of conformal prediction (Vovk et al., 2005; Gibbs et al., 2025), Z_{obs} corresponds to $\mathcal{D} = \{(X_1, Y_1), \dots, (X_n, Y_n), X_{n+1}\}$. Conditioning on \mathcal{D} yields a stronger notion of validity than approaches that condition on the test input X_{n+1} (Gibbs et al., 2025). We establish general theoretical guarantees under both distributional invariance and distribution shift settings, recovering many existing guarantees as special cases (Gibbs et al., 2025; Dobriban and Yu, 2024).

(ii). Computational efficiency.

We also develop two computationally efficient variants of **C-SymmPI**.

- We propose a projected variant, **Projected C-SymmPI**, which establishes near-conditional coverage conditional on a projection $\eta(Z_{\text{obs}})$, where η can be an arbitrary function that projects high-dimensional Z_{obs} to a lower-dimensional embedding, thereby reducing the complexity of threshold estimation for the prediction set. By doing so, our framework achieves not only near training- or test-conditional coverage, but also coverage conditional on *arbitrary embeddings* of the observed data, while simultaneously reducing computational complexity.
- **Sampled C-SymmPI**, which improves computational scalability by approximating group averaging through finite random sampling.

Both variants preserve near-conditional coverage guarantees comparable to the full procedure, enabling applications in settings with high-dimensional observations and large or infinite symmetry groups.

(iii). Statistical guarantees.

We borrow the (relaxed) multi-accuracy perspective, which reformulates conditional coverage from pointwise conditional probabilities to function-weighted averages. Leveraging this perspective, we establish statistical convergence rates for near-conditional coverage of **C-SymmPI** and its variants over various function classes, including linear models and RKHSs. In the near conditional conformal prediction setting (Gibbs et al., 2025), where guarantees are conditioned solely on the test covariate X_{n+1} , our framework with **Projected C-SymmPI** by setting $\eta(Z_{\text{obs}}) = X_{n+1}$ recovers the convergence rates established by Gibbs et al. (2025). This highlights that the broad applicability of **C-SymmPI** and its variants to general group symmetries also enjoys desirable statistical guarantees.

(iv). Broad applicability.

We illustrate the broad applicability of **C-SymmPI** through three representative examples.

- **Exchangeable data:** We show that **C-SymmPI** recovers classical distribution-free guarantees under global exchangeability.

- **Two-layer hierarchical models:** We apply C-SymmPI to two-layer hierarchical models with random cluster sizes and specialize the framework to cluster randomized trials.
- **Network-structured data:** We adapt our framework to network-assisted regression, where C-SymmPI leverages network topology to provide topology-aware conditional guarantees.

These examples illustrate the flexibility of C-SymmPI, and similar constructions can be developed for other structured data settings as well, such as trees and images with group symmetries.

(v). Empirical validation. In numerical simulations across a range of settings, C-SymmPI produces more adaptive and robust prediction intervals than SymmPI and other baselines (see Figure 1 for an illustration in two-layer hierarchical data). In particular, C-SymmPI automatically adapts to local heterogeneity in complex data structures. In real-data analyses of the PPACT cluster randomized trial (DeBar et al., 2022) and the Cora citation network dataset (McCallum et al., 2000), C-SymmPI outperforms existing approaches (Wang et al., 2024; Lunde et al., 2023) that adapt to individual- or structure-level heterogeneity, while additionally providing the first near-conditional coverage guarantees in these settings.

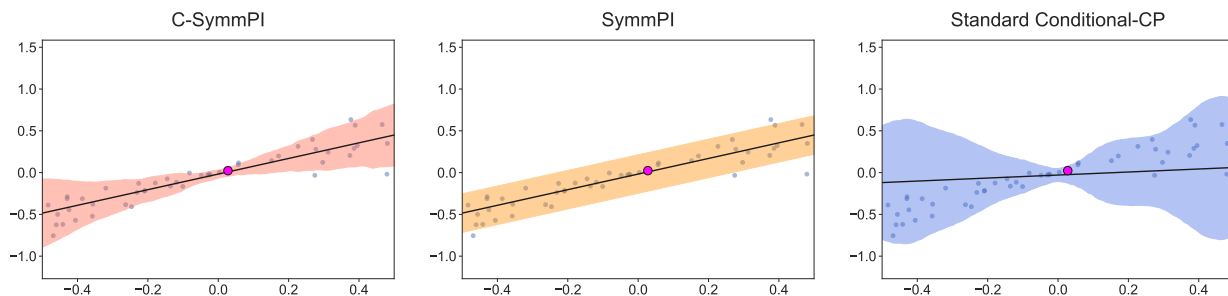


Figure 1: Comparison of prediction sets produced by C-SymmPI (our method), SymmPI (Dobriban and Yu, 2024), and Standard Conditional-CP (Gibbs et al., 2025) on simulated two-layer hierarchical data with heterogeneous noise. The data are generated with low variance near the center and higher variance in the tails within each cluster. C-SymmPI produces narrower sets in low-variance regions and wider sets in high-variance regions, adapting to local heterogeneity, whereas competing methods fail to provide comparably adaptive and robust prediction intervals. Details are provided in Section 5.1.

1.2 Related Work

Distribution-free inference has received considerable attention in recent years. Comprehensive reviews can be found in Vovk et al. (2005); Angelopoulos and Bates (2021); Shafer and Vovk (2008); Angelopoulos et al. (2024). A canonical example is conformal prediction (Vovk et al., 2005; Papadopoulos et al., 2002), which provides a general framework for predictive inference that achieves marginal coverage under the exchangeability assumption of the dataset.

However, the exchangeability assumption is often violated in practice, motivating a substantial body of work extending predictive inference to non-exchangeable data. In hierarchical data, methods exploit nested dependencies via subsampling, CDF pooling, and specialized conformal procedures (Dunn et al., 2023; Lee et al., 2023; Wang et al., 2024). For network data, topology-aware approaches are proposed to ensure valid inference on node attributes (Lunde et al., 2023; Huang et al., 2023), while for time series, block permutation schemes preserve serial dependence (Chernozhukov et al., 2018). Additionally, another major direction studies distribution shift: weighted conformal prediction maintains validity under covariate shift or outcome shift (Tibshirani et al., 2019; Park et al., 2021; Qiu et al., 2023; Yang et al., 2024; Si et al., 2023; Ai and Ren, 2024), and recent frameworks enhance robustness using weighted quantiles and randomized

adjustments (Barber et al., 2023). Recently, Dobriban and Yu (2024) developed a unified framework for predictive inference that provides valid marginal coverage guarantees across a broad class of structured data, including networks, two-layer hierarchical models, trees, and imaging data.

Even though there have been substantial developments extending coverage guarantees beyond exchangeability, most existing methods still focus on marginal coverage. However, in many settings, conditional coverage guarantees are more desirable. In light of this, recent work has sought to move beyond marginal coverage guarantees. Nevertheless, fundamental issues constrain distribution-free conditional guarantees. Vovk et al. (2005) showed that exact conditional coverage is unattainable for continuous features without producing trivial prediction sets. Subsequently, several works further highlighted the inherent challenges of conditional predictive inference, even under relaxed inferential targets (Foygel Barber et al., 2021), as well as for inference on conditional means or medians (Barber, 2020; Lee and Barber, 2021; Medarametla and Candès, 2021).

In light of these limitations, subsequent work has pursued various relaxed notions of conditional coverage. One line of research focuses on test-conditional coverage, which proves statistical validity conditional on the test input. In particular, some methods refine the standard conformal procedure to improve empirical conditional performance while formally targeting marginal coverage (Romano et al., 2019; Chernozhukov et al., 2021; Guan, 2023; Xie et al., 2024). Others pursue relaxed guarantees such as multi-accuracy or local coverage (Gibbs et al., 2025; Hore and Barber, 2024) on the test data. Another line is training-conditional coverage, where guarantees hold conditional on the training set while remaining marginal over the test point (Vovk, 2012; Bian and Barber, 2023; Liang and Barber, 2025; Gibbs and Candès, 2025). Bridging these perspectives, Zhang and Candès (2024) achieves approximate training- and test-conditional coverage by modeling conformity scores with a mixture distribution. In addition, Duchi (2025) shows that quantile regression can achieve exact training-conditional and approximate test-conditional coverage for linear function classes. Moreover, Lee and Ren (2025) proposes a relaxed inferential target that provides both training- and test-conditional ℓ_k -coverage guarantees on various function classes.

However, none of the existing methods can be directly applied to a broad class of non-exchangeable structured data while simultaneously providing near training- and test-conditional coverage guarantees (or, more generally, conditional guarantees with respect to arbitrary embeddings of the observed samples). Achieving this is non-trivial, as it requires not only adapting to local heterogeneity given the observed attributes Z_{obs} , but also handling the underlying non-exchangeable structure of the data. Our unified framework fills this gap. Table 1.2 compares our contributions with prior work.

1.3 Outline

The rest of this paper is organized as follows. In Section 2, we introduce the necessary background on the SymmPI framework. Section 3 presents our C-SymmPI methodology, along with its theoretical guarantees and computational considerations. In Section 4, we illustrate the versatility of our framework through several key examples. Section 5 provides empirical validation of our method through simulations and real-data analyses. Finally, we conclude in Section 6 with a summary and a discussion of future directions.

2 Preliminaries

In this section, we review preliminaries on (split) conformal prediction and introduce the group-theoretic framework for predictive inference (Dobriban and Yu, 2024), which underlies our approach. Our methodological development relies on several concepts from group theory, including group actions, orbits, stabilizers, cosets, and Haar probability measures. A self-contained review of these concepts is provided in Appendix A. For a comprehensive treatment, see Artin (2018); Giri (1996); Diaconis (1988); Nachbin (1976).

Paper	Data Structure	Beyond Exchangeability	Near-Conditional Coverage	
			Test Level	Training Level
Tibshirani et al. (2019) Barber et al. (2023)	Data with distribution shift	✓		
Lunde et al. (2023)	Jointly exchangeable network			
Lee et al. (2023) Wang et al. (2024)	Two-layer hierarchical model	✓		
Dobriban and Yu (2024)	Data under group symmetries	✓		
Hore and Barber (2024) Gibbs et al. (2025)	i.i.d. data		✓	
Bian and Barber (2023) Liang and Barber (2025) Gibbs and Candès (2025)	i.i.d. data			✓
Duchi (2025) Lee and Ren (2025)	i.i.d. data		✓	✓
Our work	Data under group symmetries	✓	✓	✓

Table 1: Comparison of related work.

2.1 Conformal Prediction and Group-Theoretic Predictive Inference

We begin by reviewing split conformal prediction (Papadopoulos et al., 2002; Vovk et al., 2005; Angelopoulos and Bates, 2021), interpreting distribution-free predictive inference as a procedure consisting of three key steps. We then connect this perspective to predictive inference within the group-theoretic framework.

- (i) We first impose a distributional invariance assumption on the data-generating process and observe a subset of its realizations. In split conformal prediction, we observe n labeled samples $(X_1, Y_1), \dots, (X_n, Y_n)$ from $\mathcal{X} \times \mathcal{Y}$, together with a test input X_{n+1} whose label Y_{n+1} is unobserved and we assume that all $n + 1$ points are exchangeable.
- (ii) We next transform the data into nonconformity scores. In split conformal prediction, given a pretrained black-box model $\hat{\mu} : \mathcal{X} \rightarrow \mathcal{Y}$, we compute the nonconformity scores as the absolute residuals $S_i = |Y_i - \hat{\mu}(X_i)|$ for $i = 1, \dots, n$.¹
- (iii) We then compute a data-adaptive threshold for predicting Y_{n+1} from the nonconformity scores. In split conformal prediction, we construct a prediction set for the test outcome Y_{n+1} as $\hat{C}(X_{n+1}) = [\hat{\mu}(X_{n+1}) - \hat{q}, \hat{\mu}(X_{n+1}) + \hat{q}]$, where \hat{q} denotes the $[(1 - \alpha)(n + 1)]/n$ -th quantile of the empirical distribution of S_1, \dots, S_n . This procedure guarantees the marginal coverage $\mathbb{P}(Y_{n+1} \in \hat{C}(X_{n+1})) \geq 1 - \alpha$, when the data points are exchangeable.

In what follows, we describe these three steps using group-theoretic language. This also naturally accommodates data with complex symmetry structures beyond exchangeability. See Appendix B for an example of network-structured data, and Dobriban and Yu (2024) for additional examples of other data structures.

¹Assuming that $\hat{\mu}$ is pretrained and fixed corresponds to the standard split conformal setup in Papadopoulos et al. (2002), where one subset of the data is used to fit $\hat{\mu}$ and an independent calibration subset is used to compute the scores and construct the prediction set.

Problem setup and distributional invariance. We consider a complete data vector Z taking values in a measurable space \mathcal{Z} . We assume that Z is \mathcal{G} -distributionally invariant:

$$Z \stackrel{d}{=} \rho(G)Z,$$

where $G \sim U$, with U denoting the Haar probability measure on \mathcal{G} ², and ρ representing the group action.³ This condition means that, under the group action ρ , the distribution of Z remains unchanged.

As an illustration, in split conformal, we write $Z = (Z_1, \dots, Z_{n+1})^\top = ((X_1, Y_1), \dots, (X_{n+1}, Y_{n+1}))^\top$. When $\mathcal{G} = S_{n+1}$ and ρ is the permutation action⁴, this assumption corresponds to the exchangeability of the data points $\{(X_i, Y_i)\}_{i=1}^{n+1}$. More generally, this distributionally invariant structure can accommodate broader non-exchangeable data structures, such as network data, two-layer hierarchical data, and rotationally invariant data (Dobriban and Yu, 2024).

Next, we formalize the setting where only part of the data is observed via an *observation function* $\text{obs}(\cdot) : \mathcal{Z} \rightarrow \mathcal{O}$, where \mathcal{O} is a measurable space. In the split conformal prediction example, the observation is $\text{obs}(Z) = ((X_1, Y_1), \dots, (X_n, Y_n), X_{n+1})^\top$.

Transformations. We map Z via a *transformation* $V : \mathcal{Z} \rightarrow \tilde{\mathcal{Z}}$, where $\tilde{\mathcal{Z}}$ is another measurable space equipped with a group action $\tilde{\rho}$. We assume that V is \mathcal{G} -deterministically equivariant:

$$V(\rho(g)z) = \tilde{\rho}(g)V(z),$$

for all $g \in \mathcal{G}$ and $z \in \mathcal{Z}$.⁵ This condition ensures the group action and V commute for all points in \mathcal{Z} . In split conformal prediction, the transformation V maps the dataset $Z = ((X_1, Y_1), \dots, (X_{n+1}, Y_{n+1}))^\top$ to the vector of absolute-residual nonconformity scores $V(Z) = (S_1, \dots, S_{n+1}) = (|Y_1 - \hat{\mu}(X_1)|, \dots, |Y_{n+1} - \hat{\mu}(X_{n+1})|)^\top$. Under the permutation action on both \mathcal{Z} and $\tilde{\mathcal{Z}}$, for any $g \in S_{n+1}$ we have

$$V(\rho(g)Z) = (|Y_{g^{-1}(1)} - \hat{\mu}(X_{g^{-1}(1)})|, \dots, |Y_{g^{-1}(n+1)} - \hat{\mu}(X_{g^{-1}(n+1)})|)^\top = \tilde{\rho}(g)V(Z).$$

Therefore, V is an S_{n+1} -deterministically equivariant mapping.

When the data have other structures, such as networks or images, one may use different equivariant transformations $V(\cdot)$, including equivariant graph neural networks and translation- or rotation-equivariant convolutional neural networks (LeCun et al., 1989; Finzi et al., 2020).

Threshold and Prediction Set. Next, we construct our prediction set by specifying a prediction threshold. We consider a *test function* $\psi : \tilde{\mathcal{Z}} \rightarrow \mathbb{R}$, where smaller values of $\psi(V(Z))$ indicate more plausible realizations that should be included in the prediction set. For a target coverage level $1 - \alpha \in (0, 1)$ and a realization z of Z , we define the *threshold* $t_{V(z)}$ as the $(1 - \alpha)$ -quantile of the random variable $\psi(\tilde{\rho}(G)V(z))$, where the randomness is taken over $G \sim U$:

$$t_{V(z)} = Q_{1-\alpha}(\psi(\tilde{\rho}(G)V(z)), G \sim U).$$

The resulting prediction set is defined as

$$T^{\text{SymmPI}}(z_{\text{obs}}) = \{z \in \mathcal{Z} : \psi(V(z)) \leq t_{V(z)}, \text{obs}(z) = z_{\text{obs}}\}. \quad (2.1)$$

Dobriban and Yu (2024) establish a finite-sample marginal coverage guarantee for this prediction region, ensuring that

$$\mathbb{P}(Z \in T^{\text{SymmPI}}(Z_{\text{obs}})) \geq 1 - \alpha.$$

²Throughout the paper, we assume \mathcal{G} is compact

³Here, “ $\stackrel{d}{=}$ ” denotes equality in distribution. We adopt this notation throughout this paper.

⁴Formally defined in (A.1)

⁵Dobriban and Yu (2024) consider a weaker notion of \mathcal{G} -distributional equivariance for a mapping V , requiring that for $G \sim U$, $V(\rho(G)Z) \stackrel{d}{=} \tilde{\rho}(G)V(Z)$. In practice, however, transformations are typically chosen to satisfy the stronger equivariance condition.

To connect this framework with split conformal prediction, consider the test function $\psi(\cdot) = e_{n+1}^\top \cdot$. Then we have $\psi(V(Z)) = |Y_{n+1} - \widehat{\mu}(X_{n+1})|$, which corresponds to the absolute residual used to predict the unobserved outcome Y_{n+1} . When $\mathcal{G} = S_{n+1}$, the threshold becomes

$$t_{V(Z)} = Q_{1-\alpha}\left(\{|Y_1 - \widehat{\mu}(X_1)|, \dots, |Y_n - \widehat{\mu}(X_n)|, |Y_{n+1} - \widehat{\mu}(X_{n+1})|\}\right).$$

A candidate value y is regarded as plausible if it belongs to the prediction set

$$\widehat{C}(X_{n+1}) = \left\{ y : |y - \widehat{\mu}(X_{n+1})| \leq Q_{1-\alpha}\left(\{|Y_1 - \widehat{\mu}(X_1)|, \dots, |Y_n - \widehat{\mu}(X_n)|, |y - \widehat{\mu}(X_{n+1})|\}\right) \right\},$$

which coincides with the standard split conformal prediction set.⁶

However, in many applications one may be more interested in the *conditional coverage* $\mathbb{P}(Z \in T^{\text{SymmPI}}(Z_{\text{obs}}) \mid Z_{\text{obs}}) \geq 1 - \alpha$, rather than the marginal guarantee, as it can help mitigate under- or over-coverage across different realizations of the observed sample. In the next section, we introduce (relaxed) multi-accuracy, a relaxation of exact conditional coverage.

2.2 Multi-Accuracy

We now introduce the *multi-accuracy* condition (Hébert-Johnson et al., 2018; Kim et al., 2019).

Proposition 2.1. *For any prediction set $\widehat{C} : \mathcal{O} \rightrightarrows \mathcal{Z}$ ⁷, the following two conditions are equivalent:*

- (i) $\mathbb{P}\left(Z \in \widehat{C}(Z_{\text{obs}}) \mid Z_{\text{obs}} = z_{\text{obs}}\right) = 1 - \alpha$, for $z_{\text{obs}} \in \mathcal{O}$ almost surely.
- (ii) $\mathbb{E}\left[f(Z_{\text{obs}})\left(\mathbb{1}\{Z \in \widehat{C}(Z_{\text{obs}})\} - (1 - \alpha)\right)\right] = 0$, for all bounded non-negative functions $f : \mathcal{O} \rightarrow \mathbb{R}$.⁸

Remark 2.1. *In (i), the probability is taken over the randomness of the unobserved components of Z , conditional on $Z_{\text{obs}} = z_{\text{obs}}$. In (ii), the expectation is taken over the randomness of the full data Z .*

Proposition 2.1 re-expresses the conditional coverage property in terms of *function-weighted averages* rather than pointwise conditional probabilities; its proof is provided in Section G.1. Nevertheless, achieving exact conditional coverage is generally infeasible in finite samples for distribution-free methods (Vovk et al., 2005; Foygel Barber et al., 2021). Motivated by this limitation, we consider a relaxed form of conditional coverage defined by

$$\left| \mathbb{E}\left[f(Z_{\text{obs}})\left(\mathbb{1}\{Z \in \widehat{C}(Z_{\text{obs}})\} - (1 - \alpha)\right)\right] \right| \leq \varepsilon, \text{ for all } f \in \mathcal{F}, \quad (2.2)$$

where $\mathcal{F} \subseteq \{\mathcal{O} \rightarrow \mathbb{R}\}$ is a pre-specified function class, and $\varepsilon > 0$ is a small tolerance parameter. This relaxation has two aspects: first, the equality in the multi-accuracy condition is relaxed to an inequality with tolerance ε ; second, the condition is required to hold only for $f \in \mathcal{F}$, rather than for all bounded non-negative functions.

Remark 2.2. *This form of relaxation has been studied by Gibbs et al. (2025), who consider settings where \mathcal{F} is specified as a linear function class, an RKHS, or a Lipschitz function class. Nevertheless, their approach is tailored to i.i.d. data conditioned on the test input X_{n+1} . In what follows, we develop the \mathcal{C} -SymmPI framework, which allows conditioning on general observed data Z_{obs} (or any embedding $\eta(Z_{\text{obs}})$) and accommodates data structures beyond exchangeability.*

Remark 2.3. *We can similarly generalize our framework to the setting of Lee and Ren (2025), which considers ℓ_k -coverage over $f \in \mathcal{F}$. As this extension is not our primary focus, we omit the details.*

⁶This prediction set is equivalent to the one obtained by using the $\lceil(1 - \alpha)(n + 1)\rceil/n$ empirical quantile of the conformity scores S_1, \dots, S_n as the threshold.

⁷The notation “ \rightrightarrows ” indicates that \widehat{C} maps each element in \mathcal{O} to a subset of \mathcal{Z} .

⁸All the functions we consider throughout this paper are assumed to be measurable.

3 Methodology: C-SymmPI

In this section, we introduce our method, C-SymmPI, which provides near-conditional coverage for general data structures with group symmetries.

3.1 Constructing Prediction Set

The previous SymmPI method (see Section 2.1 and (Dobriban and Yu, 2024)) attains marginal coverage by computing a *single* quantile over the orbit of transformed data. To move toward conditional coverage, we instead learn an *adaptive threshold* that depends on the observed data, allowing the prediction set to adapt to local heterogeneity. The construction of this adaptive threshold is described below.

Motivation: quantile regression. Standard quantile regression estimates a response quantile via the *pinball loss* $\ell_\alpha(t, S) := \alpha[t - S]_+ + (1 - \alpha)[S - t]_+$, where $[x]_+ = \max\{x, 0\}$. In particular, any minimizer of the empirical pinball loss over t corresponds to the empirical $(1 - \alpha)$ -quantile of S (Koenker and Bassett Jr, 1978). In our setting, suppose $|\mathcal{G}|$ is finite, for a given $z \in \mathcal{Z}$, the minimizer

$$\hat{t} = \operatorname{argmin}_{t \in \mathbb{R}} \frac{1}{|\mathcal{G}|} \sum_{i=1}^{|\mathcal{G}|} \ell_\alpha\left(t, \psi(\tilde{\rho}(g_i)V(z))\right)$$

corresponds to the $(1 - \alpha)$ -quantile of the scores $\{\psi(\tilde{\rho}(g_i)V(z)) : 1 \leq i \leq |\mathcal{G}|\}$ along the group orbit.

Function-based threshold. At a higher level, the above problem can be viewed as minimizing over the class of constant functions $\{t : t \in \mathbb{R}\}$. Now we extend this to the richer function class $\{t(\cdot) : \mathcal{O} \rightarrow \mathbb{R}\}$, which leads to an adaptive threshold function $\hat{t}_z(\cdot)$ for each $z \in \mathcal{Z}$:

$$\hat{t}_z(\cdot) = \operatorname{argmin}_{t(\cdot) \in \{\mathcal{O} \rightarrow \mathbb{R}\}} \frac{1}{|\mathcal{G}|} \sum_{i=1}^{|\mathcal{G}|} \ell_\alpha\left(t(\operatorname{obs}(\rho(g_i)z)), \psi(\tilde{\rho}(g_i)V(z))\right).^9$$

In other words, this can be viewed as a quantile regression problem that aims to estimate the conditional $(1 - \alpha)$ -quantile of $\psi(V(Z))$ given the observed features Z_{obs} . Due to the distributional invariance of the data induced by the group symmetry, we approximate this regression empirically using the orbit samples, with inputs $\{\operatorname{obs}(\rho(g_i)z)\}_{i=1}^{|\mathcal{G}|}$ and targets $\{\psi(\tilde{\rho}(g_i)V(z))\}_{i=1}^{|\mathcal{G}|}$. This formulation allows the threshold to vary along the group orbit.

Later in Section 3.4, we introduce a projected variant of the above algorithm. In this variant, we estimate the conditional $(1 - \alpha)$ -quantile of $\psi(V(Z))$ given a projection $\eta(Z_{\text{obs}})$ of the observed features, where η is an arbitrary mapping that embeds Z_{obs} into a possible lower-dimensional space.

Regularization. Quantile regression over a rich function class may interpolate the data, potentially leading to trivial prediction sets (Gibbs et al., 2025). To address this issue, we introduce a regularization term $\mathcal{R} : \{\mathcal{O} \rightarrow \mathbb{R}\} \rightarrow \mathbb{R}$ to control overfitting. We impose the following mild conditions on the regularizer:

Assumption 3.1. *The regularizer \mathcal{R} satisfies the following:*

(i) \mathcal{R} is convex on $\{\mathcal{O} \rightarrow \mathbb{R}\}$.

(ii) For all $t, f : \mathcal{O} \rightarrow \mathbb{R}$, the directional derivative $D_f \mathcal{R}(t) := \lim_{\varepsilon \rightarrow 0} \frac{\mathcal{R}(t + \varepsilon f) - \mathcal{R}(t)}{\varepsilon}$ exists.

⁹Recall that $\operatorname{obs}(\cdot)$ is a fixed function that maps \mathcal{Z} to \mathcal{O} . For example, suppose we observe the first n elements of a vector $z = (z_1, \dots, z_{n+1}) \in \mathbb{R}^{n+1}$, so that $\operatorname{obs}(z) = (z_1, \dots, z_n)^\top$. If $\rho(g)$ acts by permuting the coordinates of z with $g \in S_{n+1}$, then $\operatorname{obs}(\rho(g)z) = (z_{g^{-1}(1)}, \dots, z_{g^{-1}(n)})^\top$.

Common examples of \mathcal{R} include the squared L^2 norm $\mathcal{R}(t) = \|t\|_2^2$, the negative entropy functional $\mathcal{R}(t) = \int_{\mathcal{O}} t(o) \log t(o) d\mu(o)$ defined for $t(\cdot) > 0$, and the trivial regularizer $\mathcal{R} \equiv 0$ for simple function classes. We then arrive at the following regularized quantile regression problem:

$$\hat{t}_z(\cdot) = \operatorname{argmin}_{t(\cdot) \in \{\mathcal{O} \rightarrow \mathbb{R}\}} \frac{1}{|\mathcal{G}|} \sum_{i=1}^{|\mathcal{G}|} \ell_\alpha \left(t(\operatorname{obs}(\rho(g_i)z)), \psi(\tilde{\rho}(g_i)V(z)) \right) + \mathcal{R}(t).$$

General groups. We assumed above that $|\mathcal{G}|$ is finite. We now consider the case where $|\mathcal{G}|$ may be infinite. Note that when $|\mathcal{G}|$ is finite, the objective function is an empirical average under the uniform distribution U on \mathcal{G} . This suggests extending the formulation to general (possibly infinite) groups by replacing the empirical average with an expectation under the Haar probability measure U :

$$\hat{t}_z(\cdot) = \operatorname{argmin}_{t(\cdot) \in \{\mathcal{O} \rightarrow \mathbb{R}\}} \mathbb{E}_{G \sim U} \left[\ell_\alpha \left(t(\operatorname{obs}(\rho(G)z)), \psi(\tilde{\rho}(G)V(z)) \right) \right] + \mathcal{R}(t). \quad (3.1)$$

Equation (3.1) defines the general form of the adaptive threshold function in our framework. Our subsequent theoretical development in Section 3.2 builds upon this general definition.

C-SymmPI prediction set. Based on the adaptive threshold function in (3.1), we define the C-SymmPI prediction set in analogy with (2.1), replacing the quantile threshold with the learned threshold function:

$$T^{\text{C-SymmPI}}(z_{\text{obs}}) = \{z \in \mathcal{Z} : \psi(V(z)) \leq \hat{t}_z(z_{\text{obs}}), \operatorname{obs}(z) = z_{\text{obs}}\}. \quad (3.2)$$

The complete procedure is summarized in Algorithm 1. For each completion z^{10} of the observed data z_{obs} , the algorithm solves the optimization problem in (3.1) to obtain the corresponding threshold function $\hat{t}_z(\cdot)$, and includes z in the prediction set whenever $\psi(V(z)) \leq \hat{t}_z(z_{\text{obs}})$.

Algorithm 1 C-SymmPI: Conditional predictive inference for data with group symmetries

Input: Data z satisfying distributional invariance under group \mathcal{G} . Observation function $\operatorname{obs} : \mathcal{Z} \rightarrow \mathcal{O}$. Observed data z_{obs} . Deterministically equivariant map $V : \mathcal{Z} \rightarrow \tilde{\mathcal{Z}}$. Test function $\psi : \tilde{\mathcal{Z}} \rightarrow \mathbb{R}$. Misscoverage level $\alpha \in (0, 1)$. Penalty term \mathcal{R} satisfying Assumption 3.1.

- 1: Initialize $T^{\text{C-SymmPI}}(z_{\text{obs}}) = \emptyset$.
- 2: **for** $z \in \mathcal{Z}$ satisfying $\operatorname{obs}(z) = z_{\text{obs}}$ **do**
- 3: Solve the optimization problem (3.1) to obtain $\hat{t}_z(\cdot)$. ▷ Adaptive threshold function.
- 4: **if** $\psi(V(z)) \leq \hat{t}_z(z_{\text{obs}})$ **then**
- 5: Set $T^{\text{C-SymmPI}}(z_{\text{obs}}) \leftarrow T^{\text{C-SymmPI}}(z_{\text{obs}}) \cup \{z\}$.
- 6: **end if**
- 7: **end for**

Output: Prediction region $T^{\text{C-SymmPI}}(z_{\text{obs}})$.

Remark 3.1. We now provide several remarks on our main algorithm.

- In practice, to ensure computational tractability, we restrict the optimization problem in (3.1) to a rich parameterized function class, thereby reducing the infinite-dimensional function-space optimization to a tractable optimization problem. (see Section 3.3).
- To further alleviate computational bottlenecks, we introduce two variants of C-SymmPI (*Projected C-SymmPI* and *Sampled C-SymmPI*) tailored to solving the challenges of the high-dimensional observations and infinite groups (see Section 3.4).

¹⁰A completion z of the observed data z_{obs} is any element $z \in \mathcal{Z}$ satisfying $\operatorname{obs}(z) = z_{\text{obs}}$.

3.2 Theoretical Results

In this section, we first present two main theorems that establish near-conditional coverage guarantees under both the distributionally invariant setting and the distribution shift setting. We then provide two examples based on linear and RKHS function classes. Finally, we introduce two variants of our algorithm, **Projected C-SymmPI** and **Sampled C-SymmPI**, to improve computational efficiency in practice.

3.2.1 Near-Conditional Coverage under Distributional Invariance

We first present our main theorem establishing near-conditional coverage under the distributional invariance assumption when the group is finite. The case of an infinite group is discussed in Section E.

Theorem 3.1. *Let \mathcal{G} be a finite group equipped with the Haar probability measure U . Suppose the complete data $Z \in \mathcal{Z}$ satisfies the distributional invariance property $Z \stackrel{d}{=} \rho(G)Z$ for $G \sim U$, where ρ denotes an action of \mathcal{G} on \mathcal{Z} . Let the observed data be $Z_{\text{obs}} = \text{obs}(Z)$, where $\text{obs} : \mathcal{Z} \rightarrow \mathcal{O}$ is an observation function for some space \mathcal{O} . Consider a \mathcal{G} -deterministically equivariant function $V : \mathcal{Z} \rightarrow \tilde{\mathcal{Z}}$ for some space $\tilde{\mathcal{Z}}$, and a test function $\psi : \tilde{\mathcal{Z}} \rightarrow \mathbb{R}$. Denote $\alpha \in (0, 1)$ as the miscoverage level, and \mathcal{R} as the penalty term on the function space $\{\mathcal{O} \rightarrow \mathbb{R}\}$ satisfying Assumption 3.1. Then, for any function $f : \mathcal{O} \rightarrow \mathbb{R}$, the **C-SymmPI** prediction set defined in (3.2) satisfies*

$$\left| \mathbb{E}_Z \left[f(Z_{\text{obs}}) \left(\mathbb{1}\{Z \in T^{\text{C-SymmPI}}(Z_{\text{obs}})\} - (1 - \alpha) \right) \right] \right| \leq \varepsilon_{\text{penalty}} + \varepsilon_{\text{int}},$$

where the penalty error and interpolation error are defined as

$$\varepsilon_{\text{penalty}} = \left| \mathbb{E}_Z [D_f \mathcal{R}(\hat{t}_Z)] \right|, \quad \varepsilon_{\text{int}} = \mathbb{E}_Z [|f(Z_{\text{obs}})| \mathbb{1}\{\psi(V(Z)) = \hat{t}_Z(Z_{\text{obs}})\}].$$

Theorem 3.1 follows the relaxed multi-accuracy perspective introduced in Section 2.2. Compared with the uniform guarantee in (2.2), the bound in Theorem 3.1 holds for a fixed weighting function f . Nevertheless, by restricting f to suitable function classes, one can obtain uniform upper bounds on both the penalty error $\varepsilon_{\text{penalty}}$ and the interpolation error ε_{int} over the class, which implies that the result holds for all weighting functions f in that class (see Section 3.3 for examples).

This result generalizes the i.i.d. analysis of Gibbs et al. (2025) to general data structures with group symmetries (e.g., networks, two-layer hierarchical data) and general observation maps. The proof is deferred to Section G.2.

Remark 3.2 (Penalty error). *The term $\varepsilon_{\text{penalty}}$ captures the bias introduced by the regularization $\mathcal{R}(t)$ in the quantile regression. When the function class for $t(\cdot)$ is rich, regularization is typically required to prevent the learned threshold function \hat{t}_Z from interpolating the orbit values $\psi(\tilde{\rho}(G_i)V(z))$, which would lead to trivial prediction sets (Gibbs et al., 2025). In such cases, one may introduce a regularization parameter $\lambda > 0$ (e.g., $\mathcal{R}(t) = \lambda \|t\|_2^2$), and choosing λ sufficiently small keeps $\varepsilon_{\text{penalty}}$ small. When the function class $t(\cdot)$ is simple (e.g. the low-dimensional linear function class discussed in Section 3.3.1), we may set the regularization to zero, which gives $\varepsilon_{\text{penalty}} = 0$.*

Remark 3.3 (Interpolation error). *The term ε_{int} accounts for the error arising when the test statistic $\psi(V(Z))$ equals the learned threshold $\hat{t}_Z(Z_{\text{obs}})$. This term stems from the subgradient analysis of the pinball loss, whose subgradient is not unique at the origin, corresponding to the event $\psi(V(Z)) = \hat{t}_Z(Z_{\text{obs}})$. We analyze the magnitude of ε_{int} for specific function classes in Section 3.3.*

3.2.2 Near-Conditional Coverage under Distributional Shift

The guarantee in Theorem 3.1 relies on the \mathcal{G} -distributional invariance property $Z \stackrel{d}{=} \rho(G)Z$. In practice, this exact symmetry may be violated due to distribution shift. The following theorem characterizes the near-conditional coverage guarantee of **C-SymmPI** under distribution shift, whose proof is deferred to Section G.3.

Theorem 3.2. *Suppose the distributional invariance does not hold, i.e., $Z \stackrel{d}{\neq} \rho(G)Z$. Let \mathbb{P} denote the distribution of Z , and let \mathbb{Q} denote the distribution of $\rho(G)Z$. Further denote $Z_G := \rho(G)Z$, $Z_G^{\text{obs}} := \text{obs}(Z_G)$, and $\tilde{Z}_G := V(Z_G)$. Under the remaining conditions of Theorem 3.1, for any bounded function $f : \mathcal{O} \rightarrow \mathbb{R}$, the following bound holds:*

$$\left| \mathbb{E}_Z \left[f(Z_{\text{obs}}) \left(\mathbb{1}\{Z \in T^{\text{C-SymmPI}}(Z_{\text{obs}})\} - (1 - \alpha) \right) \right] \right| \leq \varepsilon_{\text{penalty}} + \varepsilon_{\text{int}} + 2(1 + \alpha) \|f\|_{\infty} \mathbb{E}_G [\text{TV}(\mathbb{P}, \mathbb{Q})].$$

where $\text{TV}(\mathbb{P}, \mathbb{Q})$ is the total variation distance between \mathbb{P} and \mathbb{Q} , and

$$\varepsilon_{\text{penalty}} = \left| \mathbb{E}_{G,Z} [D_f \mathcal{R}(\hat{t}_{Z_G})] \right|, \quad \varepsilon_{\text{int}} = \mathbb{E}_{G,Z} \left[|f(Z_G^{\text{obs}})| \mathbb{1}\{\psi(\tilde{Z}_G) = \hat{t}_{Z_G}(Z_G^{\text{obs}})\} \right]$$

Compared with Theorem 3.1, an additional error term arises, capturing the deviation from the invariance property via the total variation distance. Crucially, if the \mathcal{G} -distributional invariance holds ($Z \stackrel{d}{=} \rho(G)Z$), then both $\varepsilon_{\text{penalty}}$ and ε_{int} reduce to their counterparts in Theorem 3.1, and $\text{TV}(\mathbb{P}, \mathbb{Q})$ vanishes. In this case, Theorem 3.2 recovers the bound established in Theorem 3.1.

3.3 Specifying Function Classes

Note that the conditional coverage error in Theorem 3.1 depends on the choice of function class. In this section, we derive the convergence rates for two commonly used function classes: low-dimensional linear function classes and reproducing kernel Hilbert spaces (RKHSs). Throughout this subsection, without loss of generality, we assume \mathcal{G} to be finite.

3.3.1 Linear Function Class

Let \mathcal{F}_L be a d -dimensional linear function class induced by a feature map $\varphi : \mathcal{O} \rightarrow \mathbb{R}^d$:

$$\mathcal{F}_L = \{f : \mathcal{O} \rightarrow \mathbb{R} \mid f(\cdot) = \langle \theta, \varphi(\cdot) \rangle, \theta \in \mathbb{R}^d\}.$$

We impose the following boundedness conditions on the feature map and the parameter vector:

Assumption 3.2. *There exist constants $b_{\varphi} > 0$ and $b_{\theta} > 0$ such that (i) $\|\varphi(\cdot)\|_2 \leq b_{\varphi}$, and (ii) $\|\theta\|_2 \leq b_{\theta}$.*

We restrict the optimization in (3.1) to \mathcal{F}_L , and set the regularization term $\mathcal{R}(t) \equiv 0$ as the problem is low-dimensional. Under the parametrization $\hat{t}_z^L(\cdot) = \langle \hat{\theta}_z, \varphi(\cdot) \rangle$, (3.1) reduces to an optimization over $\theta \in \mathbb{R}^d$. In particular, for each $z \in \mathcal{Z}$,

$$\hat{\theta}_z = \underset{\|\theta\|_2 \leq b_{\theta}}{\text{argmin}} \frac{1}{|\mathcal{G}|} \sum_{i=1}^{|\mathcal{G}|} \ell_{\alpha} \left(\langle \theta, \varphi(\text{obs}(\rho(g_i)z)) \rangle, \psi(\tilde{\rho}(g_i)V(z)) \right). \quad (3.3)$$

Since there are multiple elements $g_i \in \mathcal{G}$, it is possible for different g_i 's to induce the same loss value, resulting in redundant terms in the summation. We therefore identify these redundancies and evaluate each distinct term only once. Define

$$F : \mathcal{Z} \rightarrow \mathbb{R}^d \times \mathbb{R}, \quad F(z) := (\varphi(\text{obs}(z)), \psi(V(z))).$$

The stabilizer subgroup of F is given by

$$\mathcal{H} := \{g \in \mathcal{G} : F(\rho(g)z) = F(z), \forall z \in \mathcal{Z}\}.$$

By construction, \mathcal{H} consists of elements $g \in \mathcal{G}$ that leave both $\varphi(\text{obs}(\cdot))$ and $\psi(V(\cdot))$ unchanged. A coset $g\mathcal{H} := \{gh : h \in \mathcal{H}\}$ can be viewed as a collection of group elements that result in the same function F . The set of distinct cosets is denoted by $\mathcal{G}/\mathcal{H} := \{g\mathcal{H} : g \in \mathcal{G}\}$. By the orbit-stabilizer theorem (see Section A),

$|\mathcal{G}/\mathcal{H}| = |\mathcal{G}|/|\mathcal{H}|$, therefore there are $|\mathcal{G}|/|\mathcal{H}|$ distinct terms, each repeated $|\mathcal{H}|$ times in the original averaged loss function (3.3). Choosing representatives $\{g_i\}_{i=1}^{|\mathcal{G}/\mathcal{H}|}$ therefore yields the equivalent formulation:

$$\widehat{\theta}_z = \operatorname{argmin}_{\|\theta\|_2 \leq b_\theta} \frac{|\mathcal{H}|}{|\mathcal{G}|} \sum_{i=1}^{|\mathcal{G}/\mathcal{H}|} \ell_\alpha \left(\langle \theta, \varphi(\operatorname{obs}(\rho(g_i)z)) \rangle, \psi(\tilde{\rho}(g_i)V(z)) \right).$$

The resulting C-SymmPI prediction set is:

$$T_L^{\text{C-SymmPI}}(z_{\text{obs}}) = \left\{ z \in \mathcal{Z} : \psi(V(z)) \leq \langle \widehat{\theta}_z, \varphi(z_{\text{obs}}) \rangle, \operatorname{obs}(z) = z_{\text{obs}} \right\}. \quad (3.4)$$

The following theorem establishes the convergence rate of the near-conditional coverage error for the low-dimensional linear function class; its proof is provided in Section G.4.

Theorem 3.3. *Let $\mathcal{F}_L \subseteq \{\mathcal{O} \rightarrow \mathbb{R}\}$ denote the class of d -dimensional linear functions with $d \leq |\mathcal{G}|/|\mathcal{H}|$ that satisfies Assumption 3.2. Assume that $\Psi := [\psi(\tilde{\rho}(g_i)V(Z))]_{1 \leq i \leq |\mathcal{G}|/|\mathcal{H}|}^\top$ admits a joint density. Then for all $f(\cdot) = \langle \theta, \varphi(\cdot) \rangle \in \mathcal{F}_L$, the C-SymmPI prediction set defined in (3.4) satisfies*

$$\left| \mathbb{E}_Z \left[f(Z_{\text{obs}}) \left(\mathbb{1}\{Z \in T_L^{\text{C-SymmPI}}(Z_{\text{obs}})\} - (1 - \alpha) \right) \right] \right| \leq \frac{b_\varphi b_\theta d}{|\mathcal{G}|/|\mathcal{H}|}.$$

Remark 3.4. *Theorem 3.3 shows that when using a d -dimensional linear function class, the near-conditional coverage error decays at a rate of $\mathcal{O}(d|\mathcal{H}|/|\mathcal{G}|)$. Since no regularization is imposed, the penalty error $\varepsilon_{\text{penalty}}$ is zero, and the error bound arises from the interpolation error ε_{int} . In Section 4.1, we show that this rate matches the result for conditional conformal prediction in (Gibbs et al., 2025) under specific choices of $\psi(\cdot)$ and $\varphi(\cdot)$.*

3.3.2 RKHS Function Class

Due to space limitations in the main text, we defer the discussion of RKHS-based function classes to the appendix; see Section D for details. We next introduce two variants of our algorithm aimed at improving computational efficiency.

3.4 Computationally Efficient Variants

Solving (3.1) can be computationally demanding for two main reasons: learning a threshold function over a high-dimensional observation space \mathcal{O} , and evaluating the Haar expectation over a large (or infinite) group \mathcal{G} . To address these challenges, we introduce two tractable variants.

(i). **Projected C-SymmPI** reduces the complexity of function learning by mapping $Z_{\text{obs}} \in \mathcal{O}$ to a lower-dimensional representation $\eta(Z_{\text{obs}})$. (ii). **Sampled C-SymmPI** reduces the cost of group averaging by replacing the Haar expectation with a Monte Carlo average over independently sampled group elements $g_i \in \mathcal{G}$.

Projected C-SymmPI. When the observation space \mathcal{O} is high-dimensional, learning a threshold function $\widehat{t}_z : \mathcal{O} \rightarrow \mathbb{R}$ may suffer from the curse of dimensionality. Moreover, the unknown entries to be predicted may depend only on a subset of the observations, or on a lower-dimensional representation of the data, rather than on the entire observation vector. To mitigate this issue, we project the observed data $\operatorname{obs}(Z) \in \mathcal{O}$ onto a lower-dimensional space via a mapping $\eta : \mathcal{O} \rightarrow \mathcal{W}$, where \mathcal{W} is a low-dimensional embedding. Composing η with the observation function, we define $\operatorname{proj}(z) := \eta(\operatorname{obs}(z))$. We then learn a threshold function

$$\widehat{t}_z^{\text{proj}}(\cdot) = \operatorname{argmin}_{t(\cdot) \in \{\mathcal{W} \rightarrow \mathbb{R}\}} \mathbb{E}_{G \sim U} \left[\ell_\alpha \left(t(\operatorname{proj}(\rho(G)z)), \psi(\tilde{\rho}(G)V(z)) \right) \right] + \mathcal{R}(t). \quad (3.5)$$

Compared with (3.1), the optimization in (3.5) is carried out over functions defined on the lower-dimensional space \mathcal{W} . This improves computational efficiency in two ways: (i) learning functions in a

lower-dimensional space is more tractable; and (ii) additional redundancies in the loss function can be eliminated, following the same approach as in Section 4.1. The corresponding **Projected C-SymmPI** prediction set is defined as follows:

$$T_p^{\text{C-SymmPI}}(z_{\text{obs}}) = \{z \in \mathcal{Z} : \psi(V(z)) \leq \hat{t}_z^{\text{proj}}(z_{\text{proj}}), \text{obs}(z) = z_{\text{obs}}\}, \quad (3.6)$$

where $z_{\text{proj}} = \text{proj}(z) = \eta(\text{obs}(z))$. The following corollary establishes the near-conditional coverage guarantee for **Projected C-SymmPI**; its proof closely follows that of Theorem 3.1 and is therefore omitted.

Corollary 3.1. *Under the same conditions as Theorem 3.1, for any function $f : \mathcal{W} \rightarrow \mathbb{R}$, the Projected C-SymmPI prediction region defined in (3.6) satisfies*

$$\left| \mathbb{E}_Z \left[f(Z_{\text{proj}}) \left(\mathbb{1}\{Z \in T_p^{\text{C-SymmPI}}(Z_{\text{obs}})\} - (1 - \alpha) \right) \right] \right| \leq \varepsilon_{\text{penalty}} + \varepsilon_{\text{int}}.$$

Here we define $Z_{\text{proj}} = \eta(Z_{\text{obs}})$, which can be arbitrary embedding of Z_{obs} . Additionally, the penalty error and interpolation error are defined as

$$\varepsilon_{\text{penalty}} = \left| \mathbb{E}_Z \left[D_f \mathcal{R}(\hat{t}_Z^{\text{proj}}) \right] \right|, \quad \varepsilon_{\text{int}} = \mathbb{E}_Z \left[|f(Z_{\text{proj}})| \mathbb{1}\{\psi(V(Z)) = \hat{t}_Z^{\text{proj}}(Z_{\text{proj}})\} \right].$$

Compared with Theorem 3.1, the near-conditional coverage guarantee in Corollary 3.1 is established with respect to conditioning on the projected data $Z_{\text{proj}} = \eta(Z_{\text{obs}})$, where η is an arbitrary mapping from the observed data Z_{obs} to a lower-dimensional representation. This demonstrates that our framework not only accommodates training- and test-conditional guarantees, but also enables conditioning on arbitrary embeddings of the observed features.

In practice, conditioning on the full data Z_{obs} is often unnecessary; instead, it suffices to condition on a reduced set of features Z_{proj} that are most relevant to the problem, thereby alleviating computational burden. In Section 4, we illustrate this variant of **C-SymmPI** through several examples.

Regarding results under different function classes \mathcal{F} , similar convergence rates hold when \mathcal{F} is specified as either a low-dimensional linear class or an RKHS, as discussed in Section 3.3. The only modification is that all occurrences of the observation map $\text{obs}(\cdot)$ are replaced by the projection map $\text{proj}(\cdot)$. The proofs are analogous and are therefore omitted.

Sampled C-SymmPI. When \mathcal{G} is large or infinite (e.g., the rotation group $\text{SO}(p)$), evaluating the group average in (3.1) becomes computationally costly or infeasible. To improve tractability, we approximate the Haar expectation by a Monte Carlo average based on a finite number of i.i.d. draws $G_1, \dots, G_N \sim U$. Appendix E formalizes this **Sampled C-SymmPI** variant and establishes two results: (i) when N is large, the sampled procedure approximates the full method; and (ii) it admits a near-conditional coverage guarantee analogous to the original procedure in Theorem 3.1.

4 Examples

In this section, we illustrate the broader applicability of the **C-SymmPI** framework across a range of data settings. Specifically, we consider (i) exchangeable data (Section 4.1), (ii) two-layer hierarchical models, including cluster randomized trials (Section 4.2), and (iii) network-structured data (Section 4.3). For each setting, we identify the underlying group symmetries, instantiate the components of the **C-SymmPI** framework, and characterize the resulting near-conditional coverage guarantees.

4.1 Exchangeable Data

In this section, we study near-conditional predictive inference under the exchangeability assumption. In particular, we demonstrate that **C-SymmPI** recovers the conditional conformal prediction method of Gibbs et al. (2025).

Problem setup. Let $Z = (X_i, Y_i)_{1 \leq i \leq n+1}^\top \in \mathcal{Z} := (\mathcal{X} \times \mathbb{R})^{n+1}$ be a random vector consisting of $n+1$ exchangeable pairs (X_i, Y_i) . Let S_{n+1} be the permutation group on the index set $[n+1]$, and let ρ be the permutation action of S_{n+1} on Z as defined in (A.1). The exchangeability assumption ensures $Z \stackrel{d}{=} \rho(G)Z$ for $G \sim U$, where U denotes the Haar probability measure on S_{n+1} . For all $z = (x_i, y_i)_{1 \leq i \leq n+1}^\top \in \mathcal{Z}$, the observation function is $\text{obs}(z) := ((x_1, y_1), \dots, (x_n, y_n), x_{n+1})^\top \in \mathcal{O} := (\mathcal{X} \times \mathbb{R})^n \times \mathcal{X}$, which reveals all the data points (both features and labels) except for y_{n+1} .

Transformations. We focus primarily on split conformal prediction due to its computational efficiency (Papadopoulos et al., 2002; Angelopoulos and Bates, 2021), and our method can be extended to full conformal prediction easily. We assume access to an arbitrary black-box predictor $\hat{\mu} : \mathcal{X} \rightarrow \mathbb{R}$ ¹¹. Define

$$V(z) := (s_1, \dots, s_{n+1})^\top := (|y_1 - \hat{\mu}(x_1)|, \dots, |y_{n+1} - \hat{\mu}(x_{n+1})|)^\top \in \tilde{\mathcal{Z}}.$$

We obtain that for all $g \in S_{n+1}$ and $z \in \mathcal{Z}$, the transformed data satisfy $V(\rho(g)z) = \rho(g)V(z)$, and hence V is S_{n+1} -deterministically equivariant. Additionally, $V(z)$ collects the non-conformity scores of the original sample z with respect to $\hat{\mu}$.

Adaptive threshold. Let the test function be $\psi(V(z)) := s_{n+1} = |y_{n+1} - \hat{\mu}(x_{n+1})|$, which extracts the last component of $V(z)$. We now construct an adaptive threshold by applying a threshold function to the scores $\{\psi(\rho(g)V(z)) : g \in S_{n+1}\}$ over the group orbit.

To recover the method of Gibbs et al. (2025), we consider the Projected C-SymmPI variant from Section 3.4, in which the threshold function is restricted to depend only on the covariates in \mathcal{X} , rather than the full observed data \mathcal{O} . Formally, we define the projection map $\text{proj} : \mathcal{Z} \rightarrow \mathcal{X}$ by $\text{proj}(z) = \eta(\text{obs}(z)) = x_{n+1}$, which yields the optimization problem in (3.5).

Next, we simplify the calculation of (3.5) by partitioning the group. For any $i \in [n+1]$, the set of permutations that map the i -th element to the last position has size $n!$. For any such permutation g , we have $\text{proj}(\rho(g)z) = x_i$ and $\psi(\rho(g)V(z)) = s_i$. Therefore, the optimization problem reduces to

$$\begin{aligned} \hat{t}_z(\cdot) &= \underset{t(\cdot) \in \{\mathcal{X} \rightarrow \mathbb{R}\}}{\text{argmin}} \frac{1}{|S_{n+1}|} \sum_{g \in S_{n+1}} \ell_\alpha \left(t(\text{proj}(\rho(g)z)), \psi(\rho(g)V(z)) \right) + \mathcal{R}(t) \\ &= \underset{t(\cdot) \in \{\mathcal{X} \rightarrow \mathbb{R}\}}{\text{argmin}} \frac{1}{(n+1)!} \sum_{i=1}^{n+1} |\{g \in S_{n+1} : \text{proj}(\rho(g)z) = x_i, \psi(\rho(g)V(z)) = s_i\}| \cdot \ell_\alpha(t(x_i), s_i) + \mathcal{R}(t) \\ &= \underset{t(\cdot) \in \{\mathcal{X} \rightarrow \mathbb{R}\}}{\text{argmin}} \frac{1}{(n+1)!} \sum_{i=1}^{n+1} n! \cdot \ell_\alpha(t(x_i), s_i) + \mathcal{R}(t) \\ &= \underset{t(\cdot) \in \{\mathcal{X} \rightarrow \mathbb{R}\}}{\text{argmin}} \frac{1}{n+1} \sum_{i=1}^{n+1} \ell_\alpha(t(x_i), s_i) + \mathcal{R}(t). \end{aligned} \tag{4.1}$$

This formulation coincides with that of Gibbs et al. (2025), where the adaptive threshold is learned by minimizing the empirical pinball loss over the calibration scores $\{s_i\}_{i=1}^{n+1}$ with a regularization term.¹²

C-SymmPI prediction region. Substituting $\hat{t}_z(\cdot)$ from (4.1) into the C-SymmPI prediction region (3.2) and isolating the unobserved component y_{n+1} , we obtain

$$T^{\text{C-SymmPI}}(z_{\text{obs}}) = \{y_{n+1} : s_{n+1} \leq \hat{t}_z(x_{n+1})\}. \tag{4.2}$$

¹¹One can always partition the sample into two disjoint subsets, using n_0 observations to train the predictor and the remaining $n_1 := n - n_0$ observations to construct the prediction set. Without loss of generality, we treat n_1 as the full calibration size n and leave the n_0 training sample implicit. This notational simplification is also adopted in Gibbs et al. (2025).

¹²Throughout this section, we omit the ‘‘proj’’ subscript and superscript from the threshold function and the prediction region for simplicity.

This prediction region coincides with that proposed by [Gibbs et al. \(2025\)](#). The following corollary, which is directly implied by [Theorem 3.1](#) and [Corollary 3.1](#), establishes the near-conditional coverage guarantee for Y_{n+1} given X_{n+1} for the prediction set in [\(4.2\)](#). Its proof closely parallels the arguments of [Theorem 3.1](#) and [Corollary 3.1](#) and is therefore omitted for brevity.

Corollary 4.1 ([Gibbs et al. \(2025\)](#), [Theorem 3](#)). *Under the split conformal prediction setup, for any function $f : \mathcal{X} \rightarrow \mathbb{R}$, the prediction region $T^{\text{C-SymmPI}}$ defined in [\(4.2\)](#) satisfies*

$$\left| \mathbb{E}_Z \left[f(X_{n+1}) \left(\mathbb{1}\{Y_{n+1} \in T^{\text{C-SymmPI}}(Z_{\text{obs}})\} - (1 - \alpha) \right) \right] \right| \leq \varepsilon_{\text{penalty}} + \varepsilon_{\text{int}},$$

where the penalty error and interpolation error are defined as

$$\varepsilon_{\text{penalty}} = \left| \mathbb{E}_Z [D_f \mathcal{R}(\hat{t}_Z)] \right|, \quad \varepsilon_{\text{int}} = \mathbb{E}_Z [|f(X_{n+1})| \mathbb{1}\{S_{n+1} = \hat{t}_Z(X_{n+1})\}].$$

Remark 4.1. *While our derivation employs the absolute residual score, $S_i = |Y_i - \hat{\mu}(X_i)|$, the framework readily accommodates other non-conformity scores through appropriate choices of the transformation V and the test function ψ .*

Specialization to a linear function class. Let $\mathcal{F}_L = \{f : \mathcal{X} \rightarrow \mathbb{R} \mid f(\cdot) = \langle \theta, \varphi(\cdot) \rangle\}$, where $\|\varphi\|_2 \leq b_\varphi$ and $\|\theta\|_2 \leq b_\theta$, as specified in [Assumption 3.2](#). By restricting [\(4.1\)](#) to the class \mathcal{F}_L and setting the penalty $\mathcal{R} \equiv 0$, we obtain the corresponding prediction region $T_L^{\text{C-SymmPI}}(Z_{\text{obs}})$. [Corollary 4.2](#) establishes a convergence rate of $\mathcal{O}(d/n)$ for the conditional coverage error, which follows directly from [Theorem 3.3](#).

Corollary 4.2 ([Gibbs et al. \(2025\)](#), [Theorem 2](#)). *Assume that the distribution of the score S is continuous. Then, in the setting above, for any function $f \in \mathcal{F}_L$, the prediction region $T_L^{\text{C-SymmPI}}(Z_{\text{obs}})$ satisfies*

$$\left| \mathbb{E}_Z \left[f(X_{n+1}) \left(\mathbb{1}\{Y_{n+1} \in T_L^{\text{C-SymmPI}}(Z_{\text{obs}})\} - (1 - \alpha) \right) \right] \right| \leq \frac{b_\varphi b_\theta d}{n+1}.$$

Specialization to an RKHS. Let \mathcal{F}_K be the RKHS with norm $\|\cdot\|_K$ induced by a positive semidefinite kernel $K : \mathcal{X} \times \mathcal{X} \rightarrow \mathbb{R}$. We assume the kernel is bounded by κ^2 , as specified in [Assumption D.1](#). By restricting [\(4.1\)](#) to the function class $B_M(\mathcal{F}_K) = \{t \in \mathcal{F}_K : \|t\|_K \leq M\}$ and choosing the penalty $\mathcal{R}(t) = \|t\|_K^2 / \sqrt{n+1}$, we obtain the corresponding prediction region $T_K^{\text{C-SymmPI}}(Z_{\text{obs}})$. [Corollary 4.3](#) establishes a convergence rate of $\mathcal{O}(1/\sqrt{n})$ for the conditional coverage error, which follows directly from [Theorem D.1](#).

Corollary 4.3. *Assume that the score S admits a density that is bounded above by a constant $b > 0$. Then, in the setting above, for any $f \in B_M(\mathcal{F}_K)$, the prediction region $T_K^{\text{C-SymmPI}}(Z_{\text{obs}})$ satisfies*

$$\left| \mathbb{E}_Z \left[f(X_{n+1}) \left(\mathbb{1}\{Y_{n+1} \in T_K^{\text{C-SymmPI}}(Z_{\text{obs}})\} - (1 - \alpha) \right) \right] \right| \leq \frac{2M^2 + b\kappa^3 M}{\sqrt{n+1}}.$$

Remark 4.2. [Gibbs et al. \(2025\)](#) considered a richer function class $\mathcal{F} = \{f = f_1 + f_2 : \mathcal{X} \rightarrow \mathbb{R} \mid f_1 \in \mathcal{F}_L, f_2 \in \mathcal{F}_K\}$, defined as the sum of a d -dimensional linear component and an RKHS component. A direct consequence of their [Proposition 1](#) is a statistical rate of $\mathcal{O}(\sqrt{d \log n/n})$ for the conditional coverage error. Our analysis considers the RKHS function class only and establishes a convergence rate of $\mathcal{O}(1/\sqrt{n})$ under standard boundedness assumptions.

4.2 Two-Layer Hierarchical Models

We apply C-SymmPI to two-layer hierarchical data, a structure commonly arising in applications like meta-learning ([Park et al., 2022](#)) and cluster randomized trials ([Wang et al., 2024](#)). We show that C-SymmPI extends prior marginal coverage results ([Lee et al., 2023](#); [Dobriban and Yu, 2024](#)) by providing a stronger near-conditional coverage guarantee. We next illustrate this methodology in supervised meta-learning and for estimating treatment effects in cluster-randomized trials.

4.2.1 Setup: Data with Hierarchical Symmetries

Let $Z = (Z_1^\top, \dots, Z_K^\top)^\top$ be a random vector consisting of K clusters, drawn from a joint distribution \mathbb{P}_Z over the space $\mathcal{Z}_0^* := \bigcup_{j \geq 0} \mathcal{Z}_0^j$. For each $i \in [K]$, the i -th cluster is denoted by $Z_i = (Z_1^{(i)}, \dots, Z_{N_i}^{(i)})^\top$, where the cluster size N_i is a random variable taking values in \mathbb{N} . Let $N = (N_1, \dots, N_K) \in \mathbb{N}^K$ denote the vector of cluster sizes, where each N_i is independently drawn from a distribution P_N . We impose the following assumptions:

Assumption 4.1. *The distribution \mathbb{P}_N of the cluster sizes is independent of the distribution \mathbb{P}_Z of the data.*

For $n = (n_1, \dots, n_K) \in \text{supp}(N)$, we assume that the data exhibit a two-layer exchangeability structure (Lee et al., 2023; Dobriban and Yu, 2024; Wang et al., 2024), as formalized by the following two assumptions.

Assumption 4.2 (Within-cluster exchangeability). *For each cluster $i \in [K]$, the individual data points $Z_1^{(i)}, \dots, Z_{n_i}^{(i)}$ within the cluster vector $Z_i = (Z_1^{(i)}, \dots, Z_{n_i}^{(i)})^\top \in \mathcal{Z}_0^{n_i}$ are exchangeable.*

Assumption 4.3 (Between-cluster exchangeability). *The cluster vectors Z_1, \dots, Z_K that constitute the full data vector $Z = (Z_1^\top, \dots, Z_K^\top)^\top \in \mathcal{Z} := \prod_{i=1}^K \mathcal{Z}_0^{n_i}$ are exchangeable.*

To formalize the two-layer exchangeability via group actions, for any $n = (n_1, \dots, n_K) \in \text{supp}(N)$, we introduce two groups, S_{in} and S_{out} , which correspond to the within-cluster and between-cluster exchangeability, respectively. We define the inner group as the direct product $S_{\text{in}} := S_{n_1} \times \dots \times S_{n_K}$, where each S_{n_i} acts on the index set $[n_i]$. Any element $\sigma \in S_{\text{in}}$ can be written as $\sigma = (\sigma_1, \dots, \sigma_K)$, where $\sigma_i \in S_{n_i}$ acts on Z_i^\top by

$$\sigma_i \cdot Z_i = \left(Z_{\sigma_i^{-1}(1)}^{(i)}, \dots, Z_{\sigma_i^{-1}(n_i)}^{(i)} \right)^\top.$$

Let $S_{\text{out}} := S_K$ be the symmetric group acting on $[K]$, with its permutation action on the cluster vectors Z_1, \dots, Z_K given by

$$\pi \cdot Z = \left(Z_{\pi^{-1}(1)}^\top, \dots, Z_{\pi^{-1}(K)}^\top \right)^\top.$$

We then define the group $\mathcal{G} := S_{\text{in}} \times S_{\text{out}}$ ¹³, where each element $g = (\sigma, \pi) \in \mathcal{G}$ consists of a permutation $\sigma \in S_{\text{in}}$ and a permutation $\pi \in S_{\text{out}}$. The action of an element $g = (\sigma, \pi) \in \mathcal{G}$ on Z is defined by the composition of a within-cluster permutation σ and a between-cluster permutation π . Specifically, for $g = (\sigma, \pi)$, the action $\rho(g)$ on Z is given by:

$$\rho(g)Z := \pi \cdot (\sigma_1 \cdot Z_1^\top, \dots, \sigma_K \cdot Z_K^\top)^\top.$$

Let U denote the Haar probability measure on the group \mathcal{G} . Assumptions 4.2 and 4.3 together imply that the data vector Z is distributionally invariant under the action of \mathcal{G} , i.e., $Z \stackrel{d}{=} \rho(G)Z$ for $G \sim U$.

4.2.2 Example: Supervised Learning with Two-Layer Hierarchical Data

We now apply the C-SymmPI framework to a supervised learning problem with two-layer hierarchical data, a setting also considered in Lee et al. (2023); Dobriban and Yu (2024). For each $n = (n_1, \dots, n_K) \in \text{supp}(N)$, conditional on $N = n$, let the complete data be

$$z = (z_i^\top)_{1 \leq i \leq K}^\top = \left((x_1^{(i)}, y_1^{(i)}), \dots, (x_{n_i}^{(i)}, y_{n_i}^{(i)}) \right)_{1 \leq i \leq K}^\top \in \mathcal{Z} := \prod_{i=1}^K (\mathcal{X} \times \mathbb{R})^{n_i},$$

which satisfies the two-layer exchangeability structure described in Section 4.2.1. We consider the problem of predicting the response of the last individual in the final cluster, denoted by $y_{n_K}^{(K)}$. Accordingly, the observation function reveals all observed data points except for this target response:

$$\text{obs}(z) := (z_1^\top, \dots, z_{K-1}^\top, o_K^\top)^\top, \quad \text{where } o_K := \left((x_1^{(K)}, y_1^{(K)}), \dots, (x_{n_K-1}^{(K)}, y_{n_K-1}^{(K)}), x_{n_K}^{(K)} \right)^\top.$$

¹³See the definition of the notation “ \times ” in Section A.

Transformation and adaptive threshold. Suppose we are given a pretrained black-box predictor $\widehat{\mu} : \mathcal{X} \rightarrow \mathbb{R}$. We define a transformation that maps the data to non-conformity scores. Here, we use the absolute residuals as the non-conformity scores:

$$V(z) := (s_j^{(i)})_{1 \leq i \leq K, 1 \leq j \leq n_i}^\top := \left(|y_1^{(i)} - \widehat{\mu}(x_1^{(i)})|, \dots, |y_{n_i}^{(i)} - \widehat{\mu}(x_{n_i}^{(i)})| \right)_{1 \leq i \leq K}^\top \in \widetilde{\mathcal{Z}} := \prod_{i=1}^K \mathbb{R}^{n_i}.$$

It is straightforward to verify that $V(\rho(g)z) = \rho(g)V(z)$ for all $g \in \mathcal{G}$ and $z \in \mathcal{Z}$, indicating that V is \mathcal{G} -deterministically equivariant. Let the test function be $\psi(V(z)) := s_{n_K}^{(K)} = |y_{n_K}^{(K)} - \widehat{\mu}(x_{n_K}^{(K)})|$, which extracts the non-conformity score of the target individual.

For computational efficiency, we adopt the **Projected C-SymmPI** approach introduced in Section 3.4, which leads to the optimization problem in (3.5). In particular, we choose η such that $\text{proj}(z) = x_{n_K}^{(K)}$, allowing the threshold function to depend only on the covariate of the target individual, $x_{n_K}^{(K)}$.

We now simplify the calculation in (3.5) by partitioning the group. For any $i \in [K]$ and $j \in [n_i]$, the set of permutations in \mathcal{G} that map the j -th individual in the i -th cluster to the last position of the last cluster has size $(K-1)! \cdot (n_i-1)! \cdot \prod_{k \neq i} n_k!$. For any such permutation g , we have $\text{proj}(\rho(g)z) = x_j^{(i)}$ and $\psi(\rho(g)V(z)) = s_j^{(i)}$. Therefore, the optimization problem reduces to

$$\begin{aligned} \widehat{t}_z(\cdot) &= \underset{t(\cdot) \in \{\mathcal{X} \rightarrow \mathbb{R}\}}{\text{argmin}} \frac{1}{|\text{S}_{\text{out}}| \cdot |\text{S}_{\text{in}}|} \sum_{\pi \in \text{S}_{\text{out}}} \sum_{\sigma \in \text{S}_{\text{in}}} \ell_\alpha \left(t(\text{proj}(\rho(\sigma, \pi)z)), \psi(\rho(\sigma, \pi)V(z)) \right) + \mathcal{R}(t) \\ &= \underset{t(\cdot) \in \{\mathcal{X} \rightarrow \mathbb{R}\}}{\text{argmin}} \frac{1}{K! \cdot \prod_{k=1}^K n_k!} \sum_{i=1}^K \sum_{j=1}^{n_i} \left| \left\{ g = (\sigma, \pi) \in \mathcal{G} : \text{proj}(\rho(g)z) = x_j^{(i)}, \psi(\rho(g)V(z)) = s_j^{(i)} \right\} \right| \ell_\alpha \left(t(x_j^{(i)}), s_j^{(i)} \right) + \mathcal{R}(t) \\ &= \underset{t(\cdot) \in \{\mathcal{X} \rightarrow \mathbb{R}\}}{\text{argmin}} \frac{1}{K!} \sum_{i=1}^K \frac{1}{n_i! \cdot \prod_{k \neq i} n_k!} \sum_{j=1}^{n_i} (K-1)! \cdot (n_i-1)! \cdot \prod_{k \neq i} n_k! \cdot \ell_\alpha \left(t(x_j^{(i)}), s_j^{(i)} \right) + \mathcal{R}(t) \\ &= \underset{t(\cdot) \in \{\mathcal{X} \rightarrow \mathbb{R}\}}{\text{argmin}} \frac{1}{K} \sum_{i=1}^K \frac{1}{n_i} \sum_{j=1}^{n_i} \ell_\alpha \left(t(x_j^{(i)}), s_j^{(i)} \right) + \mathcal{R}(t). \end{aligned} \tag{4.3}$$

This formulation corresponds to a *weighted* empirical pinball loss with regularization, where each cluster is assigned equal weight, and observations within a cluster are weighted inversely proportional to the cluster size. Similar weighting schemes have appeared in prior work (Lee et al., 2023; Dobriban and Yu, 2024; Wang et al., 2024), which established marginal coverage guarantees for prediction sets under two-layer hierarchical data structures. Our framework extends these results by incorporating adaptive thresholds, thereby yielding a stronger near-conditional coverage guarantee.

C-SymmPI prediction region. Substituting $\widehat{t}_z(\cdot)$ from (4.3) into the C-SymmPI prediction set (3.2) and isolating the unobserved component $y_{n_K}^{(K)}$, we obtain

$$T^{\text{C-SymmPI}}(z_{\text{obs}}) = \left\{ y_{n_K}^{(K)} : s_{n_K}^{(K)} \leq \widehat{t}_z(x_{n_K}^{(K)}) \right\}.$$

By Corollary 3.1, this prediction set satisfies a corresponding near-conditional coverage guarantee under a two-layer hierarchical exchangeability structure; we omit the formal statement for brevity. This result provides a stronger guarantee than the marginal coverage results established in Dobriban and Yu (2024). Appendix F presents a computationally efficient algorithm for constructing the prediction set. More generally, our framework can also be used to predict other components by specifying alternative forms of ψ .

4.2.3 Example: Cluster Randomized Trials

We now apply the C-SymmPI framework to cluster randomized trials (CRTs), building on the two-layer hierarchical data structure introduced in Section 4.2.1 (Wang et al., 2024). We begin by introducing the

setup and notation for CRTs.

Consider a trial with K clusters indexed by $i = 1, \dots, K$, where a cluster i contains N_i individuals. All individuals within each cluster receive the same binary treatment assignment $A_i \in \{0, 1\}$, where $A_i = 1$ denotes treatment and $A_i = 0$ denotes control. For each individual $j = 1, \dots, N_i$ in cluster i , we denote the potential outcomes as $Y_{ij}(1) \in \mathcal{Y}$ (under treatment) and $Y_{ij}(0) \in \mathcal{Y}$ (under control). The available covariates are $C_i \in \mathcal{C}$ (cluster-level) and $X_{ij} \in \mathcal{X}$ (individual-level).

To embed this CRT setting within our framework, we define the entire trial as $Z = (Z_1^\top, \dots, Z_K^\top)^\top$. The complete data for each cluster is given by $Z_i = (Z_1^{(i)}, \dots, Z_{N_i}^{(i)})^\top$, and the complete data for each individual is $Z_j^{(i)} = (Y_{ij}(1), Y_{ij}(0), X_{ij}, C_i)$. The data is assumed to satisfy the \mathcal{G} -distributional invariance discussed in Section 4.2.1. The observed data Z_{obs} consist of all covariates and the outcomes $Y_{ij}(A_i)$ observed under each individual's assigned treatment $A = (A_1, \dots, A_K)$:

$$\text{obs}(Z) = ((Y_{ij}(A_i), X_{ij}, C_i))_{1 \leq i \leq K, 1 \leq j \leq N_i}^\top.$$

We now demonstrate how to construct prediction sets for both individual- and cluster-level treatment effects.

Individual-level treatment effect. Our objective is to construct a prediction set for the individual treatment effect $\Delta_{mn} := Y_{mn}(1) - Y_{mn}(0)$ for individual n in cluster m . Since we observe $Y_{mn}(A_m)$, this requires constructing a prediction set for the unobserved potential outcome $Y_{mn}(1 - A_m)$.

We begin by defining the non-conformity scores. Assume we are given two pretrained models, $\hat{\mu}_a : \mathcal{X} \times \mathcal{C} \rightarrow \mathcal{Y}$ for $a \in \{0, 1\}$, which predict the potential outcome under each treatment assignment based on covariates. For the complete data vector Z , we define the transformation $V_a(Z)$ for each treatment assignment $a \in \{0, 1\}$ as the vector of absolute residuals:

$$V_a(Z) := (S_{ij}(a))_{1 \leq i \leq K, 1 \leq j \leq N_i}^\top := (|Y_{ij}(a) - \hat{\mu}_a(X_{ij}, C_i)|)_{1 \leq i \leq K, 1 \leq j \leq N_i}^\top.$$

Among these scores, $S_{ij}(A_i)$ is a known quantity computed from the observed data, whereas $S_{ij}(1 - A_i)$ is unknown. Under Assumptions 4.1, 4.2, and 4.3, this transformation V_a is \mathcal{G} -deterministically equivariant for $a \in \{0, 1\}$, preserving the group symmetry required by our framework. To focus on the individual (m, n) , we define the test function ψ to extract the corresponding non-conformity score for $a \in \{0, 1\}$:

$$\psi(V_a(Z)) := S_{mn}(a) := |Y_{mn}(a) - \hat{\mu}_a(X_{mn}, C_m)|.$$

To construct the adaptive threshold for the unobserved potential outcome $Y_{mn}(1 - A_m)$, we leverage the non-conformity scores from clusters that received treatment assignment $1 - A_m$. Let $a^* = 1 - A_m$ be the unobserved treatment assignment for individual (m, n) , and let $\mathcal{I}_{a^*} = \{1 \leq i \leq K : A_i = a^*\}$ denote the set of clusters that received this treatment. Similar to the approach in Section 4.2.2, we restrict the threshold function to the covariate space $\mathcal{X} \times \mathcal{C}$. For computational efficiency, we extract individual n from cluster m and treat it as a singleton cluster containing only that individual. This leads to the following optimization problem analogous to (4.3):

$$\hat{t}_Z(\cdot) = \underset{t(\cdot) \in \{\mathcal{X} \times \mathcal{C} \rightarrow \mathbb{R}\}}{\text{argmin}} \frac{1}{|\mathcal{I}_{a^*}| + 1} \left\{ \sum_{i \in \mathcal{I}_{a^*}} \frac{1}{N_i} \sum_{j=1}^{N_i} \ell_\alpha(t(X_{ij}, C_i), S_{ij}(a^*)) + \ell_\alpha(t(X_{mn}, C_m), S_{mn}(a^*)) \right\} + \mathcal{R}(t).$$

The scores $S_{ij}(a^*)$ for $i \in \mathcal{I}_{a^*}$ are known (as $A_i = a^*$), while the score $S_{mn}(a^*)$ is the unknown quantity associated with individual (m, n) . This adaptive threshold allows us to define a prediction set for the potential outcome $Y_{mn}(1 - A_m)$:

$$\hat{C}_{mn}(1 - A_m) = \{y \in \mathbb{R} : |y - \hat{\mu}_{1-A_m}(X_{mn}, C_m)| \leq \hat{t}_Z(X_{mn}, C_m)\}.$$

To construct the final prediction set for $\Delta_{mn} = Y_{mn}(1) - Y_{mn}(0)$, we utilize the observed potential outcome $Y_{mn}(A_m)$ and the prediction set $\hat{C}_{mn}(1 - A_m)$ for the unobserved potential outcome $Y_{mn}(1 - A_m)$.

The C-SymmPI prediction set for Δ_{mn} is therefore defined as

$$T^{\text{C-SymmPI}}(Z_{\text{obs}}) = \begin{cases} \widehat{C}_{mn}(1) - Y_{mn}(0), & \text{if } A_m = 0, \\ Y_{mn}(1) - \widehat{C}_{mn}(0), & \text{if } A_m = 1. \end{cases}$$

By Corollary 3.1, this prediction set satisfies a corresponding near-conditional coverage guarantee; the formal statement is omitted for brevity. This provides a stronger guarantee compared to existing methods for constructing prediction sets for treatment effects in CRTs (Lee et al., 2023; Dobriban and Yu, 2024; Wang et al., 2024), which only ensure marginal coverage. Appendix F provides a computationally efficient algorithm for constructing this prediction set.

Cluster-Level Treatment Effect. We now relax the within-cluster exchangeability Assumption 4.2 and construct a prediction set for the cluster-level treatment effect. This approach aggregates all information to the cluster level. First, we define the cluster-average potential outcome $\bar{Y}_i(a) = \sum_{j=1}^{N_i} Y_{ij}(a)/N_i$ for $a \in \{0, 1\}$ and the corresponding average covariate $\bar{X}_i = \sum_{j=1}^{N_i} X_{ij}/N_i$. The complete data Z then consist of the cluster-level tuples $(\bar{Y}_i(0), \bar{Y}_i(1), \bar{X}_i, C_i)_{1 \leq i \leq K}$. Consequently, the observation function reveals the observed tuples $(\bar{Y}_i(A_i), \bar{X}_i, C_i)_{1 \leq i \leq K}$.

Our objective is to construct a prediction set for $\Delta_m = \bar{Y}_m(1) - \bar{Y}_m(0)$. The methodology proceeds analogously to the individual-level case. We first define cluster-level non-conformity scores $S_i(a) = |\bar{Y}_i(a) - \widehat{\mu}_a(\bar{X}_i, C_i)|$ using pretrained models $\widehat{\mu}_a$. An adaptive threshold $\widehat{t}_Z(\cdot)$ is then constructed by solving the function-based quantile regression, using the observed scores $S_i(1 - A_m)$ from clusters $i \in \mathcal{I}_{1-A_m}$. The final prediction set for Δ_m is formed by combining the observed outcome $\bar{Y}_m(A_m)$ with the prediction set for the unobserved outcome, $\widehat{C}_m(1 - A_m)$. By Theorem 3.1, the resulting C-SymmPI prediction set for Δ_m satisfies a near-conditional coverage guarantee, providing a stronger assurance than existing marginal coverage results in the literature (Wang et al., 2024). Appendix F provides a computationally efficient algorithm for constructing this prediction set.

4.3 Network-Structured Data

We also consider settings in which the data exhibit a jointly exchangeable network structure, following the framework of Lunde et al. (2023). Due to space limitations, we defer the relevant discussion and results to Appendix C. Furthermore, in Appendix C.3, we extend our analysis to more general network models that do not satisfy joint exchangeability.

5 Experiments

We evaluate C-SymmPI through a simulation on a hierarchical model and two real-world applications: the PPACT cluster randomized trial and the Cora citation network. These experiments demonstrate the advantages of our method over existing benchmarks in constructing valid and adaptive prediction intervals.

5.1 Numerical Simulation

Data-generating process. We consider a supervised learning task from a hierarchical model with $K = 5$ clusters, as described in Section 4.2.2. For each cluster $i \in \{1, \dots, K\}$, the number of samples N_i is drawn from $\text{Poisson}(100)$. The covariates are drawn i.i.d. as $X_j^{(i)} \sim \text{Unif}([-0.5, 0.5])$. The response $Y_j^{(i)}$ is generated from a linear heterogeneous model:

$$Y_j^{(i)} = X_j^{(i)} \cdot (\theta_i + \varepsilon_j^{(i)}),$$

where $\theta_i \sim \mathcal{N}(0, \sigma_\theta^2 = 1.0^2)$ are the slopes for each cluster, and $\varepsilon_j^{(i)} \sim \mathcal{N}(0, \sigma_\varepsilon^2 = 0.5^2)$ are independent noise terms for each individual. This model exhibits covariate-dependent heterogeneity, since the conditional

variance of the response is a function of the covariate:

$$\text{Var}\left(Y_j^{(i)}|X_j^{(i)}\right) = (X_j^{(i)})^2(\sigma_\theta^2 + \sigma_\varepsilon^2).$$

The task is to construct a prediction interval for a new response $Y_{n_K}^{(K)}$ from a test covariate $X_{n_K}^{(K)}$ in the K -th cluster.

Methods for comparison. We compare the performance of our proposed C-SymmPI with several benchmarks. For all methods, we use linear regression predictors, and we set the target miscoverage level to $\alpha = 0.1$.

- (i) **Standard Split-CP¹⁴**: Since standard split conformal prediction does not account for hierarchical structure, we pool all training data from all clusters to fit a single predictor $\hat{\mu}$. We also pool all calibration data from all clusters into one set. We then compute a standard split conformal interval using the residuals from the pooled predictor as scores.
- (ii) **Standard Conditional-CP**: This method applies the conditional calibration technique of [Gibbs et al. \(2025\)](#) to the pooled data. It uses the residuals from the single pooled predictor as scores and computes an adaptive interval using function-based quantile regression.
- (iii) **Single-Tree Split-CP**: This benchmark uses only the training and calibration data from the target cluster $i = K$. It computes a standard split conformal interval using the cluster-specific predictor $\hat{\mu}_K$. While this respects the local data distribution, it suffers from a small effective sample size.
- (iv) **Single-Tree Conditional-CP**: This method is the conditional counterpart to the single-tree split conformal approach. It uses only the data from the target cluster K and applies conditional calibration to compute an adaptive interval.
- (v) **SymmPI**: Proposed by [Dobriban and Yu \(2024\)](#). This method computes residuals using per-cluster predictors and then pools these scores from all clusters. A constant-width interval is constructed based on the weighted quantile of the pooled scores.
- (vi) **C-SymmPI**: Our proposed method. We first compute non-conformity scores using per-cluster predictors trained on each cluster’s data. Next, we pool the calibration scores from all clusters into a unified, symmetry-aware calibration set. Finally, we apply the conditional calibration technique to this set and compute an adaptive quantile via function-based quantile regression.

Experimental details. We evaluate the proposed procedure over $N_{\text{trials}} = 40$ independent trials, each consisting of $N_{\text{reps}} = 100$ repetitions with independently generated datasets. For each of the K clusters, the dataset $\mathcal{D}^{(i)} = \{(X_j^{(i)}, Y_j^{(i)})\}_{j=1}^{N_i}$ is randomly split in a 50/50 ratio into a training set $\mathcal{D}_{\text{train}}^{(i)}$ and a calibration set $\mathcal{D}_{\text{cal}}^{(i)}$. The training set is used to fit linear regression models. The calibration set is used to compute non-conformity scores and to construct prediction intervals for $Y_{n_K}^{(K)}$. For the function-based quantile regression, we employ an RKHS with a Gaussian kernel of length scale $L = 0.1$ and regularization parameter $\lambda = 0.005$.

We compute the *average empirical coverage* and *average interval length* for prediction intervals over the 100 repetitions. The final table reports the mean and standard deviation of these 40 trial-level averages. To assess conditional coverage, we report the empirical coverage and average interval length both marginally and conditionally on regions of the covariate space that represent different levels of variance: $R_1 = \{x : |x| \leq 0.1\}$, $R_2 = \{x : 0.1 < |x| \leq 0.3\}$, and $R_3 = \{x : 0.3 < |x| \leq 0.5\}$.

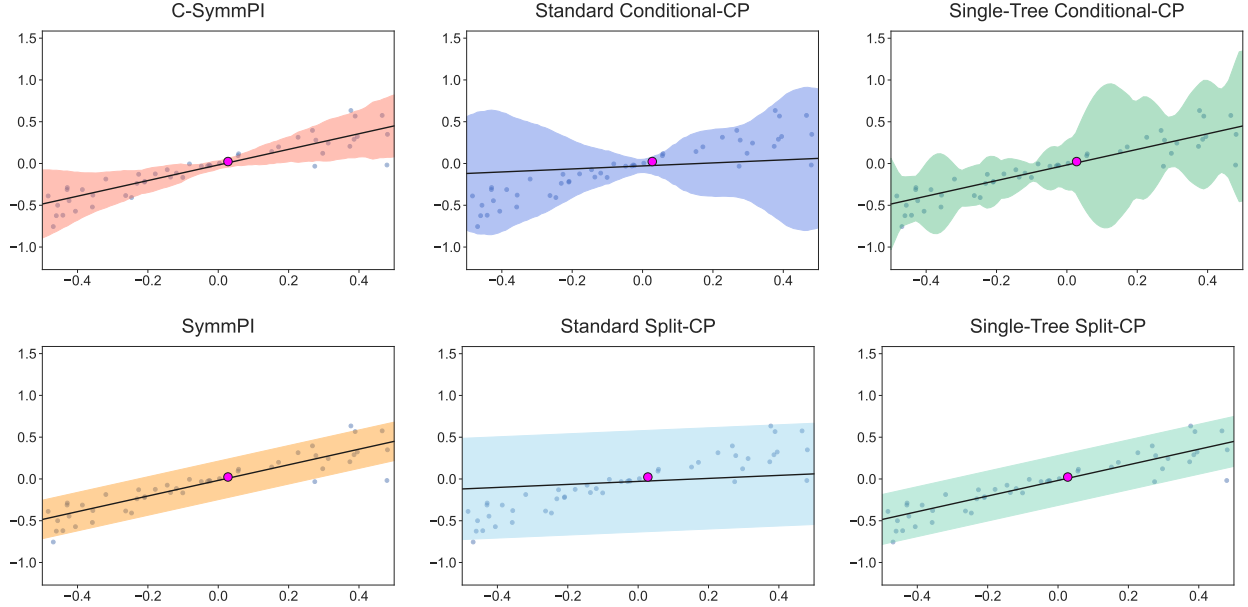


Figure 2: Visual comparison of 90% prediction intervals for a single test point (magenta dot) from one cluster of the simulated linear heterogeneous model. **Top row:** Methods adaptive to the covariate $X_{nK}^{(K)}$. **Bottom row:** Constant-width methods. **Left column:** SymmPI methods that are adaptive to the hierarchical structure. **Center column:** Standard conformal methods that pool all data naively. **Right column:** Single-tree methods that use data only from the target cluster. **Top left:** C-SymmPI produces a tight, adaptive interval by leveraging the hierarchical group symmetry and the full calibration set.

Results and discussion. Figure 2 provides a visual comparison of the six methods on a single realization of the data, and Table 2 summarizes the average empirical coverage and average interval length across all simulation trials.

As demonstrated in Table 2, our proposed C-SymmPI method outperforms the marginal-only methods, which produce constant-width intervals and suffer from two key deficiencies. First, they exhibit significant under-coverage in high-variance regions; for instance, SymmPI (Dobriban and Yu, 2024) achieves an empirical coverage of only 0.764 in region R_3 , which is below the target 0.9 level. Second, they are overly conservative in low-variance regions, producing unnecessarily wide intervals; for instance, in region R_1 , SymmPI has an average interval length of 0.59, whereas C-SymmPI achieves a tighter interval of length 0.13 while maintaining valid coverage of 0.932.

C-SymmPI also outperforms other conditional methods. The standard conditional approach ignores the hierarchical structure, resulting in wider intervals with an average length of 0.71, compared to 0.46 for C-SymmPI. Conversely, the single-tree conditional method uses only local data, which leads to small sample sizes and thus inefficient, overly conservative intervals with an average length of 0.91, compared to 0.46 for C-SymmPI. Moreover, as seen in Figure 2, the single-tree conditional intervals are visibly less stable than those from C-SymmPI.

5.2 Real Data Applications

5.2.1 PPACT Cluster Randomized Trial

The Pain Program for Active Coping and Training (PPACT) study is a CRT designed to evaluate a care-based cognitive behavioral therapy (CBT) intervention for long-term opioid users with chronic pain (DeBar

¹⁴Here, “CP” stands for “conformal prediction”.

Region	Method	Interval Length	Coverage Probability
Overall	C-SymmPI	0.46 (0.28)	0.917 (0.056)
	SymmPI	0.59 (0.01)	0.910 (0.111)
	Standard Conditional-CP	0.71 (0.44)	0.909 (0.052)
	Standard Split-CP	1.02 (0.06)	0.924 (0.100)
	Single-Tree Conditional-CP	0.91 (0.29)	0.982 (0.024)
	Single-Tree Split-CP	0.71 (0.03)	0.939 (0.085)
$0.0 \leq x \leq 0.1$	C-SymmPI	0.13 (0.01)	0.932 (0.062)
	SymmPI	0.59 (0.01)	1.000 (0.000)
	Standard Conditional-CP	0.20 (0.03)	0.938 (0.056)
	Standard Split-CP	1.02 (0.08)	1.000 (0.000)
	Single-Tree Conditional-CP	0.63 (0.09)	0.994 (0.016)
	Single-Tree Split-CP	0.70 (0.03)	1.000 (0.000)
$0.1 < x \leq 0.3$	C-SymmPI	0.42 (0.02)	0.920 (0.051)
	SymmPI	0.59 (0.01)	0.967 (0.028)
	Standard Conditional-CP	0.67 (0.04)	0.903 (0.041)
	Standard Split-CP	1.01 (0.05)	0.980 (0.018)
	Single-Tree Conditional-CP	0.81 (0.06)	0.975 (0.024)
	Single-Tree Split-CP	0.71 (0.02)	0.983 (0.022)
$0.3 < x \leq 0.5$	C-SymmPI	0.82 (0.02)	0.898 (0.048)
	SymmPI	0.59 (0.01)	0.764 (0.062)
	Standard Conditional-CP	1.27 (0.05)	0.887 (0.045)
	Standard Split-CP	1.01 (0.04)	0.792 (0.058)
	Single-Tree Conditional-CP	1.29 (0.06)	0.975 (0.025)
	Single-Tree Split-CP	0.71 (0.03)	0.833 (0.066)

Table 2: Comparison of average prediction interval length and empirical coverage probability for the two-layer linear heterogeneous model with 90% target coverage. Interval length and coverage probability are evaluated marginally and conditionally on three disjoint covariate regions. We display the average and the standard error over 40 independent trials.

et al., 2022). This dataset was previously analyzed by Wang et al. (2024), who proposed the Split-CCI method.¹⁵ Following their experimental setup, our goal is to construct confidence intervals for both cluster-level and individual-level treatment effects using C-SymmPI, and to compare its performance with that of the Split-CCI method.

Experimental details. The PPACT study randomized 106 primary care providers (clusters) to either the CBT intervention or usual care. The dataset includes 1 to 10 participants per cluster. Our analysis focuses on the primary outcome: the PEGS (pain intensity and interference with enjoyment of life, general activity, and sleep) score at 12 months, which is a continuous measure of pain intensity and interference on a scale from 1 to 10. We adjust for a set of 13 individual-level baseline variables: baseline PEGS score (Y_0), age, gender, disability, smoking status, body mass index, alcohol abuse, drug abuse, comorbidity, depression, number of pain types, average morphine dose, and heavy opioid usage.

We conduct 100 independent trials. In each trial, 20 clusters are held out as a test set, while the remaining 86 clusters are evenly split into training and calibration sets, stratified by the intervention arm A . We implement the C-SymmPI method described in Section 4.2.3, using the efficient computation strategy

¹⁵Here, “CCI” stands for “conformal causal inference”.

α	Method	Cluster-level Treatment Effect		Individual-level Treatment Effect	
		Interval Length	Negative Fraction	Interval Length	Negative Fraction
0.10	C-SymmPI	3.968(0.019)	0.143(0.008)	4.391(0.009)	0.180(0.003)
	Split-CCI	4.056(0.557)	0.089(0.069)	6.908(0.590)	0.055(0.026)
0.20	C-SymmPI	3.354(0.023)	0.204(0.009)	3.816(0.009)	0.225(0.004)
	Split-CCI	2.874(0.412)	0.173(0.092)	4.800(0.345)	0.132(0.044)
0.30	C-SymmPI	2.861(0.025)	0.261(0.010)	3.293(0.009)	0.270(0.004)
	Split-CCI	2.233(0.313)	0.238(0.104)	3.811(0.220)	0.199(0.052)
0.40	C-SymmPI	2.443(0.024)	0.319(0.010)	2.800(0.009)	0.314(0.004)
	Split-CCI	1.799(0.255)	0.304(0.117)	3.108(0.189)	0.257(0.055)

Table 3: Comparison of treatment effects for the C-SymmPI and Split-CCI methods (Wang et al., 2024). For both the length of intervals and the fraction, we display the average and standard error over 100 independent trials.

detailed in Appendix F. The predictor $\hat{\mu}_a$ is specified as an ensemble learner combining linear regression and random forest models. We condition on the baseline PEGS score Y_0 , which serves as an important determinant of the 12-month outcome. We employ an RKHS with a Gaussian kernel of length scale $L = 0.1$ and regularization parameter $\lambda = 0.01$.

We report the average and standard error for two performance metrics: *length of intervals* and *fraction of negatives*. Here, the fraction of negatives is the proportion of conformal intervals that are subsets of $(-\infty, 0)$ among the test data. Since negative values indicate treatment benefits, this metric reveals how many clusters or individuals are associated with beneficial treatment effects with probability $1 - \alpha$. A higher fraction of negatives indicates a more effective method for identifying treatment benefits.

Results and discussion. Table 3 summarizes the performance of C-SymmPI and the Split-CCI benchmark for both cluster-level and individual-level treatment effects across four target coverage levels $1 - \alpha$. At the cluster level, when $\alpha = 0.10$, C-SymmPI attains a higher fraction of negatives (0.143 vs. 0.089) while keeping the interval length similar to that of the Split-CCI method (3.968 vs. 4.056). At the individual level, C-SymmPI attains both shorter intervals and a higher fraction of negatives compared to the Split-CCI method across all target coverage levels. The improvement is particularly obvious for $\alpha = 0.10$, where C-SymmPI achieves an average interval length of 4.391 (compared to 6.908) and a negative fraction of 0.180 (compared to 0.055). In both cluster-level and individual-level analyses, C-SymmPI attains a lower standard deviation for both metrics, indicating more stable performance across trials.

The left panel of Figure 3 presents the 90% prediction intervals for cluster 145 and four of its individuals. The top panel shows that the cluster-level interval contains zero, indicating no statistically significant aggregate effect. The bottom panel reveals individual-level heterogeneity: the interval for individual 145-3 lies entirely below zero, indicating a statistically significant beneficial treatment effect. This highlights the importance of analyzing individual-level effects, which C-SymmPI is designed to capture more effectively. The middle and right panels of Figure 3 display the distributions of interval lengths across all clusters and individuals, respectively. This illustrates the adaptivity of our method, as interval lengths vary with the underlying uncertainty for different individuals and clusters.

5.2.2 Network-Assisted Classification on Cora Dataset

In this subsection, we study the network dataset (Cora dataset) consists of 2708 machine learning papers categorized into 7 research topics (McCallum et al., 2000). It includes the contents of the papers and a

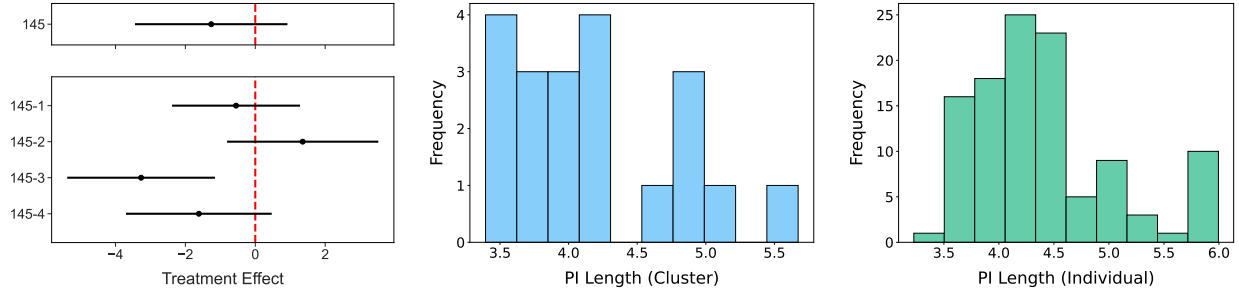


Figure 3: **Left:** 90% prediction intervals for the treatment effects of cluster 145 and its individuals. **Middle:** Distribution of cluster-level treatment-effect interval lengths across all clusters. **Right:** Distribution of individual-level treatment-effect interval lengths across all individuals.

citation network, which are represented by a document-word matrix and an adjacency matrix, respectively. Leveraging these features, we consider the task of predicting whether a paper belongs to the “Neural Networks” category. This classification problem was also studied by Lunde et al. (2023), who applied split conformal prediction to network-assisted models. We illustrate our C-SymmPI method for this problem and compare its performance with standard split conformal prediction. Due to space limitations, we defer the details to Section C.2.

6 Discussion

We propose C-SymmPI, a distribution-free method that strengthens marginal guarantees to near-conditional guarantees for data with symmetries. This is achieved by learning an adaptive threshold that keeps a function-weighted average of coverage errors small. We prove fast convergence rates for linear function spaces and RKHSs. We also provide computationally efficient variants that work with high-dimensional observation spaces and infinite groups. Our method recovers the globally exchangeable setting and extends to hierarchical and network data, where our studies show that it yields more adaptive and robust prediction intervals than prior methods. For future work, it would be interesting to learn a deterministic equivariant map V beyond the non-conformity scores used in this paper, and to explore how such a map could further improve adaptivity.

References

- Ai, J. and Ren, Z. (2024). Not all distributional shifts are equal: Fine-grained robust conformal inference. *arXiv preprint arXiv:2402.13042*.
- Angelopoulos, A. N., Barber, R. F., and Bates, S. (2024). Theoretical foundations of conformal prediction. *arXiv preprint arXiv:2411.11824*.
- Angelopoulos, A. N. and Bates, S. (2021). A gentle introduction to conformal prediction and distribution-free uncertainty quantification. *arXiv preprint arXiv:2107.07511*.
- Artin, M. (2018). *Algebra*. Pearson, 2nd edition.
- Barber, R. F. (2020). Is distribution-free inference possible for binary regression?
- Barber, R. F., Candès, E. J., Ramdas, A., and Tibshirani, R. J. (2023). Conformal prediction beyond exchangeability. *The Annals of Statistics*, 51(2):816–845.

- Bian, M. and Barber, R. F. (2023). Training-conditional coverage for distribution-free predictive inference. *Electronic Journal of Statistics*, 17(2):2044–2066.
- Bickel, P. J. and Chen, A. (2009). A nonparametric view of network models and newman–girvan and other modularities. *Proceedings of the National Academy of Sciences*, 106(50):21068–21073.
- Bousquet, O. and Elisseeff, A. (2002). Stability and generalization. *J. Mach. Learn. Res.*, 2:499–526.
- Chernozhukov, V., Wüthrich, K., and Yinchu, Z. (2018). Exact and robust conformal inference methods for predictive machine learning with dependent data. In *Conference On learning theory*, pages 732–749. PMLR.
- Chernozhukov, V., Wüthrich, K., and Zhu, Y. (2021). Distributional conformal prediction. *Proceedings of the National Academy of Sciences*, 118(48):e2107794118.
- DeBar, L., Mayhew, M., Benes, L., Bonifay, A., Deyo, R. A., Elder, C. R., Keefe, F. J., Leo, M. C., McMullen, C., Owen-Smith, A., et al. (2022). A primary care–based cognitive behavioral therapy intervention for long-term opioid users with chronic pain: a randomized pragmatic trial. *Annals of Internal Medicine*, 175(1):46–55.
- Diaconis, P. (1988). Group representations in probability and statistics. *Lecture notes-monograph series*, 11:i–192.
- Diestel, J. and Spalsbury, A. (2014). *The joys of Haar measure*. American Mathematical Soc.
- Dixon, J. D. and Mortimer, B. (1996). *Permutation groups*, volume 163. Springer Science & Business Media.
- Dobriban, E. and Yu, M. (2024). Symmpi: Predictive inference for data with group symmetries.
- Duchi, J. C. (2025). A few observations on sample-conditional coverage in conformal prediction.
- Dunn, R., Wasserman, L., and Ramdas, A. (2023). Distribution-free prediction sets for two-layer hierarchical models. *Journal of the American Statistical Association*, 118(544):2491–2502.
- Finzi, M., Stanton, S., Izmailov, P., and Wilson, A. G. (2020). Generalizing convolutional neural networks for equivariance to lie groups on arbitrary continuous data. In *International conference on machine learning*, pages 3165–3176. PMLR.
- Foygel Barber, R., Candès, E. J., Ramdas, A., and Tibshirani, R. J. (2021). The limits of distribution-free conditional predictive inference. *Information and Inference: A Journal of the IMA*, 10(2):455–482.
- Gibbs, I. and Candès, E. J. (2025). Characterizing the training-conditional coverage of full conformal inference in high dimensions. *arXiv preprint arXiv:2502.20579*.
- Gibbs, I., Cherian, J. J., and Candès, E. J. (2025). Conformal prediction with conditional guarantees. *Journal of the Royal Statistical Society Series B: Statistical Methodology*, page qkaf008.
- Gilmer, J., Schoenholz, S. S., Riley, P. F., Vinyals, O., and Dahl, G. E. (2017). Neural message passing for quantum chemistry. In *International conference on machine learning*, pages 1263–1272. Pmlr.
- Giri, N. C. (1996). *Group invariance in statistical inference*. World Scientific.
- Guan, L. (2023). Localized conformal prediction: A generalized inference framework for conformal prediction. *Biometrika*, 110(1):33–50.
- Hébert-Johnson, U., Kim, M., Reingold, O., and Rothblum, G. (2018). Multicalibration: Calibration for the (computationally-identifiable) masses. In *International Conference on Machine Learning*, pages 1939–1948. PMLR.

- Hore, R. and Barber, R. F. (2024). Conformal prediction with local weights: randomization enables local guarantees.
- Huang, K., Jin, Y., Candes, E., and Leskovec, J. (2023). Uncertainty quantification over graph with conformalized graph neural networks. *Advances in Neural Information Processing Systems*, 36:26699–26721.
- Kim, M. P., Ghorbani, A., and Zou, J. (2019). Multiaccuracy: Black-box post-processing for fairness in classification. In *Proceedings of the 2019 AAAI/ACM Conference on AI, Ethics, and Society*, pages 247–254.
- Koenker, R. and Bassett Jr, G. (1978). Regression quantiles. *Econometrica: journal of the Econometric Society*, pages 33–50.
- LeCun, Y., Boser, B., Denker, J. S., Henderson, D., Howard, R. E., Hubbard, W., and Jackel, L. D. (1989). Backpropagation applied to handwritten zip code recognition. *Neural computation*, 1(4):541–551.
- Lee, Y. and Barber, R. (2021). Distribution-free inference for regression: discrete, continuous, and in between. *Advances in Neural Information Processing Systems*, 34:7448–7459.
- Lee, Y., Barber, R. F., and Willett, R. (2023). Distribution-free inference with hierarchical data. *arXiv preprint arXiv:2306.06342*.
- Lee, Y. and Ren, Z. (2025). Conditional predictive inference with l^k -coverage control.
- Liang, R. and Barber, R. F. (2025). Algorithmic stability implies training-conditional coverage for distribution-free prediction methods. *The Annals of Statistics*, 53(4):1457–1482.
- Lunde, R., Levina, E., and Zhu, J. (2023). Conformal prediction for network-assisted regression.
- Ma, Z., Ma, Z., and Yuan, H. (2020). Universal latent space model fitting for large networks with edge covariates. *Journal of Machine Learning Research*, 21(4):1–67.
- Manski, C. F. (1993). Identification of endogenous social effects: The reflection problem. *The review of economic studies*, 60(3):531–542.
- McCallum, A. K., Nigam, K., Rennie, J., and Seymore, K. (2000). Automating the construction of internet portals with machine learning. *Information Retrieval*, 3(2):127–163.
- Medarametla, D. and Candes, E. (2021). Distribution-free conditional median inference. *Electronic Journal of Statistics*, 15(2):4625–4658.
- Nachbin, L. (1976). The haar integral, re kriegler pub.
- Papadopoulos, H., Proedrou, K., Vovk, V., and Gammerman, A. (2002). Inductive confidence machines for regression. In *European conference on machine learning*, pages 345–356. Springer.
- Park, S., Dobriban, E., Lee, I., and Bastani, O. (2021). Pac prediction sets under covariate shift. *arXiv preprint arXiv:2106.09848*.
- Park, S., Dobriban, E., Lee, I., and Bastani, O. (2022). Pac prediction sets for meta-learning. *Advances in neural information processing systems*, 35:37920–37931.
- Qiu, H., Dobriban, E., and Tchetgen Tchetgen, E. (2023). Prediction sets adaptive to unknown covariate shift. *Journal of the Royal Statistical Society Series B: Statistical Methodology*, 85(5):1680–1705.
- Romano, Y., Patterson, E., and Candes, E. (2019). Conformalized quantile regression. *Advances in neural information processing systems*, 32.

- Romano, Y., Sesia, M., and Candes, E. (2020). Classification with valid and adaptive coverage. *Advances in neural information processing systems*, 33:3581–3591.
- Schölkopf, B., Herbrich, R., and Smola, A. J. (2001). A generalized representer theorem. In *International conference on computational learning theory*, pages 416–426. Springer.
- Shafer, G. and Vovk, V. (2008). A tutorial on conformal prediction. *Journal of Machine Learning Research*, 9(3).
- Si, W., Park, S., Lee, I., Dobriban, E., and Bastani, O. (2023). Pac prediction sets under label shift. *arXiv preprint arXiv:2310.12964*.
- Tibshirani, R. J., Foygel Barber, R., Candes, E., and Ramdas, A. (2019). Conformal prediction under covariate shift. *Advances in neural information processing systems*, 32.
- Vovk, V. (2012). Conditional validity of inductive conformal predictors. In *Asian conference on machine learning*, pages 475–490. PMLR.
- Vovk, V., Gammerman, A., and Shafer, G. (2005). *Algorithmic learning in a random world*. Springer.
- Wang, B., Li, F., and Yu, M. (2024). Conformal causal inference for cluster randomized trials: Model-robust inference without asymptotic approximations. *arXiv preprint arXiv:2401.01977*.
- Xie, R., Barber, R., and Candes, E. (2024). Boosted conformal prediction intervals. *Advances in Neural Information Processing Systems*, 37:71868–71899.
- Xu, K., Li, C., Tian, Y., Sonobe, T., Kawarabayashi, K.-i., and Jegelka, S. (2018). Representation learning on graphs with jumping knowledge networks. In *International conference on machine learning*, pages 5453–5462. pmlr.
- Yang, Y., Kuchibhotla, A. K., and Tchetgen Tchetgen, E. (2024). Doubly robust calibration of prediction sets under covariate shift. *Journal of the Royal Statistical Society Series B: Statistical Methodology*, 86(4):943–965.
- Zhang, Y. and Candès, E. J. (2024). Posterior conformal prediction.

Roadmap for the Appendix

This appendix is organized as follows. In Section A, we provide a brief review of group-theoretic concepts that are essential for understanding the SymmPI framework. In Section B, we present an additional example of the SymmPI framework involving network-structured data. In Section C, we apply the SymmPI framework to a real-world network dataset. In Section D, we provide an RKHS-based analysis of the C-SymmPI method. In Section E, we discuss the details of the **S**ampled C-SymmPI variant. In Section F, we discuss computational strategies for efficiently implementing the C-SymmPI method in practice. Finally, in Section G, we provide detailed proofs of the theoretical results stated in the main text.

A Review of Group Theory

A *group* is a set \mathcal{G} equipped with a binary operation $\cdot : \mathcal{G} \times \mathcal{G} \rightarrow \mathcal{G}$ ¹⁶ that satisfies three axioms: (i) *Associativity*: for all $g, g', g'' \in \mathcal{G}$, $(gg')g'' = g(g'g'')$; (ii) *Identity element*: there exists an element $e \in \mathcal{G}$ such that for every $g \in \mathcal{G}$, $eg = ge = g$; (iii) *Inverse element*: for each $g \in \mathcal{G}$, there exists an element $g^{-1} \in \mathcal{G}$ such that $gg^{-1} = g^{-1}g = e$. For example, symmetric group S_n is the group of all permutations on a set of n elements. The group operation is the composition of functions (\circ). The identity element is the identity map (i.e., the permutation that leaves all elements fixed), and the inverse of a permutation is its functional inverse.

A group \mathcal{G} can act on a set \mathcal{Z} through a *group action*, which is a map $\rho : \mathcal{G} \times \mathcal{Z} \rightarrow \mathcal{Z}$ satisfying two conditions for all $g, g' \in \mathcal{G}$ and $z \in \mathcal{Z}$: (i) $\rho(gg', z) = \rho(g, \rho(g', z))$; and (ii) $\rho(e, z) = z$. Throughout this paper, we use the simplified notations $\rho(g)z$ and $g \cdot z$ interchangeably for $\rho(g, z)$. For example, the symmetric group S_n acts on a space \mathcal{Z}_0^n by permuting the coordinates of its elements. For any $g \in S_n$ and $z = (z_1, \dots, z_n)^\top \in \mathcal{Z}_0^n$, this permutation action is defined as

$$g \cdot z := \rho(g)z := (z_{g^{-1}(1)}, \dots, z_{g^{-1}(n)})^\top. \quad (\text{A.1})$$

Throughout this paper, we will use this permutation action whenever we consider an action of the symmetric group S_n .

Given a group action “ \cdot ” of \mathcal{G} on \mathcal{Z} , there is a natural induced action on a function $F : \mathcal{Z} \rightarrow \mathcal{W}$, defined by $(g \cdot F)(z) := F(g^{-1} \cdot z)$, where \mathcal{W} is another measurable space.¹⁸ The *orbit* of the function F is the set of all functions obtainable by acting on F , formally defined as

$$O_F := \{g \cdot F : g \in \mathcal{G}\}.$$

For example, define $F : \mathcal{Z}_0^n \rightarrow \mathcal{Z}_0$ as $F(z) = z_n$. The orbit of F under the permutation action of S_n is $O_F = \{F_1, \dots, F_n\}$, where $F_i(z) = z_i$ for $i = 1, \dots, n$. In other words, O_F consists of all coordinate projection functions.

The *stabilizer* of the function $F : \mathcal{Z} \rightarrow \mathcal{W}$ is the subgroup¹⁹ of \mathcal{G} that leaves F unchanged, formally defined as $\text{Stab}(F) := \{g \in \mathcal{G} : g \cdot F = F\}$, or equivalently,

$$\text{Stab}(F) = \{g \in \mathcal{G} : F(g \cdot z) = F(z), \forall z \in \mathcal{Z}\}.$$

Continuing the example above, for the function $F(z) = z_n$, the stabilizer of F under the permutation action of S_n is $\text{Stab}(F) = \{g \in S_n : g(n) = n\}$, which is isomorphic to S_{n-1} . Equivalently, $\text{Stab}(F)$ is the set of all permutations that fix the last coordinate.

¹⁶For brevity, the operation $g \cdot g'$ is often written simply as gg' .

¹⁷By definition, we have $(g_1 \cdot (g_2 \cdot z))_i = (g_2 \cdot z)_{g_1^{-1}(i)} = z_{g_2^{-1}(g_1^{-1}(i))} = z_{(g_1 g_2)^{-1}(i)}$. The second condition is trivial.

¹⁸By definition, $((g_1 g_2) \cdot F)(z) = F((g_1 g_2)^{-1} \cdot z) = F(g_2^{-1} \cdot (g_1^{-1} \cdot z)) = (g_1 \cdot (g_2 \cdot F))(z)$. Also, $(e \cdot F)(z) = F(e^{-1} \cdot z) = F(z)$. When there is no ambiguity, we use “ \cdot ” for both actions on \mathcal{Z} and on functions.

¹⁹A subset \mathcal{H} of \mathcal{G} is called a *subgroup* of \mathcal{G} , if \mathcal{H} also forms a group under the operation of \mathcal{G} .

There is a fundamental relationship between the orbit O_F and the stabilizer $\text{Stab}(F)$. To state it, we first introduce some additional concepts. Given $g \in \mathcal{G}$ and the subgroup $\text{Stab}(F)$, the (left) *coset* of $\text{Stab}(F)$ associated with g is defined as $g\text{Stab}(F) := \{gh : h \in \text{Stab}(F)\}$. Intuitively, a coset is a “bundle” of group elements that are indistinguishable in their effect on F , since all elements of the coset $g\text{Stab}(F)$ produce the same element of the orbit.²⁰ The set of all distinct cosets of $\text{Stab}(F)$ in \mathcal{G} is denoted by $\mathcal{G}/\text{Stab}(F) := \{g\text{Stab}(F) : g \in \mathcal{G}\}$. We are now ready to state the *orbit-stabilizer theorem*:

$$O_F \cong \mathcal{G}/\text{Stab}(F).$$

Here, “ \cong ” means that there exists a natural bijection. This theorem states that there is a one-to-one correspondence between the elements of the orbit and the cosets of the stabilizer subgroup. In particular, when \mathcal{G} is finite, it implies that

$$|O_F| = \frac{|\mathcal{G}|}{|\text{Stab}(F)|},$$

where $|\cdot|$ denotes the cardinality of a set. Continuing the previous example, since $|\mathbb{S}_n| = n!$ and $|\text{Stab}(F)| = (n-1)!$, the orbit O_F has size $|O_F| = n!/(n-1)! = n$, which aligns with our earlier observation that $O_F = \{F_1, \dots, F_n\}$.

Finally, a *Haar probability measure* U on a group \mathcal{G} formalizes the notion of a uniform distribution over its elements. Its key property is invariance under the group operation: if $G \sim U$ ²¹, then for any fixed $g \in \mathcal{G}$, we have $gG \sim U$ and $Gg \sim U$. Haar probability measures exist for a broad class of groups, including all finite groups and many common infinite groups (e.g., the rotation group).²² For any finite group, the Haar probability measure is the discrete uniform distribution over its elements. Throughout this paper, all groups we consider are equipped with their corresponding Haar probability measure.

To illustrate these concepts with a structure beyond global exchangeability, we consider a “nested” symmetric group (Dixon and Mortimer, 1996), which is relevant to two-layer hierarchical settings discussed in Section 4.2.

Example A.1. Suppose the data is a vector $Z = (Z_1^\top, \dots, Z_K^\top)^\top$ composed of K distinct clusters. Each cluster $Z_i = (Z_1^{(i)}, \dots, Z_n^{(i)})^\top$ in turn contains n data points for all $i = 1, \dots, K$.

The symmetries of this structure arise from a two-layer permutation mechanism: first, permuting the elements within each cluster, and second, permuting the clusters themselves. This hierarchical symmetry is formally represented by a “nested” symmetric group $\mathcal{G} := (\mathbb{S}_n)^K \rtimes \mathbb{S}_K$, which can be described as follows:

- (i) Each group element $g \in \mathcal{G}$ is a pair $((\sigma_1, \dots, \sigma_K), \pi)$, where $\sigma_i \in \mathbb{S}_n$ permutes the elements within the i -th cluster, and $\pi \in \mathbb{S}_K$ permutes the clusters themselves.
- (ii) The group operation between $g_1 = ((\sigma_1, \dots, \sigma_K), \pi)$ and $g_2 = ((\tau_1, \dots, \tau_K), \eta)$ is defined as $g_1 g_2 = ((\sigma_1 \tau_{\pi^{-1}(1)}, \dots, \sigma_K \tau_{\pi^{-1}(K)}), \pi \eta)$. In other words, the cluster permutation is directly given by composition, while the within-cluster permutations are composed after reordering according to the cluster permutation π .

The group action of $g = ((\sigma_1, \dots, \sigma_K), \pi) \in \mathcal{G}$ on the data vector Z proceeds in two stages: first, the clusters are permuted according to π , and then the elements within each cluster are permuted according to σ_i . Formally, this action is expressed as

$$\rho(g)Z := \pi \cdot (\sigma_1 \cdot Z_1^\top, \dots, \sigma_K \cdot Z_K^\top)^\top, \quad (\text{A.2})$$

where the symbol “ \cdot ” denotes the permutation action defined in (A.1).

²⁰Indeed, for any $h \in \text{Stab}(F)$, we have $(gh) \cdot F = g \cdot (h \cdot F) = g \cdot F$.

²¹The expression “ $G \sim U$ ” means that G is a random variable taking values in \mathcal{G} whose distribution is the Haar probability measure U .

²²Formally, any unimodular group admits a unique Haar probability measure that is both left- and right-invariant (Diestel and Spalsbury, 2014).

Suppose we are interested in the function $F : \mathcal{Z} \rightarrow \mathcal{Z}_0$ that extracts the last data point from the last cluster, i.e., $F(Z) = Z_n^{(K)}$. Because π can send any cluster $i \in [K]$ to the last cluster K , and within that cluster σ_i can send any element $j \in [n]$ to the last element n , the orbit consists of all coordinate projections: $O_F = \{F_j^{(i)}\}_{1 \leq i \leq K, 1 \leq j \leq n}$, where $F_j^{(i)}(Z) = Z_j^{(i)}$. The stabilizer $\text{Stab}(F)$ consists of all group elements that fix the last data point in the last cluster. Specifically, π must fix cluster K , and σ_K must fix element n . The other permutations $\sigma_1, \dots, \sigma_{K-1}$ can be arbitrary. Therefore, $\text{Stab}(F) \cong (\mathbb{S}_n)^{K-1} \times \mathbb{S}_{n-1} \times \mathbb{S}_{K-1}$. As a check, we can verify the orbit-stabilizer theorem:

$$\frac{|\mathcal{G}|}{|\text{Stab}(F)|} = \frac{(n!)^K \cdot K!}{(n!)^{K-1} \cdot (n-1)! \cdot (K-1)!} = Kn = |O_F|.$$

Finally, since \mathcal{G} is a finite group, its Haar probability measure corresponds to the uniform distribution over its elements. This allows us to define a probability space $(\mathcal{G}, 2^{\mathcal{G}}, U)$, which enables probabilistic analysis on the group.²³ \square

B Examples of the SymmPI Framework

The SymmPI framework introduced in Section 2.1 is highly general and accommodates a wide range of data structures and group actions, including network-structured data, rotationally invariant data, and two-layer hierarchical data. In this section, we present an additional example involving network-structured data to further demonstrate the versatility of the SymmPI framework. For further examples and a more detailed discussion, readers are referred to Dobriban and Yu (2024).

Problem setup. We consider an illustration of the SymmPI framework for random variables whose symmetries are characterized by a graph structure. Let $Z = (Z_1, \dots, Z_{n+1})^\top \in \mathcal{Z}_0^{n+1} =: \mathcal{Z}$. In this setting, we are given an undirected graph with adjacency matrix $A \in [0, \infty)^{(n+1) \times (n+1)}$. We assume the data Z is distributionally invariant under the automorphism group $\text{Aut}(A) \subseteq \mathbb{S}_{n+1}$ with the permutation action defined in (A.1). The elements of $\text{Aut}(A)$ are permutations g that satisfy $gAg^\top = A$ when viewed as linear maps $\mathbb{R}^{n+1} \rightarrow \mathbb{R}^{n+1}$. See Figure 4 for examples of the adjacency matrices of undirected graphs and their corresponding automorphism group actions. This framework generalizes the classical notion of exchangeability, which is recovered by taking the identity matrix $A = I_{n+1}$.

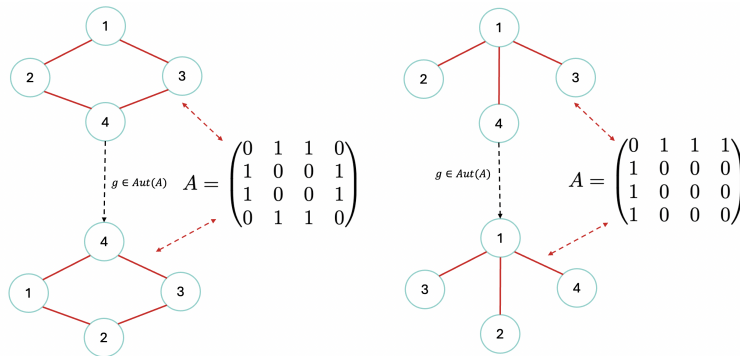


Figure 4: Examples of undirected graphs along with their adjacency matrices. Relabeling the vertices of a graph according to its automorphism group leaves the adjacency matrix unchanged. Adapted from Dobriban and Yu (2024).

²³Here, $2^{\mathcal{G}}$ denotes the power set of \mathcal{G} , representing the sigma-algebra of all subsets of \mathcal{G} .

Transformation. In machine learning, numerous graph neural network (GNN) architectures exhibiting deterministic equivariance have been developed, and a prominent class among them is the message-passing GNN (Gilmer et al., 2017; Xu et al., 2018). For a chosen depth L , we define the layers sequentially as $z^0 := z$ and z^1, \dots, z^L . For any $l \geq 0$ and any $i \in [n+1]$, the i -th coordinate of z^{l+1} is computed by first aggregating information from the neighborhood $N(i)$ of node i via a message function λ_1 , and then applying a node update function λ_0 :

$$z_i^{l+1} = \lambda_0 \left(z_i^l, \sum_{j \in N(i)} \lambda_1(z_i^l, z_j^l) \right) := F_l(z^l)_i.$$

The message-passing GNN is then defined as $\text{MPGNN}_L(z) := F_L \circ F_{L-1} \circ \dots \circ F_1(z)$ for all $z \in \mathcal{Z}$. Since all nodes apply the same functions and aggregate neighbor information using a permutation-invariant operation, relabeling the nodes only relabels the outputs without changing their values. Therefore, any message-passing GNN is $\text{Aut}(A)$ -deterministically equivariant under the permutation action defined in (A.1), i.e., $\text{MPGNN}_L(g \cdot z) = g \cdot \text{MPGNN}_L(z)$, for all $g \in \text{Aut}(A)$ and $z \in \mathcal{Z}$.

Threshold. In general, determining the automorphism group of a graph is a hard problem, and therefore we do not provide the details of the threshold calculation here. Instead, we refer readers to Dobriban and Yu (2024) for a comprehensive discussion of how to compute the SymmPI threshold in this setting.

C Real-World Example of Network Data

C.1 Network-Structured Data

We first consider the setting where data possess a joint exchangeable network structure, following the framework of Lunde et al. (2023). Our analysis is later extended in Appendix C.3 to accommodate more general network models that do not satisfy joint exchangeability.

Problem setup. Let $Y_1, \dots, Y_{n+1} \in \mathcal{Y} \subseteq \mathbb{R}$ denote response variables, $X_1, \dots, X_{n+1} \in \mathcal{X}$ denote covariates, and let A denote the $(n+1) \times (n+1)$ adjacency matrix, where A_{ij} encodes the relationship between nodes i and j . For $1 \leq i, j \leq n+1$, define $V_{ij} = (Y_i, Y_j, X_i, X_j, A_{ij})$. We posit the following joint exchangeability assumption, a general condition in many common network models, including sparse graphon models (Bickel and Chen, 2009) and spatial autoregressive models (Manski, 1993).

Assumption C.1. For any permutation $\sigma : [n+1] \rightarrow [n+1]$, we have

$$(V_{\sigma^{-1}(i)\sigma^{-1}(j)})_{1 \leq i, j \leq n+1} \stackrel{d}{=} (V_{ij})_{1 \leq i, j \leq n+1}.$$

To leverage the network structure for prediction, we define local statistics $C_i \in \mathcal{C}$ for each node i . These statistics are functions of the adjacency matrix A and the covariates (X_1, \dots, X_{n+1}) . Many natural network summaries, such as the node degree $D_i = \sum_{j \neq i} A_{ij}$ or the neighborhood covariate average $\bar{X}_i = \sum_{j \neq i} A_{ij} X_j / D_i$, exhibit inherent symmetry properties. We formalize this requirement in the following exchangeability assumption on the network statistics:

Assumption C.2. Let $(C_1, \dots, C_{n+1}) = \zeta(A, X_1, \dots, X_{n+1})$ for some function ζ . For any permutation $\sigma : [n+1] \rightarrow [n+1]$, the network statistics (C_1, \dots, C_{n+1}) satisfy

$$(C_{\sigma^{-1}(1)}, \dots, C_{\sigma^{-1}(n+1)}) = \zeta(A_{\sigma^{-1}}, X_{\sigma^{-1}(1)}, \dots, X_{\sigma^{-1}(n+1)}) \quad \text{a.s.}$$

where $A_{\sigma^{-1}}$ is the permuted adjacency matrix with entries $A_{ij}^{\sigma^{-1}} = A_{\sigma^{-1}(i)\sigma^{-1}(j)}$ for $1 \leq i, j \leq n+1$.

Assumption C.2 thus ensures that a permutation of the node labels induces a corresponding permutation of the network statistics vector. A key result from Lunde et al. (2023, Theorem 1) establishes that under Assumptions C.1 and C.2, the triplets (X_i, C_i, Y_i) for $1 \leq i \leq n+1$ are exchangeable.

This exchangeability allows us to embed the problem within our framework. We define the complete data space as $\mathcal{Z} = (\mathcal{X} \times \mathcal{C} \times \mathcal{Y})^{n+1}$ and the complete data vector as $Z = (X_i, C_i, Y_i)_{1 \leq i \leq n+1}^\top \in \mathcal{Z}$. The relevant symmetry group is the permutation group S_{n+1} , acting on Z via the permutation action $\rho(\sigma)Z := (X_{\sigma^{-1}(i)}, C_{\sigma^{-1}(i)}, Y_{\sigma^{-1}(i)})_{1 \leq i \leq n+1}^\top$. Let U denote the Haar probability measure on S_{n+1} , and the exchangeability of the triplets implies that Z is S_{n+1} -distributionally invariant. In the standard predictive inference task, we observe all data except for the final response. For $z = (x_i, c_i, y_i)_{1 \leq i \leq n+1}^\top \in \mathcal{Z}$, the observation function is thus

$$\text{obs}(z) := ((x_1, c_1, y_1), \dots, (x_n, c_n, y_n), (x_{n+1}, c_{n+1}))^\top,$$

which reveals all components of z except the response y_{n+1} .

C-SymmPI methodology. We construct non-conformity scores using a black-box predictor $\hat{\mu} : \mathcal{X} \times \mathcal{C} \rightarrow \mathbb{R}$. This defines the transformation

$$V(z) := (s_i)_{1 \leq i \leq n+1}^\top := (|y_i - \hat{\mu}(x_i, c_i)|)_{1 \leq i \leq n+1}^\top \in \tilde{\mathcal{Z}} := \mathbb{R}^{n+1}.$$

The transformed data $V(z)$ represent the non-conformity scores for all nodes. Since $\hat{\mu}$ is applied element-wise, V is S_{n+1} -deterministically equivariant. The test function isolates the score of the target node:

$$\psi(V(z)) := s_{n+1} := |y_{n+1} - \hat{\mu}(x_{n+1}, c_{n+1})|.$$

We now construct the adaptive threshold function $\hat{t}_z(\cdot)$ using **Sampled C-SymmPI**. Specifically, we define the threshold as a function over the space $\mathcal{X} \times \mathcal{C}$. This yields the following optimization problem, analogous to (4.1):

$$\hat{t}_z(\cdot) = \underset{t \in \{\mathcal{X} \times \mathcal{C} \rightarrow \mathbb{R}\}}{\text{argmin}} \frac{1}{n+1} \sum_{i=1}^{n+1} \ell_\alpha(t(x_i, c_i), s_i) + \mathcal{R}(t).$$

The C-SymmPI prediction set for y_{n+1} is then given by

$$T^{\text{C-SymmPI}}(z_{\text{obs}}) = \{y_{n+1} : s_{n+1} \leq \hat{t}_z(x_{n+1}, c_{n+1})\}.$$

By construction, this prediction set satisfies the conditional coverage guarantees of Theorem 3.1. This result strengthens the marginal coverage guarantee provided by standard network-assisted conformal prediction (Lunde et al., 2023). Appendix F provides a computationally efficient algorithm for constructing this prediction set.

C.2 Network-Assisted Classification on Cora Dataset

The Cora dataset consists of 2708 machine learning papers categorized into 7 research topics (McCallum et al., 2000). It includes the contents of the papers and a citation network, which are represented by a document-word matrix and an adjacency matrix, respectively. Leveraging these features, we consider the task of predicting whether a paper belongs to the ‘‘Neural Networks’’ category. This classification problem was also studied by Lunde et al. (2023), who applied split conformal prediction to network-assisted models. We illustrate our C-SymmPI method for this problem and compare its performance with standard split conformal prediction.²⁴

²⁴We do not include a direct comparison with the results in Lunde et al. (2023), as the evaluation metrics and score definitions are not directly comparable. Their approach measures predictive performance by the size of the prediction set, which takes only discrete values in $\{0, 1, 2\}$. In contrast, we evaluate performance using a continuous interval length on the outcome scale to better reflect adaptivity. Moreover, they adopt the score function from Romano et al. (2020), whereas our method consistently employs an absolute residual score.

α	Prediction Region	Mean Interval Length		Coverage Probability	
		C-SymmPI	Split-CP	C-SymmPI	Split-CP
0.05	Overall	1.4511	1.6121	0.9450	0.9600
	$0.0 \leq P \leq 0.3$	1.4513	1.6121	0.9407	0.9481
	$0.3 < P < 0.7$	1.5575	1.6121	1.0000	1.0000
	$0.7 \leq P \leq 1.0$	1.4213	1.6121	0.9412	0.9804
0.10	Overall	1.0437	1.2667	0.9100	0.9100
	$0.0 \leq P \leq 0.3$	1.0319	1.2667	0.9111	0.9111
	$0.3 < P < 0.7$	1.1871	1.2667	0.9286	0.9286
	$0.7 \leq P \leq 1.0$	1.0355	1.2667	0.9020	0.9020

Table 4: Comparison of mean interval length and coverage probability for C-SymmPI and split conformal prediction at different target miscoverage levels and prediction regions.

Experimental details. We construct the covariate X using three groups of features: (i) the top 20 principal components extracted from the document-word matrix; (ii) 3-dimensional latent position embeddings and degree-related parameters obtained from the logit model of Ma et al. (2020); and (iii) the node degrees and neighborhood averages of the response variable Y . The dataset is divided into a training set ($n_{\text{train}} = 1254$), a calibration set ($n_{\text{cal}} = 1254$), and a test set ($n_{\text{test}} = 200$). A logistic regression model is then fit on the training data to produce the predicted probability $\mathbb{P}(Y = 1)$, where $Y = 1$ indicates that the paper belongs to the ‘‘Neural Networks’’ category. We implement the C-SymmPI method described in Section C.1, using the efficient computation strategy detailed in Appendix F. We condition on the covariate set X using an RKHS with a Gaussian kernel of length scale $L = 5.0$ and a regularization parameter $\lambda = 0.004$. We use the absolute residual score function for both C-SymmPI and standard split conformal prediction. We evaluate the performance of both methods at target miscoverage levels $\alpha = 0.05$ and $\alpha = 0.10$.

Results and discussion. Table 4 summarizes the mean interval length and coverage probability for both C-SymmPI and split conformal prediction, evaluated overall and conditionally on three prediction regions defined by the predicted probability $P = \mathbb{P}(Y = 1)$: a low-confidence region ($0.3 < P < 0.7$) and two high-confidence regions ($0.0 \leq P \leq 0.3$ and $0.7 \leq P \leq 1.0$). Overall, C-SymmPI produces shorter intervals than split conformal prediction while maintaining valid coverage. Moreover, as shown in Figure 5, the adaptive intervals are shorter in the high-confidence regions and longer in the low-confidence region, demonstrating our method’s adaptivity to prediction uncertainty.

C.3 Network Data Beyond Joint Exchangeability

In this section, we consider a generalized setting for network-structured data that extends beyond the joint exchangeability assumption in Lunde et al. (2023). In this setting, we assume that the edges of the network are observed and that the adjacency matrix $A \in \mathbb{R}^{(n+1) \times (n+1)}$ is fixed and known. For $1 \leq i, j \leq n+1$, define $V_{ij} = (Y_i, Y_j, X_i, X_j)$, where $X_i \in \mathcal{X}$ and $Y_i \in \mathbb{R}$ denote the covariate and response associated with node i , respectively. We assume that the array $(V_{ij})_{1 \leq i, j \leq n+1}$ is distributionally invariant under the automorphism group $\text{Aut}(A) \subseteq S_{n+1}$ of the graph with adjacency matrix A . This assumption is formally stated as follows.

Assumption C.3. For any $g \in \text{Aut}(A)$, i.e., for any permutation g satisfying $gAg^\top = A$, we have

$$(V_{g^{-1}(i)g^{-1}(j)})_{1 \leq i, j \leq n+1} \stackrel{d}{=} (V_{ij})_{1 \leq i, j \leq n+1}.$$

Heuristically, Assumption C.3 posits that relabeling the nodes of the graph according to its automorphism group does not affect the joint distribution of the edge variables (see Figure 4 for an illustration). This

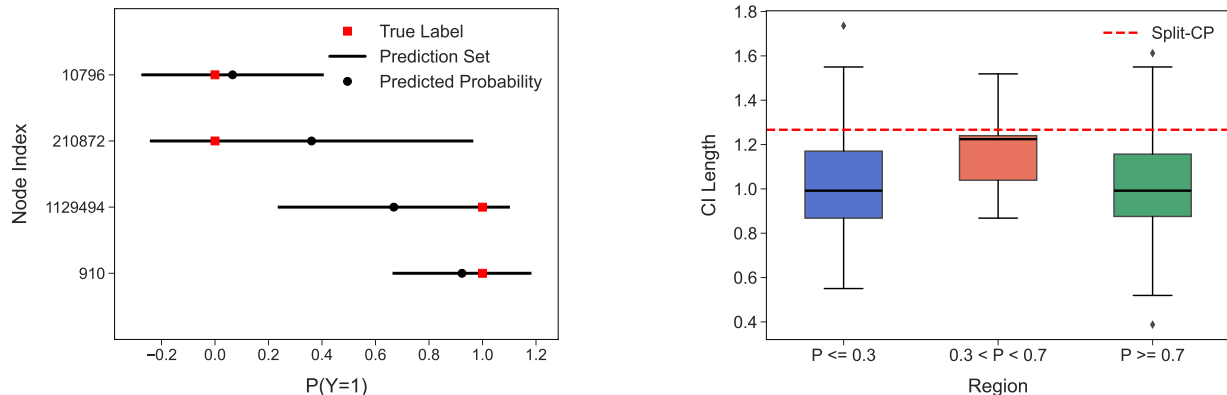


Figure 5: **Left:** Prediction intervals produced by C-SymmPI for selected nodes at $\alpha = 0.10$. **Right:** Boxplots of interval lengths for C-SymmPI across all test nodes, stratified by predicted-probability region.

assumption is less restrictive than the joint exchangeability condition in Assumption C.1. For network statistics (C_1, \dots, C_{n+1}) , we also consider a relaxation of Assumption C.2.

Assumption C.4. Let $(C_1, \dots, C_{n+1}) = \zeta(X_1, \dots, X_{n+1})$ for some function ζ . For any $g \in \text{Aut}(A)$, the network statistics (C_1, \dots, C_{n+1}) satisfy

$$(C_{g^{-1}(1)}, \dots, C_{g^{-1}(n+1)}) = \zeta(X_{g^{-1}(1)}, \dots, X_{g^{-1}(n+1)}) \quad a.s.$$

Under Assumptions C.3 and C.4, we can conclude that the triple $(X_i, C_i, Y_i)_{1 \leq i \leq n+1}$ is distributionally invariant under the automorphism group $\text{Aut}(A)$. This is a direct consequence of Lunde et al. (2023, Proposition 2), and we omit the details here for brevity. Consequently, we can directly apply the SymmPI framework introduced in Section 2.1 to construct valid predictive inference for the unobserved response Y_{n+1} based on the observed data $\{(X_i, C_i, Y_i) : 1 \leq i \leq n\}$ and (X_{n+1}, C_{n+1}) .

D Reproducing Kernel Hilbert Space

Let $K : \mathcal{O} \times \mathcal{O} \rightarrow \mathbb{R}$ be a positive semidefinite kernel function that induces an RKHS \mathcal{F}_K , equipped with an inner product $\langle \cdot, \cdot \rangle_K$ and norm $\|\cdot\|_K$. We restrict the function class to a ball of radius M within the RKHS:

$$B_M(\mathcal{F}_K) = \{f \in \mathcal{F}_K : \|f\|_K \leq M\}.$$

We impose the following boundedness condition on the kernel K :

Assumption D.1. There exists a constant $\kappa > 0$ such that $K(\cdot, \cdot) \leq \kappa^2$.

Now we restrict the optimization in (3.1) to $B_M(\mathcal{F}_K)$, and set the penalty term $\mathcal{R}(t) = \lambda \|t\|_K^2$, where $\lambda > 0$ is a regularization parameter. Using the same coset decomposition trick as in Section 3.3.1, for each $z \in \mathcal{Z}$, the adaptive threshold $\hat{t}_z^K(\cdot)$ is given by:

$$\hat{t}_z^K(\cdot) = \underset{t(\cdot) \in B_M(\mathcal{F}_K)}{\text{argmin}} \frac{|\mathcal{H}|}{|\mathcal{G}|} \sum_{i=1}^{|\mathcal{G}/\mathcal{H}|} \ell_\alpha \left(t(\text{obs}(\rho(g_i)z)), \psi(\tilde{\rho}(g_i)V(z)) \right) + \lambda \|t\|_K^2.$$

To make the computation tractable, let $\mathbf{K} \in \mathbb{R}^{|\mathcal{G}/\mathcal{H}| \times |\mathcal{G}/\mathcal{H}|}$ denote the Gram matrix with entries $\mathbf{K}_{ij} = K(z_i^{\text{obs}}, z_j^{\text{obs}})$, where $z_i^{\text{obs}} := \text{obs}(\rho(g_i)z)$. Common choices of the kernel function K include linear, polynomial, and Gaussian kernels. By the representer theorem (Schölkopf et al., 2001), any minimizer $\hat{t}_z^K(\cdot) \in$

$B_M(\mathcal{F}_K)$ admits a finite expansion of the form $\widehat{t}_z^K(z_i^{\text{obs}}) = (\mathbf{K}c)_i$ for some coefficient vector $c \in \mathbb{R}^{|\mathcal{G}/\mathcal{H}|}$, and its squared RKHS norm is given by $\|\widehat{t}_z^K\|_K^2 = c^\top \mathbf{K}c$. Consequently, the optimization problem reduces to

$$\min_{c \in \mathbb{R}^{|\mathcal{G}/\mathcal{H}|}} \frac{|\mathcal{H}|}{|\mathcal{G}|} \sum_{i=1}^{|\mathcal{G}/\mathcal{H}|} \ell_\alpha \left((\mathbf{K}c)_i, \psi(\tilde{\rho}(g_i)V(z)) \right) + \lambda c^\top \mathbf{K}c, \quad \text{subject to } c^\top \mathbf{K}c \leq M^2.$$

This is a standard convex optimization problem that can be solved efficiently using existing algorithms. The **C-SymmPI** prediction region is then given by:

$$T_K^{\text{C-SymmPI}}(z_{\text{obs}}) = \{z \in \mathcal{Z} : \psi(V(z)) \leq \widehat{t}_z^K(z_{\text{obs}}), \text{obs}(z) = z_{\text{obs}}\}. \quad (\text{D.1})$$

The following theorem provides the convergence rate for the near-conditional coverage error when using an RKHS. The proof is provided in Section G.5.

Theorem D.1. *Let $\mathcal{F}_K \subseteq \{\mathcal{O} \rightarrow \mathbb{R}\}$ be an RKHS with a bounded kernel satisfying Assumption D.1, and let $B_M(\mathcal{F}_K)$ be a closed ball of radius M in \mathcal{F}_K . Assume that $\psi(V(Z))$ admits a density $p_\psi(z)$ bounded above by a constant $b_\psi > 0$ on \mathcal{Z} . Choose the regularization parameter $\lambda = 1/\sqrt{|\mathcal{G}|/|\mathcal{H}|}$. Then, for all $f \in B_M(\mathcal{F}_K)$, the **C-SymmPI** prediction region defined in (D.1) satisfies*

$$\left| \mathbb{E}_Z \left[f(Z_{\text{obs}}) \left(\mathbb{1}\{Z \in T_K^{\text{C-SymmPI}}(Z_{\text{obs}})\} - (1 - \alpha) \right) \right] \right| \leq \frac{2M^2 + b_\psi \kappa^3 M}{\sqrt{|\mathcal{G}|/|\mathcal{H}|}}.$$

Remark D.1. *Theorem D.1 demonstrates that for the RKHS function class with squared RKHS norm, the near-conditional coverage error decays at a rate of $\mathcal{O}(1/\sqrt{|\mathcal{G}|/|\mathcal{H}|})$. In Section 4.1, we compare this rate with the state-of-the-art result for conditional conformal prediction in the standard i.i.d. setting.*

E Sampled C-SymmPI Algorithm

We sample N elements G_1, \dots, G_N i.i.d. from the Haar probability measure U . We then replace the expectation in (3.1) with the empirical average over these samples. For a given $z \in \mathcal{Z}$, the sampled adaptive threshold $\widehat{t}_{\text{samp}}(\cdot)$ ²⁵ is defined as:

$$\widehat{t}_{\text{samp}}(\cdot) = \underset{t(\cdot) \in \{\mathcal{O} \rightarrow \mathbb{R}\}}{\text{argmin}} \frac{1}{N} \sum_{i=1}^N \ell_\alpha \left(t(\text{obs}(\rho(G_i)z)), \psi(\tilde{\rho}(G_i)V(z)) \right) + \mathcal{R}(t). \quad (\text{E.1})$$

The corresponding prediction region $T_s^{\text{C-SymmPI}}(z_{\text{obs}})$ is analogous to (3.2):

$$T_s^{\text{C-SymmPI}}(z_{\text{obs}}) = \{z \in \mathcal{Z} : \psi(V(z)) \leq \widehat{t}_{\text{samp}}(z_{\text{obs}}), \text{obs}(z) = z_{\text{obs}}\}. \quad (\text{E.2})$$

The full procedure is outlined in Algorithm 2.

Sampled C-SymmPI closely approximates the full method when N is large. To formalize this, we first introduce some notations. Let Δ denote the coverage error of the full **C-SymmPI** method, and let Δ_{samp} denote the coverage error of **Sampled C-SymmPI**:

$$\begin{aligned} \Delta &= \mathbb{E}_Z \left[f(Z_{\text{obs}}) \left(\mathbb{1}\{Z \in T^{\text{C-SymmPI}}(Z_{\text{obs}})\} - (1 - \alpha) \right) \right], \\ \Delta_{\text{samp}} &= \mathbb{E}_Z \left[f(Z_{\text{obs}}) \left(\mathbb{1}\{Z \in T_s^{\text{C-SymmPI}}(Z_{\text{obs}})\} - (1 - \alpha) \right) \right]. \end{aligned}$$

Define $\nu(z) = \psi(V(z)) - \widehat{t}_z^K(z_{\text{obs}})$ and $\nu_{\text{samp}}(z) = \psi(V(z)) - \widehat{t}_{\text{samp}}(z_{\text{obs}})$. For any non-negative, bounded function $f : \mathcal{O} \rightarrow \mathbb{R}$, we define the f -tilted measure \mathbb{P}_f : for any $z \in \mathcal{Z}$,

$$d\mathbb{P}_f(z) = \frac{f(\text{obs}(z))}{\mathbb{E}_Z[f(\text{obs}(z))]} d\mathbb{P}_Z(z). \quad (\text{E.3})$$

²⁵We keep the dependence on z implicit in the notation.

Algorithm 2 Sampled C-SymmPI: conditional predictive inference using sampled group elements

Input: Data z satisfying distributional invariance under group \mathcal{G} . Observation function $\text{obs} : \mathcal{Z} \rightarrow \mathcal{O}$. Observed data z_{obs} . Deterministically equivariant map $V : \mathcal{Z} \rightarrow \tilde{\mathcal{Z}}$. Test function $\psi : \tilde{\mathcal{Z}} \rightarrow \mathbb{R}$. Miscoverage level $\alpha \in (0, 1)$. Penalty term \mathcal{R} satisfying Assumption 3.1. Number of samples N .

- 1: Initialize $T_s^{\text{C-SymmPI}}(z_{\text{obs}}) = \emptyset$.
- 2: Sample $G_1, \dots, G_N \stackrel{\text{i.i.d.}}{\sim} U$.
- 3: **for** $z \in \mathcal{Z}$ satisfying $\text{obs}(z) = z_{\text{obs}}$ **do**
- 4: Solve the optimization problem in (E.1) to obtain $\hat{t}_{\text{samp}}(\cdot)$. ▷ Adaptive threshold function.
- 5: **if** $\psi(V(z)) \leq \hat{t}_{\text{samp}}(z_{\text{obs}})$ **then**
- 6: Set $T_s^{\text{C-SymmPI}}(z_{\text{obs}}) \leftarrow T_s^{\text{C-SymmPI}}(z_{\text{obs}}) \cup \{z\}$.
- 7: **end if**
- 8: **end for**

Output: Prediction region $T_s^{\text{C-SymmPI}}(z_{\text{obs}})$.

We further consider the total variation distance between the distribution of $\nu(Z)$ and the distribution of $\nu_{\text{samp}}(Z)$ under the tilted measure \mathbb{P}_f :

$$\text{TV}_f(\nu(Z), \nu_{\text{samp}}(Z)) = \sup_{A \in \mathcal{B}(\mathbb{R})} |\mathbb{P}_f(\nu(Z) \in A) - \mathbb{P}_f(\nu_{\text{samp}}(Z) \in A)|, \quad (\text{E.4})$$

where $\mathcal{B}(\mathbb{R})$ is the Borel σ -algebra on \mathbb{R} . With these notations in place, we state the following theorem, which quantifies the difference between Δ and Δ_{samp} ; its proof is provided in Section G.6.

Theorem E.1. *Under the setting of Theorem 3.1, for a group \mathcal{G} that is not necessarily finite, and for any non-negative, upper-bounded function $f : \mathcal{O} \rightarrow \mathbb{R}$ satisfying $\mathbb{E}_Z[f(Z_{\text{obs}})] > 0$, with probability at least $1 - \delta$, the following holds:*

$$|\Delta - \Delta_{\text{samp}}| \leq \|f\|_{\infty} \sqrt{\frac{8 \log(2/\delta)}{N}} + \mathbb{E}_Z[f(Z_{\text{obs}})] \text{TV}_f(\nu(Z), \nu_{\text{samp}}(Z)).$$

Remark E.1. *Theorem E.1 shows that the coverage error of the sampled method, Δ_{samp} , closely approximates that of the full method, Δ . The first error term arises from using a sample average of size N to approximate the expectation over the group and vanishes at a rate of $\mathcal{O}(1/\sqrt{N})$ due to standard concentration inequalities. The second term captures the effect of using the sampled threshold $\hat{t}_{\text{samp}}(\cdot)$ instead of the exact one $\hat{t}_z(\cdot)$. As N grows, $\hat{t}_{\text{samp}}(\cdot)$ converges to $\hat{t}_z(\cdot)$, causing this total variation distance term to shrink. Therefore, for a large number of samples N , the coverage error of the sampled method is a good approximation of the full method's error with high probability.*

Next, Corollary E.1 provides a near-conditional coverage guarantee for Sampled C-SymmPI, averaged over the randomness in the sampled group elements $G_{1:N}$. The proof is provided in Section G.7, which is analogous to that of Theorem 3.1.

Corollary E.1. *Under the setting of Theorem 3.1, the Sampled C-SymmPI prediction region from Algorithm 2 satisfies*

$$\left| \mathbb{E}_{Z, G_{1:N}} \left[f(Z_{\text{obs}}) \left(\mathbb{1}\{Z \in T_s^{\text{C-SymmPI}}(Z_{\text{obs}})\} - (1 - \alpha) \right) \right] \right| \leq \varepsilon_{\text{penalty}} + \varepsilon_{\text{int}},$$

where the penalty error and interpolation error are defined as

$$\varepsilon_{\text{penalty}} = \left| \mathbb{E}_{Z, G_{1:N}} [D_f \mathcal{R}(\hat{t}_{\text{samp}})] \right|, \quad \varepsilon_{\text{int}} = \mathbb{E}_{Z, G_{1:N}} [|f(Z_{\text{obs}})| \mathbb{1}\{\psi(V(Z)) = \hat{t}_{\text{samp}}(Z_{\text{obs}})\}].$$

Remark E.2. *Analogous to Section 3.3, if we specify the function class to be a d -dimensional linear class, the convergence rate is $\mathcal{O}(d/N)$; if we specify the function class to be an RKHS, the convergence rate is $\mathcal{O}(1/\sqrt{N})$.*

Together, Theorem E.1 and Corollary E.1 establish that, for data with large or infinite group symmetries, **Sampled C-SymmPI** provides a computationally feasible approximation to the full method, while also achieving near-conditional coverage guarantees.

F Dual Formulation for Efficient Computation

In this section, we present a dual formulation of the optimization problem in (3.1) to enable efficient computation of the prediction region. This type of duality-based approach has been previously explored by Gibbs et al. (2025), who considered quantile regression with regularization under uniform weights. Our approach generalizes their framework to accommodate *arbitrary* weights, thereby extending it to the broader setting of weighted quantile regression with regularization.

Dual formulation. Consider a dataset $z = ((x_1, y_1), \dots, (x_n, y_n)) \in (\mathcal{X} \times \mathbb{R})^n$, where the covariates x_1, \dots, x_n are fully observed, the responses y_1, \dots, y_{n-1} are observed, and y_n is unobserved. Define the score for each observation by $s_i = s(x_i, y_i)$ for some score function $s(\cdot, \cdot)$. Accordingly, s_1, \dots, s_{n-1} are fixed, while s_n is treated as a parameter. We then formulate the following regularized, weighted quantile regression problem, whose decision variable is a function $t(\cdot) \in \{\mathcal{X} \rightarrow \mathbb{R}\}$:

$$\text{minimize} \quad \sum_{i=1}^n w_i \cdot \ell_\alpha(t(x_i), s_i) + \mathcal{R}(t). \quad (\text{F.1})$$

Here, $w = [w_i]_{1 \leq i \leq n}$ is a vector of non-negative weights, which we assume are normalized such that $\sum_{i=1}^n w_i = 1$. The following proposition presents the dual formulation of this optimization problem, whose proof is provided in Section G.8.

Proposition F.1. *The dual problem of the optimization problem in (F.1) is given by*

$$\begin{aligned} & \text{maximize} \quad (w \odot \lambda)^\top s - \mathcal{R}^*(w \odot \lambda) \\ & \text{subject to} \quad -\alpha \mathbf{1} \preceq \lambda \preceq (1 - \alpha) \mathbf{1}, \end{aligned} \quad (\text{F.2})$$

where $\lambda \in \mathbb{R}^n$ is the dual variable, and $\mathcal{R}^*(\alpha) := \sup_t \{\sum_{i=1}^n \alpha_i t(x_i) - \mathcal{R}(t)\}$ is the Fenchel conjugate of \mathcal{R} .²⁶

Remark F.1. *The Fenchel conjugate $\mathcal{R}^*(\cdot)$ often admits a closed-form expression for many commonly used regularizers. As an illustrative example, consider the RKHS setting. Let $K \in \mathbb{R}^{n \times n}$ be the Gram matrix with entries $K_{ij} = K(x_i, x_j)$, where common choices of the kernel function K include the linear, polynomial, and Gaussian RBF kernels. By the representer theorem (Schölkopf et al., 2001), any function t in the RKHS admits a finite expansion of the form $t(x_i) = (Kc)_i$ for some coefficient vector $c = (c_1, \dots, c_n)^\top \in \mathbb{R}^n$, and its squared RKHS norm is given by $\|t\|_K^2 = c^\top Kc$. Consequently, the conjugate is expressed as $\mathcal{R}^*(\alpha) = \sup_{c \in \mathbb{R}^n} \{\alpha^\top Kc - \lambda c^\top Kc\}$, and solving this quadratic maximization problem yields*

$$\mathcal{R}^*(\alpha) = \frac{1}{4\lambda} \alpha^\top K \alpha.$$

In the experiments presented in Section 5, we employ this RKHS kernel to enable efficient computation.

Let $\hat{t}_z(\cdot) \in \{\mathcal{X} \rightarrow \mathbb{R}\}$ and $\hat{\lambda} = [\hat{\lambda}_i]_{1 \leq i \leq n}$ denote the primal and dual optimal solutions, respectively. Recall that the scores s_1, \dots, s_{n-1} are fixed, while s_n is treated as a parameter. Consequently, the optimal dual solution $\hat{\lambda}$ is a function of s_n . Among the dual variables, our primary interest lies in the n -th component $\hat{\lambda}_n = \hat{\lambda}_n(s_n)$. The following proposition identifies the precise form of $\hat{\lambda}_n(s_n)$, whose proof is provided in Section G.9.

²⁶ $w \odot \lambda := [w_i \lambda_i]_{i=1}^n$ denotes the Hadamard product of vectors w and λ , $\mathbf{1}$ denotes the vector of all ones, and “ \preceq ” denotes element-wise inequality.

Proposition F.2. Let $\hat{t}_z : \mathcal{X} \rightarrow \mathbb{R}$ and $\hat{\lambda}(s_n) = [\hat{\lambda}_i(s_n)]_{1 \leq i \leq n}$ denote the optimal primal and dual solutions to (F.1). Then $\hat{\lambda}_n(s_n)$ satisfies:

$$\hat{\lambda}_n(s_n) \in \begin{cases} -\alpha & \text{if } s_n < \hat{t}_z(x_n), \\ [-\alpha, 1 - \alpha] & \text{if } s_n = \hat{t}_z(x_n), \\ 1 - \alpha & \text{if } s_n > \hat{t}_z(x_n). \end{cases}$$

Remark F.2. For the prediction set $\hat{C}(x_n) = \{y_n : s_n \leq \hat{t}_z(x_n)\}$, Proposition F.2 reveals that evaluating the condition $s_n \leq \hat{t}_z(x_n)$ is nearly equivalent to verifying whether $\hat{\lambda}_n(s_n) < 1 - \alpha$. This motivates the following dual representation of the prediction region:

$$\hat{C}^*(x_n) = \{y_n : \hat{\lambda}_n(s_n) < 1 - \alpha\}. \quad (\text{F.3})$$

Under strong duality, Gibbs et al. (2025) show that $\hat{C}^*(x_n)$ attains the same near-conditional coverage guarantee as $\hat{C}(x_n)$.

Efficient computation. To enable efficient computation of $\hat{C}^*(x_n)$ in (F.3), the following proposition establishes a key monotonicity property that facilitates fast search procedures. Its proof is provided in Section G.10.

Proposition F.3. The function $\hat{\lambda}_n(\cdot)$ is a monotonically increasing function.

Leveraging this monotonicity, we can recover the prediction region by identifying the largest value of s_n for which the dual feasibility condition holds. Specifically, we compute $s^* = \sup\{s_n : \hat{\lambda}_n(s_n) < 1 - \alpha\}$ using binary search and return the prediction region $\hat{C}^*(x_n) = \{y_n : s_n \leq s^*\}$. The detailed algorithmic steps are provided in Algorithm 3.

Algorithm 3 Computation of the prediction region via dual formulation

Input: Observed data $z = ((x_1, y_1), \dots, (x_{n-1}, y_{n-1}), x_n)$, score function $s(\cdot, \cdot)$, miscoverage level α , weights $w = [w_i]_{1 \leq i \leq n}$, regularizer $\mathcal{R}(\cdot)$, tolerance $\varepsilon > 0$.

- 1: Initialize s_{\min} and s_{\max} as lower and upper bounds for s_n .
- 2: **while** $s_{\max} - s_{\min} > \varepsilon$ **do** ▷ Binary search.
- 3: Set $s_n = (s_{\min} + s_{\max})/2$.
- 4: Solve the dual problem in (F.2) to obtain $\hat{\lambda}_n(s_n)$.
- 5: **if** $\hat{\lambda}_n(s_n) < 1 - \alpha$ **then**
- 6: Set $s_{\min} = s_n$.
- 7: **else**
- 8: Set $s_{\max} = s_n$.
- 9: **end if**
- 10: **end while**
- 11: Set $s^* = s_{\min}$. ▷ An approximation of $\sup\{s_n : \hat{\lambda}_n(s_n) < 1 - \alpha\}$.

Output: Prediction region $\hat{C}^*(x_n) = \{y_n : s(x_n, y_n) \leq s^*\}$.

Remark F.3. In the final step of Algorithm 3, the dual formulation enables efficient recovery of the prediction region when $s_n = s(x_n, y_n)$ is defined as a non-conformity score, such as $s_n = |\hat{\mu}(x_{n+1}) - y_{n+1}|$, where $\hat{\mu}(x_{n+1})$ denotes the predicted response. In this case, once s^* is obtained, the prediction region immediately reduces to the closed-form interval $[\hat{\mu}(x_{n+1}) - s^*, \hat{\mu}(x_{n+1}) + s^*]$.

G Proofs

G.1 Proof of Proposition 2.1

For (i) implies (ii), taking conditional expectation with respect to Z_{obs} on (ii), we have

$$\begin{aligned} & \mathbb{E} \left[f(Z_{\text{obs}}) \left(\mathbb{1}\{Z \in \widehat{C}(Z_{\text{obs}})\} - (1 - \alpha) \right) \right] \\ &= \mathbb{E} \left[f(Z_{\text{obs}}) \mathbb{E} \left[\mathbb{1}\{Z \in \widehat{C}(Z_{\text{obs}})\} - (1 - \alpha) \mid Z_{\text{obs}} \right] \right] \\ &= \mathbb{E} \left[f(Z_{\text{obs}}) \left(\mathbb{P} \left(Z \in \widehat{C}(Z_{\text{obs}}) \mid Z_{\text{obs}} \right) - (1 - \alpha) \right) \right] = 0, \end{aligned}$$

where the last equality follows from assumption (i).

For (ii) implies (i), the above calculation implies that for all bounded non-negative $f : \mathcal{O} \rightarrow \mathbb{R}$, we have

$$\mathbb{E} \left[f(Z_{\text{obs}}) \left(\mathbb{P} \left(Z \in \widehat{C}(Z_{\text{obs}}) \mid Z_{\text{obs}} \right) - (1 - \alpha) \right) \right] = 0.$$

Take $f = \mathbb{1}_B$ for any measurable set $B \subseteq \mathcal{O}$ and define $g(Z_{\text{obs}}) = \mathbb{P} \left(Z \in \widehat{C}(Z_{\text{obs}}) \mid Z_{\text{obs}} \right) - (1 - \alpha)$. Then for any measurable set $B \subseteq \mathcal{O}$, we have

$$\mathbb{E} [\mathbb{1}_B(Z_{\text{obs}})g(Z_{\text{obs}})] = \int_B g(z_{\text{obs}}) d\mathbb{P}_{Z_{\text{obs}}}(z_{\text{obs}}) = 0.$$

Suppose there is a measurable set $B_+ \subseteq \mathcal{O}$ with positive measure such that $g(z_{\text{obs}}) > 0$ on B_+ . Then choosing $B = B_+$ gives

$$\int_{B_+} g(z_{\text{obs}}) d\mathbb{P}_{Z_{\text{obs}}}(z_{\text{obs}}) > 0,$$

which contradicts the above equation. Similar results can be shown for the case when $g(z_{\text{obs}}) < 0$ on some measurable set B_- . Therefore, we conclude that $g(z_{\text{obs}}) = 0$ almost surely, which is equivalent to (i). This completes the proof. \square

G.2 Proof of Theorem 3.1

We begin by introducing the shorthand $\widetilde{Z} := V(Z)$, and let $|\mathcal{G}|$ denote the cardinality of the finite group \mathcal{G} . For notational convenience, define $Z_i := \rho(g_i)Z$, $\widetilde{Z}_i := \widetilde{\rho}(g_i)\widetilde{Z}$, and $Z_i^{\text{obs}} := \text{obs}(Z_i)$ for each $i = 1, \dots, |\mathcal{G}|$. With these definitions, (3.1) can be equivalently rewritten as

$$\widehat{t}_Z(\cdot) = \underset{t(\cdot) \in \{\mathcal{O} \rightarrow \mathbb{R}\}}{\text{argmin}} \frac{1}{|\mathcal{G}|} \sum_{i=1}^{|\mathcal{G}|} \ell_\alpha(t(Z_i^{\text{obs}}), \psi(\widetilde{Z}_i)) + \mathcal{R}(t). \quad (\text{G.1})$$

Define the evaluation operators $\delta_i(\cdot) : \{\mathcal{O} \rightarrow \mathbb{R}\} \rightarrow \mathbb{R}$ by $\delta_i(t) = t(Z_i^{\text{obs}})$, which are linear in t . It is easy to verify that the pinball loss $\ell_\alpha(\theta, S) := \alpha[\theta - S]_+ + (1 - \alpha)[S - \theta]_+$ is convex in its first argument. Since convexity is preserved under linear transformations, it follows that $\ell_\alpha(t(Z_i^{\text{obs}}), \psi(\widetilde{Z}_i)) = \ell_\alpha(\delta_i(t), \psi(\widetilde{Z}_i))$ is convex in t for all $i = 1, \dots, |\mathcal{G}|$. By Assumption 3.1, the regularization term \mathcal{R} is also convex in t . Therefore, the optimization problem in (G.1) is an unconstrained convex optimization problem.

For any $f : \mathcal{O} \rightarrow \mathbb{R}$, the minimizer \widehat{t}_Z satisfies the first-order optimality condition

$$0 \in \partial_f \left(\frac{1}{|\mathcal{G}|} \sum_{i=1}^{|\mathcal{G}|} \ell_\alpha(\delta_i(\widehat{t}_Z), \psi(\widetilde{Z}_i)) + \mathcal{R}(\widehat{t}_Z) \right),$$

where ∂_f denotes the set of subgradients in the direction of f .

Let $A := \{1 \leq i \leq |\mathcal{G}| : \psi(\tilde{Z}_i) = \hat{t}_Z(Z_i^{\text{obs}})\}$ be the index set of interpolation points. By direct computation, we have

$$\begin{aligned}
& \partial_f \left(\frac{1}{|\mathcal{G}|} \sum_{i=1}^{|\mathcal{G}|} \ell_\alpha(\delta_i(\hat{t}_Z), \psi(\tilde{Z}_i)) \right) \\
&= \left\{ \frac{1}{|\mathcal{G}|} \left(\sum_{i \in A^c} \left(-(1-\alpha)f(Z_i^{\text{obs}}) \mathbb{1}\{\psi(\tilde{Z}_i) > \hat{t}_Z(Z_i^{\text{obs}})\} + \alpha f(Z_i^{\text{obs}}) \mathbb{1}\{\psi(\tilde{Z}_i) < \hat{t}_Z(Z_i^{\text{obs}})\} \right) + \sum_{i \in A} s_i f(Z_i^{\text{obs}}) \right) : s_i \in [\alpha-1, \alpha] \right\} \\
&= \left\{ \frac{1}{|\mathcal{G}|} \left(\sum_{i \in A^c} f(Z_i^{\text{obs}}) \left(\alpha - \mathbb{1}\{\psi(\tilde{Z}_i) > \hat{t}_Z(Z_i^{\text{obs}})\} \right) + \sum_{i \in A} s_i f(Z_i^{\text{obs}}) \right) : s_i \in [\alpha-1, \alpha] \right\} \\
&= \left\{ \frac{1}{|\mathcal{G}|} \left(\sum_{i=1}^{|\mathcal{G}|} f(Z_i^{\text{obs}}) \left(\alpha - \mathbb{1}\{\psi(\tilde{Z}_i) > \hat{t}_Z(Z_i^{\text{obs}})\} \right) + \sum_{i \in A} (s_i - \alpha) f(Z_i^{\text{obs}}) \right) : s_i \in [\alpha-1, \alpha] \right\}.
\end{aligned}$$

Let $s_i^* \in [\alpha-1, \alpha]$ be the coefficients that make the subgradient zero. Since \mathcal{R} is differentiable, its subgradient is a singleton set containing only the directional derivative, i.e., $\partial_f \mathcal{R}(\hat{t}_Z) = \{D_f \mathcal{R}(\hat{t}_Z)\}$. Therefore, we have

$$\frac{1}{|\mathcal{G}|} \sum_{i=1}^{|\mathcal{G}|} f(Z_i^{\text{obs}}) \left(\alpha - \mathbb{1}\{\psi(\tilde{Z}_i) > \hat{t}_Z(Z_i^{\text{obs}})\} \right) = -D_f \mathcal{R}(\hat{t}_Z) + \frac{1}{|\mathcal{G}|} \sum_{i \in A} (\alpha - s_i^*) f(Z_i^{\text{obs}}). \quad (\text{G.2})$$

We claim that for all $1 \leq i \leq |\mathcal{G}|$,

$$\mathbb{E}_Z \left[f(Z_i^{\text{obs}}) \left(\alpha - \mathbb{1}\{\psi(\tilde{Z}_i) > \hat{t}_Z(Z_i^{\text{obs}})\} \right) \right] = \mathbb{E}_Z \left[f(Z_{\text{obs}}) \left(\alpha - \mathbb{1}\{\psi(\tilde{Z}) > \hat{t}_Z(Z_{\text{obs}})\} \right) \right]. \quad (\text{G.3})$$

To prove this claim, we first show that $f(Z_i^{\text{obs}}) \left(\alpha - \mathbb{1}\{\psi(\tilde{Z}_i) > \hat{t}_Z(Z_i^{\text{obs}})\} \right)$ is a function of Z_i . Indeed, by the \mathcal{G} -deterministic equivariance property of V , we have $\tilde{Z}_i = V(Z_i)$. Moreover, recall the definition of $\hat{t}_Z(\cdot)$ in (3.1), and it holds that

$$\begin{aligned}
\hat{t}_{\rho(g)Z}(\cdot) &= \operatorname{argmin}_{t(\cdot) \in \{\mathcal{O} \rightarrow \mathbb{R}\}} \mathbb{E}_{G \sim U} \left[\ell_\alpha \left(t(\text{obs}(\rho(G)\rho(g)Z)), \psi(\tilde{\rho}(G)V(\rho(g)Z)) \right) \right] + \mathcal{R}(t) \\
&= \operatorname{argmin}_{t(\cdot) \in \{\mathcal{O} \rightarrow \mathbb{R}\}} \mathbb{E}_{G \sim U} \left[\ell_\alpha \left(t(\text{obs}(\rho(Gg)Z)), \psi(\tilde{\rho}(Gg)V(Z)) \right) \right] + \mathcal{R}(t) \\
&= \operatorname{argmin}_{t(\cdot) \in \{\mathcal{O} \rightarrow \mathbb{R}\}} \mathbb{E}_{G \sim U} \left[\ell_\alpha \left(t(\text{obs}(\rho(G)Z)), \psi(\tilde{\rho}(G)V(Z)) \right) \right] + \mathcal{R}(t) \\
&= \hat{t}_Z(\cdot),
\end{aligned}$$

where the first equality follows from the definition of $\hat{t}_Z(\cdot)$, the second equality follows from the definition of action ρ and the \mathcal{G} -deterministic equivariance property of V , the third equality follows from the invariance property of the Haar probability measure U , and the last equality follows from the definition of $\hat{t}_Z(\cdot)$ again. Therefore, we write

$$f(Z_i^{\text{obs}}) \left(\alpha - \mathbb{1}\{\psi(\tilde{Z}_i) > \hat{t}_Z(Z_i^{\text{obs}})\} \right) = f(\text{obs}(Z_i)) \left(\alpha - \mathbb{1}\{\psi(V(Z_i)) > \hat{t}_{Z_i}(\text{obs}(Z_i))\} \right) := \varphi(Z_i),$$

which shows that the randomness in this expression lies only in Z_i .

Next, notice that for all $g \in \mathcal{G}$, we have

$$\rho(g)Z \stackrel{d}{=} \rho(g)\rho(G)Z = \rho(gG)Z \stackrel{d}{=} \rho(G)Z \stackrel{d}{=} Z,$$

where the first equality follows from distributional invariance property of Z , the second equality follows from the definition of action ρ , the third equality follows from the property of the Haar probability measure U ,

and the last equality also follows from the distributional invariance. Therefore, for the function $\varphi(\cdot)$ defined above, we have $\varphi(Z_i) \stackrel{d}{=} \varphi(Z)$. This directly implies (G.3).

We next proceed to compute coverage error terms:

$$\begin{aligned}
& \mathbb{E}_Z \left[f(Z_{\text{obs}}) \left(\mathbb{1}\{Z \in T^{\text{C-SymmPI}}(Z_{\text{obs}})\} - (1 - \alpha) \right) \right] \\
&= \mathbb{E}_Z \left[f(Z_{\text{obs}}) \left(\mathbb{1}\{\psi(\tilde{Z}) \leq \hat{t}_Z(Z_{\text{obs}})\} - (1 - \alpha) \right) \right] \\
&= \mathbb{E}_Z \left[f(Z_{\text{obs}}) \left(\alpha - \mathbb{1}\{\psi(\tilde{Z}) > \hat{t}_Z(Z_{\text{obs}})\} \right) \right] \\
&= \mathbb{E}_Z \left[\frac{1}{|\mathcal{G}|} \sum_{i=1}^{|\mathcal{G}|} f(Z_i^{\text{obs}}) \left(\alpha - \mathbb{1}\{\psi(\tilde{Z}_i) > \hat{t}_Z(Z_i^{\text{obs}})\} \right) \right] \tag{G.4} \\
&= -\mathbb{E}_Z [D_f \mathcal{R}(\hat{t}_Z)] + \mathbb{E}_Z \left[\frac{1}{|\mathcal{G}|} \sum_{i \in A} (\alpha - s_i^*) f(Z_i^{\text{obs}}) \right],
\end{aligned}$$

where the first equality follows from Algorithm 1, the third equality follows from (G.3), and the last equality follows from (G.2).

We next derive an upper bound for the second term on the last line of (G.4). Since $\alpha - s_i^* \in [0, 1]$, it follows that

$$\begin{aligned}
\left| \mathbb{E}_Z \left[\frac{1}{|\mathcal{G}|} \sum_{i \in A} (\alpha - s_i^*) f(Z_i^{\text{obs}}) \right] \right| &\leq \mathbb{E}_Z \left[\frac{1}{|\mathcal{G}|} \sum_{i \in A} (\alpha - s_i^*) |f(Z_i^{\text{obs}})| \right] \\
&\leq \mathbb{E}_Z \left[\frac{1}{|\mathcal{G}|} \sum_{i \in A} |f(Z_i^{\text{obs}})| \right] \\
&= \mathbb{E}_Z \left[\frac{1}{|\mathcal{G}|} \sum_{i=1}^{|\mathcal{G}|} |f(Z_i^{\text{obs}})| \mathbb{1}\{\psi(\tilde{Z}_i) = \hat{t}_Z(Z_i^{\text{obs}})\} \right] \\
&= \mathbb{E}_Z \left[|f(Z_{\text{obs}})| \mathbb{1}\{\psi(\tilde{Z}) = \hat{t}_Z(Z_{\text{obs}})\} \right], \tag{G.5}
\end{aligned}$$

where the last equality follows from the same reasoning as (G.3).

Finally, applying the triangle inequality to (G.4) and combining with (G.5), we obtain

$$\left| \mathbb{E}_Z \left[f(Z_{\text{obs}}) \left(\mathbb{1}\{Z \in T^{\text{C-SymmPI}}(Z_{\text{obs}})\} - (1 - \alpha) \right) \right] \right| \leq \left| \mathbb{E}_Z [D_f \mathcal{R}(\hat{t}_Z)] \right| + \mathbb{E}_Z \left[|f(Z_{\text{obs}})| \mathbb{1}\{\psi(\tilde{Z}) = \hat{t}_Z(Z_{\text{obs}})\} \right],$$

which completes the proof. \square

G.3 Proof of Theorem 3.2

Recall that $Z_G := \rho(G)Z$, $\tilde{Z}_G := V(Z_G)$, and $Z_G^{\text{obs}} := \text{obs}(Z_G)$ for $G \sim U$. Following the same reasoning as in the first two steps of (G.4), we have

$$\mathbb{E}_Z \left[f(Z_{\text{obs}}) \left(\mathbb{1}\{Z \in T^{\text{C-SymmPI}}(Z_{\text{obs}})\} - (1 - \alpha) \right) \right] = \mathbb{E}_Z \left[f(Z_{\text{obs}}) \left(\alpha - \mathbb{1}\{\psi(\tilde{Z}) > \hat{t}_Z(Z_{\text{obs}})\} \right) \right].$$

We now decompose this expression into two terms:

$$\begin{aligned}
& \mathbb{E}_Z [f(Z_{\text{obs}}) (\mathbb{1}\{Z \in T^{\text{C-SymmPI}}(Z_{\text{obs}})\} - (1 - \alpha))] \\
&= \underbrace{\mathbb{E}_{G,Z} \left[f(Z_{\text{obs}}) \left(\alpha - \mathbb{1}\{\psi(\tilde{Z}) > \hat{t}_Z(Z_{\text{obs}})\} \right) - \frac{1}{|\mathcal{G}|} \sum_{i=1}^{|\mathcal{G}|} f(Z_i^{\text{obs}}) \left(\alpha - \mathbb{1}\{\psi(\tilde{Z}_i) > \hat{t}_{Z_G}(Z_i^{\text{obs}})\} \right) \right]}_{\text{(I)}} \\
& \quad + \underbrace{\mathbb{E}_{G,Z} \left[\frac{1}{|\mathcal{G}|} \sum_{i=1}^{|\mathcal{G}|} f(Z_i^{\text{obs}}) \left(\alpha - \mathbb{1}\{\psi(\tilde{Z}_i) > \hat{t}_{Z_G}(Z_i^{\text{obs}})\} \right) \right]}_{\text{(II)}}.
\end{aligned} \tag{G.6}$$

We begin by analyzing term (I). Using the invariance property of the Haar probability measure U , we can rewrite (I) as

$$\text{(I)} = \mathbb{E}_{G,Z} \left[f(Z_{\text{obs}}) \left(\alpha - \mathbb{1}\{\psi(\tilde{Z}) > \hat{t}_Z(Z_{\text{obs}})\} \right) - f(Z_G^{\text{obs}}) \left(\alpha - \mathbb{1}\{\psi(\tilde{Z}_G) > \hat{t}_{Z_G}(Z_G^{\text{obs}})\} \right) \right].$$

Define

$$\varphi(z) = f(\text{obs}(z)) \left(\alpha - \mathbb{1}\{\psi(V(z)) > \hat{t}_z(\text{obs}(z))\} \right).$$

Recall that \mathbb{P} and \mathbb{Q} denote the distributions of Z and Z_G , respectively. Then we can write (I) in the following integral form:

$$\text{(I)} = \mathbb{E}_G \left[\int_{\mathcal{Z}} \varphi(\cdot) d\mathbb{P} - \varphi(\cdot) d\mathbb{Q} \right].$$

Then we have

$$\begin{aligned}
|\text{(I)}| &\leq \|\varphi\|_{\infty} \mathbb{E}_G \left[\int_{\mathcal{Z}} |d\mathbb{P} - d\mathbb{Q}| \right] \\
&\leq (1 + \alpha) \|f\|_{\infty} \mathbb{E}_G \left[\int_{\mathcal{Z}} |d\mathbb{P} - d\mathbb{Q}| \right] \\
&= 2(1 + \alpha) \|f\|_{\infty} \mathbb{E}_G [\text{TV}(\mathbb{P}, \mathbb{Q})],
\end{aligned} \tag{G.7}$$

where the last step follows from the definition of total variation distance.

We now turn to term (II). By the same reasoning as in (G.2), we have

$$\text{(II)} = -\mathbb{E}_{G,Z} [D_f \mathcal{R}(\hat{t}_{Z_G})] + \mathbb{E}_{G,Z} \left[\frac{1}{|\mathcal{G}|} \sum_{i \in A} (\alpha - s_i^*) f(Z_i^{\text{obs}}) \right], \tag{G.8}$$

where $s_i^* \in [\alpha - 1, \alpha]$ for $i \in A$, and $A := \{1 \leq i \leq |\mathcal{G}| : \psi(\tilde{Z}_i) = \hat{t}_{Z_G}(Z_i^{\text{obs}})\}$. For the second term on the right-hand side of (G.8), it follows that

$$\begin{aligned}
\left| \mathbb{E}_{G,Z} \left[\frac{1}{|\mathcal{G}|} \sum_{i \in A} (\alpha - s_i^*) f(Z_i^{\text{obs}}) \right] \right| &\leq \mathbb{E}_{G,Z} \left[\frac{1}{|\mathcal{G}|} \sum_{i \in A} (\alpha - s_i^*) |f(Z_i^{\text{obs}})| \right] \\
&\leq \mathbb{E}_{G,Z} \left[\frac{1}{|\mathcal{G}|} \sum_{i \in A} |f(Z_i^{\text{obs}})| \right] \\
&= \mathbb{E}_{G,Z} \left[\frac{1}{|\mathcal{G}|} \sum_{i=1}^{|\mathcal{G}|} |f(Z_i^{\text{obs}})| \mathbb{1}\{\psi(\tilde{Z}_i) = \hat{t}_{Z_G}(Z_i^{\text{obs}})\} \right] \\
&= \mathbb{E}_{G,Z} \left[|f(Z_G^{\text{obs}})| \mathbb{1}\{\psi(\tilde{Z}_G) = \hat{t}_{Z_G}(Z_G^{\text{obs}})\} \right],
\end{aligned} \tag{G.9}$$

where the first three steps mirror the results in (G.5), and the last equality follows from the invariance property of the Haar probability measure U .

Combining (G.8) and (G.9), we have

$$|(\text{II})| \leq |\mathbb{E}_{G,Z} [D_f \mathcal{R}(\hat{t}_{Z_G})]| + \mathbb{E}_{G,Z} [|f(Z_G^{\text{obs}})| \mathbb{1}\{\psi(\tilde{Z}_G) = \hat{t}_{Z_G}(Z_G^{\text{obs}})\}] := \varepsilon_{\text{penalty}} + \varepsilon_{\text{int}}. \quad (\text{G.10})$$

Finally, taking the absolute value of both sides of (G.6), applying the triangle inequality, and combining (G.7) and (G.10) together, we complete the proof. \square

G.4 Proof of Theorem 3.3

We define $Z_i := \rho(g_i)Z$, $\tilde{Z}_i := \tilde{\rho}(g_i)\tilde{Z}$, and $Z_i^{\text{obs}} := \text{obs}(Z_i)$ for $i = 1, \dots, |\mathcal{G}|/|\mathcal{H}|$. The same reasoning as in (G.4) combined with the fact that $\mathcal{R} \equiv 0$ yields

$$\mathbb{E}_Z \left[f(Z_{\text{obs}}) \left(\mathbb{1}\{Z \in T_L^{\text{C-SymmPI}}(Z_{\text{obs}})\} - (1 - \alpha) \right) \right] = \mathbb{E}_Z \left[\frac{|\mathcal{H}|}{|\mathcal{G}|} \sum_{i \in A} (\alpha - s_i^*) f(Z_i^{\text{obs}}) \right]. \quad (\text{G.11})$$

where $s_i^* \in [\alpha - 1, \alpha]$ for $1 \leq i \leq |\mathcal{G}|/|\mathcal{H}|$, and $A := \{1 \leq i \leq |\mathcal{G}|/|\mathcal{H}| : \psi(\tilde{Z}_i) = \hat{t}_{Z_i}^L(Z_i^{\text{obs}})\}$.

We first claim that $|A| \leq d$ almost surely. Consider the matrix $\Phi_A = [\varphi(Z_i^{\text{obs}})]_{i \in A} \in \mathbb{R}^{|A| \times d}$ and the vector $\Psi_A = [\psi(\tilde{Z}_i)]_{i \in A}^\top \in \mathbb{R}^{|A|}$. By the definition of the index set A and the fact that $\hat{t}_{Z_i}^L(Z_i^{\text{obs}}) = \langle \hat{\theta}, \varphi(Z_i^{\text{obs}}) \rangle$, the following linear system holds almost surely:

$$\Phi_A \hat{\theta} = \Psi_A. \quad (\text{G.12})$$

Suppose for contradiction that $|A| > d$ with positive probability δ . Conditional on $|A| > d$, the dimension of the range of $\Phi_A \in \mathbb{R}^{|A| \times d}$ satisfies $\dim(\text{range}(\Phi_A)) = \text{rank}(\Phi_A) \leq d < |A|$. Consequently, $\text{range}(\Phi_A)$ forms a subset of $\mathbb{R}^{|A|}$ with Lebesgue measure zero. Since the random vector Ψ has a joint density, the subset Ψ_A also has a joint density p_{Ψ_A} in $\mathbb{R}^{|A|}$. Noting that the integral over a zero-measure set is zero, we have

$$\mathbb{P}_Z (\Psi_A \in \text{range}(\Phi_A) \mid |A| > d) = \int_{\text{range}(\Phi_A)} p_{\Psi_A}(z) dz = 0.$$

Then

$$\begin{aligned} \mathbb{P}_Z (\Psi_A \in \text{range}(\Phi_A)) &= \mathbb{P}_Z (\Psi_A \in \text{range}(\Phi_A) \mid |A| > d) \mathbb{P}_Z (|A| > d) \\ &\quad + \mathbb{P}_Z (\Psi_A \in \text{range}(\Phi_A) \mid |A| \leq d) \mathbb{P}_Z (|A| \leq d) \\ &\leq 0 \cdot \delta + 1 \cdot (1 - \delta) = 1 - \delta. \end{aligned}$$

Since $\Psi_A \in \text{range}(\Phi_A)$ is a necessary condition for the linear system (G.12) to hold, we have

$$\mathbb{P}_Z (\Phi_A \hat{\theta} = \Psi_A) \leq \mathbb{P}_Z (\Psi_A \in \text{range}(\Phi_A)) = 1 - \delta < 1,$$

which contradicts the assumption that Ψ_A satisfies (G.12) almost surely. Therefore, we conclude that $|A| \leq d$ almost surely.

Having established this claim, we proceed to bound $f(Z_i^{\text{obs}})$ in the right-hand side of (G.11):

$$|f(Z_i^{\text{obs}})| = |\langle \theta, \varphi(Z_i^{\text{obs}}) \rangle| \leq \|\theta\|_2 \|\varphi(Z_i^{\text{obs}})\|_2 \leq b_\theta b_\varphi,$$

where the first inequality follows from the Cauchy-Schwarz inequality, and the second inequality is a consequence of Assumption 3.2.

With these observations, we can bound the expectation on the right-hand side of (G.11) as follows:

$$\left| \mathbb{E}_Z \left[\frac{|\mathcal{H}|}{|\mathcal{G}|} \sum_{i \in A} (\alpha - s_i^*) f(Z_i^{\text{obs}}) \right] \right| \leq \frac{|\mathcal{H}|}{|\mathcal{G}|} \mathbb{E}_Z \left[\sum_{i \in A} |(\alpha - s_i^*) f(Z_i^{\text{obs}})| \right] \leq \frac{|\mathcal{H}|}{|\mathcal{G}|} \mathbb{E}_Z \left[|A| \cdot \max_{1 \leq i \leq |\mathcal{G}|/|\mathcal{H}|} |f(Z_i^{\text{obs}})| \right] \leq \frac{b_\theta b_\varphi d}{|\mathcal{G}|/|\mathcal{H}|},$$

where the first inequality uses the triangle inequality, the second inequality uses the fact that $\alpha - s_i^* \in [0, 1]$, and the final inequality uses the bounds $|f(Z_i^{\text{obs}})| \leq b_\theta b_\varphi$ and the claim that $|A| \leq d$ almost surely. This completes the proof. \square

G.5 Proof of Theorem D.1

We define $Z_i := \rho(g_i)Z$, $\tilde{Z}_i := \tilde{\rho}(g_i)\tilde{Z}$, and $Z_i^{\text{obs}} := \text{obs}(Z_i)$ for $i = 1, \dots, |\mathcal{G}|/|\mathcal{H}|$. The same reasoning as in (G.4) yields

$$\mathbb{E}_Z \left[f(Z_{\text{obs}}) \left(\mathbb{1}\{Z \in T_K^{\text{C-SymmPI}}(Z_{\text{obs}})\} - (1 - \alpha) \right) \right] = - \underbrace{\mathbb{E}_Z [D_f \mathcal{R}(\hat{t}_Z)]}_{\text{(I)}} + \underbrace{\mathbb{E}_Z \left[\frac{1}{|\mathcal{G}|/|\mathcal{H}|} \sum_{i \in A} (\alpha - s_i^*) f(Z_i^{\text{obs}}) \right]}_{\text{(II)}}. \quad (\text{G.13})$$

For term (I), we have

$$\begin{aligned} \text{(I)} &= \lambda \mathbb{E}_Z \left[\frac{d}{d\varepsilon} \|\hat{t}_Z + \varepsilon f\|_K^2 \Big|_{\varepsilon=0} \right] \\ &= \mathbb{E}_Z \left[\frac{d}{d\varepsilon} \left(\langle \hat{t}_Z, \hat{t}_Z \rangle_K + 2\varepsilon \langle \hat{t}_Z, f \rangle_K + \varepsilon^2 \langle f, f \rangle_K \right) \Big|_{\varepsilon=0} \right] \\ &= 2\lambda \mathbb{E}_Z [\langle \hat{t}_Z, f \rangle_K] \leq 2\lambda \mathbb{E}_Z [\|\hat{t}_Z\|_K \|f\|_K] \leq 2\lambda M^2, \end{aligned} \quad (\text{G.14})$$

where the first inequality follows from the Cauchy-Schwarz inequality and the second inequality follows from the definition of $B_M(\mathcal{F}_K)$.

For term (II), we have

$$|\text{(II)}| \leq \mathbb{E}_Z [|f(Z_{\text{obs}})| \mathbb{1}\{\psi(V(Z)) = \hat{t}_Z(Z_{\text{obs}})\}] \leq \|f\|_\infty \mathbb{P}_Z (\psi(V(Z)) = \hat{t}_Z(Z_{\text{obs}})), \quad (\text{G.15})$$

where the first inequality follows from the same calculation as (G.5).

We first upper bound the probability term in (G.15). Define the leave-one-out estimator

$$\hat{t}_z^{-e}(\cdot) = \underset{t(\cdot) \in B_M(\mathcal{F}_K)}{\text{argmin}} \frac{1}{|\mathcal{G}|/|\mathcal{H}| - 1} \sum_{g \neq e} \ell_\alpha \left(t(\text{obs}(\rho(g)z)), \psi(\tilde{\rho}(g)V(z)) \right) + \lambda \|t\|_K^2.$$

Since the pinball loss ℓ_α is 1-Lipchitz in the first entry, [Bousquet and Elisseeff \(2002, Theorem 22, the fourth equation in the proof\)](#) implies that

$$\|\hat{t}_z - \hat{t}_z^{-e}\|_K \leq \frac{\kappa}{2\lambda|\mathcal{G}|/|\mathcal{H}|}. \quad (\text{G.16})$$

Then we apply the reproducing property of the RKHS to obtain

$$\|\hat{t}_z - \hat{t}_z^{-e}\|_\infty = \sup_{o \in \mathcal{O}} |(\hat{t}_z - \hat{t}_z^{-e})(o)| = \sup_{o \in \mathcal{O}} |\langle \hat{t}_z - \hat{t}_z^{-e}, K(\cdot, o) \rangle_K|. \quad (\text{G.17})$$

By the Cauchy-Schwarz inequality, we have

$$|\langle \hat{t}_z - \hat{t}_z^{-e}, K(\cdot, o) \rangle_K| \leq \|\hat{t}_z - \hat{t}_z^{-e}\|_K \cdot \|K(\cdot, o)\|_K. \quad (\text{G.18})$$

Applying the reproducing property again, the RKHS norm of the kernel feature map $\|K(\cdot, o)\|_K$ satisfies, for any $z \in \mathcal{Z}$,

$$\|K(\cdot, o)\|_K = \sqrt{\langle K(\cdot, o), K(\cdot, o) \rangle_K} = \sqrt{K(o, o)} \leq \kappa, \quad (\text{G.19})$$

where the last inequality follows from Assumption D.1. Combining these results, we obtain

$$\|\hat{t}_z - \hat{t}_z^{-e}\|_\infty \leq \sup_{o \in \mathcal{O}} \|\hat{t}_z - \hat{t}_z^{-e}\|_K \cdot \|K(\cdot, o)\|_K \leq \frac{\kappa^2}{2\lambda|\mathcal{G}|/|\mathcal{H}|} := \delta, \quad (\text{G.20})$$

where the first inequality follows from (G.17) and (G.18), and the second inequality follows from (G.16) and (G.19). From (G.20), we have

$$\hat{t}_Z^{-e}(Z_{\text{obs}}) - \delta \leq \hat{t}_Z(Z_{\text{obs}}) \leq \hat{t}_Z^{-e}(Z_{\text{obs}}) + \delta$$

almost surely. Therefore, we can bound the probability term as follows:

$$\begin{aligned} \mathbb{P}_Z (\psi(V(Z)) = \widehat{t}_Z(Z_{\text{obs}})) &\leq \mathbb{P}_Z (\widehat{t}_Z^-(Z_{\text{obs}}) - \delta \leq \psi(V(Z)) \leq \widehat{t}_Z^-(Z_{\text{obs}}) + \delta) \\ &= \int_{\widehat{t}_Z^-(Z_{\text{obs}}) - \delta}^{\widehat{t}_Z^-(Z_{\text{obs}}) + \delta} p_\psi(z) dz \leq 2\delta b_\psi = \frac{b_\psi \kappa^2}{\lambda |\mathcal{G}|/|\mathcal{H}|}, \end{aligned} \quad (\text{G.21})$$

where the last inequality follows from the bounded density assumption that $p_\psi(z) \leq b_\psi$ for all $z \in \mathcal{Z}$, and the last equality follows from the definition of δ in (G.20).

We now upper bound $\|f\|_\infty$ in (G.15). Applying the reproducing property of the RKHS again, we have

$$\|f\|_\infty = \sup_{o \in \mathcal{O}} |f(o)| = \sup_{o \in \mathcal{O}} |\langle f, K(\cdot, o) \rangle_K| \leq \sup_{o \in \mathcal{O}} \|f\|_K \cdot \|K(\cdot, o)\|_K \leq \kappa \|f\|_K \leq \kappa M, \quad (\text{G.22})$$

where the first inequality follows from the Cauchy-Schwarz inequality, the second inequality follows from (G.19), and the last inequality follows from the definition of $B_M(\mathcal{F}_K)$.

Substituting (G.21) and (G.22) into (G.15), we obtain

$$|\text{(II)}| \leq 2\delta b_\psi \|f\|_\infty = \frac{b_\psi \kappa^3 M}{\lambda |\mathcal{G}|/|\mathcal{H}|}. \quad (\text{G.23})$$

Finally, from (G.13), (G.14), and (G.23), it follows that

$$\left| \mathbb{E}_Z \left[f(Z_{\text{obs}}) \left(\mathbb{1}\{Z \in T_K^{\text{C-SymmPI}}(Z_{\text{obs}})\} - (1 - \alpha) \right) \right] \right| \leq |\text{(I)}| + |\text{(II)}| \leq 2\lambda M^2 + \frac{b_\psi \kappa^3 M}{\lambda |\mathcal{G}|/|\mathcal{H}|}.$$

Choosing $\lambda = 1/\sqrt{|\mathcal{G}|/|\mathcal{H}|}$ completes the proof. \square

G.6 Proof of Theorem E.1

Following the same reasoning as in (G.4), we obtain

$$\begin{aligned} \Delta &= \mathbb{E}_Z \left[f(Z_{\text{obs}}) \left(\alpha - \mathbb{1}\{\psi(V(Z)) > \widehat{t}_Z(Z_{\text{obs}})\} \right) \right], \\ \Delta_{\text{samp}} &= \mathbb{E}_Z \left[f(Z_{\text{obs}}) \left(\alpha - \mathbb{1}\{\psi(V(Z)) > \widehat{t}_{\text{samp}}(Z_{\text{obs}})\} \right) \right]. \end{aligned} \quad (\text{G.24})$$

Note that $\widehat{t}_{\text{samp}}(\cdot)$ depends on the random samples G_1, \dots, G_N , and therefore Δ_{samp} is a random variable with regard to G_1, \dots, G_N . In contrast, (3.1) indicates that the $\widehat{t}_Z(\cdot)$ has no dependence on G , and therefore Δ is a fixed value in \mathbb{R} .

By the distributional invariance of Z , we have $G_i \cdot Z \stackrel{d}{=} Z$ for all $i = 1, \dots, N$. Then it follows that

$$\Delta_{\text{samp}} \stackrel{d}{=} \frac{1}{N} \sum_{i=1}^N \mathbb{E}_Z \left[f(\text{obs}(G_i \cdot Z)) \left(\alpha - \mathbb{1}\{\psi(V(G_i \cdot Z)) > \widehat{t}_{\text{samp}}(\text{obs}(G_i \cdot Z))\} \right) \right]. \quad (\text{G.25})$$

Define $\varphi : \mathcal{G} \rightarrow \mathbb{R}$ such that

$$\varphi(g) = \mathbb{E}_Z \left[f(\text{obs}(g \cdot Z)) \left(\alpha - \mathbb{1}\{\psi(V(g \cdot Z)) > \widehat{t}_{\text{samp}}(\text{obs}(g \cdot Z))\} \right) \right]. \quad (\text{G.26})$$

Then (G.25) can be rewritten as

$$\Delta_{\text{samp}} \stackrel{d}{=} \frac{1}{N} \sum_{i=1}^N \varphi(G_i).$$

Now, we introduce an independent random variable $G \sim U$ and estimate the difference between Δ and Δ_{samp} as follows:

$$\begin{aligned} |\Delta - \Delta_{\text{samp}}| &\stackrel{d}{=} \left| \frac{1}{N} \sum_{i=1}^N \varphi(G_i) - \Delta \right| \\ &\leq \underbrace{\left| \frac{1}{N} \sum_{i=1}^N \varphi(G_i) - \mathbb{E}_G [\varphi(G)] \right|}_{|\text{(I)}|} + \underbrace{|\mathbb{E}_G [\varphi(G)] - \Delta|}_{|\text{(II)}|}. \end{aligned} \quad (\text{G.27})$$

We first bound term (I). Since $f(\cdot)$ is nonnegative and upper-bounded, we have for all $g \in \mathcal{G}$,

$$\begin{aligned} |\varphi(g)| &\leq \mathbb{E}_Z [f(\text{obs}(g \cdot Z)) \cdot |\alpha - \mathbb{1}\{\psi(V(g \cdot Z)) > \hat{t}_{\text{samp}}(\text{obs}(g \cdot Z))\}|] \\ &\leq (1 + \alpha) \mathbb{E}_Z [f(\text{obs}(g \cdot Z))] \\ &\leq 2\|f\|_\infty < \infty. \end{aligned}$$

Therefore, $\varphi(G_i)$ is a bounded random variable with $|\varphi(G_i)| \leq 2\|f\|_\infty$, for all $i = 1, \dots, N$. By Hoeffding's inequality, with probability $1 - \delta$, we have

$$|\text{(I)}| = \left| \frac{1}{N} \sum_{i=1}^N \varphi(G_i) - \mathbb{E}_G [\varphi(G)] \right| \leq 2\|f\|_\infty \sqrt{\frac{2 \log(2/\delta)}{N}} = \|f\|_\infty \sqrt{\frac{8 \log(2/\delta)}{N}}. \quad (\text{G.28})$$

We now turn to term (II). By the definition of φ in (G.26), we have

$$\begin{aligned} \mathbb{E}_G [\varphi(G)] &= \mathbb{E}_{G,Z} [f(\text{obs}(G \cdot Z)) (\alpha - \mathbb{1}\{\psi(V(G \cdot Z)) > \hat{t}_{\text{samp}}(\text{obs}(G \cdot Z))\})] \\ &= \mathbb{E}_Z [f(Z_{\text{obs}}) (\alpha - \mathbb{1}\{\psi(V(Z)) > \hat{t}_{\text{samp}}(Z_{\text{obs}})\})], \end{aligned} \quad (\text{G.29})$$

where the last equality follows from the fact that $G \cdot Z \stackrel{d}{=} Z$. Here $\hat{t}_{\text{samp}}(\cdot)$ indicates that $\mathbb{E}_G [\varphi(G)]$ is a random variable with regard to G_1, \dots, G_N . Now we further compute the difference between $\mathbb{E}_G [\varphi(G)]$ and Δ as follows:

$$\begin{aligned} \text{(II)} &= \mathbb{E}_G [\varphi(G)] - \Delta \\ &= \mathbb{E}_Z [f(Z_{\text{obs}}) (\alpha - \mathbb{1}\{\psi(V(Z)) > \hat{t}_{\text{samp}}(Z_{\text{obs}})\})] - \mathbb{E}_Z [f(Z_{\text{obs}}) (\alpha - \mathbb{1}\{\psi(V(Z)) > \hat{t}_Z(Z_{\text{obs}})\})] \\ &= \mathbb{E}_Z [f(Z_{\text{obs}}) (\mathbb{1}\{\psi(V(Z)) > \hat{t}_Z(Z_{\text{obs}})\} - \mathbb{1}\{\psi(V(Z)) > \hat{t}_{\text{samp}}(Z_{\text{obs}})\})] \\ &= \mathbb{E}_Z [f(Z_{\text{obs}}) (\mathbb{1}\{\nu(Z) > 0\} - \mathbb{1}\{\nu_{\text{samp}}(Z) > 0\})], \end{aligned}$$

where the second equality follows from (G.24) and (G.29), and the last equality follows from the definition of $\nu(\cdot)$ and $\nu_{\text{samp}}(\cdot)$. Rewriting this as an integral and applying the tilted measure \mathbb{P}_f defined in (E.3), we obtain

$$\begin{aligned} \text{(II)} &= \int_{\mathcal{Z}} f(z_{\text{obs}}) (\mathbb{1}\{\nu(z) > 0\} - \mathbb{1}\{\nu_{\text{samp}}(z) > 0\}) d\mathbb{P}_Z(z) \\ &= \mathbb{E}_Z [f(Z_{\text{obs}})] \int_{\mathcal{Z}} (\mathbb{1}\{\nu(z) > 0\} - \mathbb{1}\{\nu_{\text{samp}}(z) > 0\}) \frac{f(z_{\text{obs}})}{\mathbb{E}_Z [f(Z_{\text{obs}})]} d\mathbb{P}_Z(z) \\ &= \mathbb{E}_Z [f(Z_{\text{obs}})] \int_{\mathcal{Z}} (\mathbb{1}\{\nu(z) > 0\} - \mathbb{1}\{\nu_{\text{samp}}(z) > 0\}) d\mathbb{P}_f(z) \\ &= \mathbb{E}_Z [f(Z_{\text{obs}})] \{\mathbb{P}_f(\nu(Z) > 0) - \mathbb{P}_f(\nu_{\text{samp}}(Z) > 0)\}. \end{aligned}$$

By the definition of total variation distance, we have

$$|\text{(II)}| \leq \mathbb{E}_Z [f(Z_{\text{obs}})] \text{TV}_f(\nu(Z), \nu_{\text{samp}}(Z)). \quad (\text{G.30})$$

Finally, combining (G.27), (G.28), and (G.30), we conclude that with probability at least $1 - \delta$,

$$|\Delta - \Delta_{\text{samp}}| \leq \|f\|_\infty \sqrt{\frac{8 \log(2/\delta)}{N}} + \mathbb{E}_Z [f(Z_{\text{obs}})] \text{TV}_f(\nu(Z), \nu_{\text{samp}}(Z)),$$

which completes the proof. \square

G.7 Proof of Corollary E.1

The proof is similar to that of Theorem 3.1. For each $1 \leq i \leq N$, denote $Z_i := \rho(G_i)Z$, $Z_i^{\text{obs}} := \text{obs}(Z_i)$, and $\tilde{Z}_i := \tilde{\rho}(G_i)\tilde{Z}$ for $\tilde{Z} := V(Z)$. Following the same reasoning as in (G.2), we have

$$\frac{1}{N} \sum_{i=1}^N f(Z_i^{\text{obs}}) \left(\alpha - \mathbb{1}\{\psi(\tilde{Z}_i) > \hat{t}_{\text{samp}}(Z_i^{\text{obs}})\} \right) = -D_f \mathcal{R}(\hat{t}_{\text{samp}}) + \frac{1}{N} \sum_{i \in A} (\alpha - s_i^*) f(Z_i^{\text{obs}}),$$

where $A := \{1 \leq i \leq N : \psi(\tilde{Z}_i) = \hat{t}_{\text{samp}}(Z_i^{\text{obs}})\}$ is the index set of interpolation points, and $s_i^* \in [\alpha - 1, \alpha]$ for $1 \leq i \leq N$.

By the distributional invariance of Z and the deterministic equivariance property of V , we have $Z_i \stackrel{d}{=} Z$ and $\tilde{Z}_i \stackrel{d}{=} \tilde{Z}$ for all $1 \leq i \leq N$. Therefore,

$$\begin{aligned}
& \mathbb{E}_{Z, G_{1:N}} [f(Z_{\text{obs}}) (\mathbb{1}\{Z \in T_s^{\text{C-SymmPI}}(Z_{\text{obs}})\} - (1 - \alpha))] \\
&= \mathbb{E}_{Z, G_{1:N}} [f(Z_{\text{obs}}) (\alpha - \mathbb{1}\{\psi(\tilde{Z}) > \hat{t}_{\text{samp}}(Z_{\text{obs}})\})] \\
&= \mathbb{E}_{Z, G_{1:N}} \left[\frac{1}{N} \sum_{i=1}^N f(Z_i^{\text{obs}}) (\alpha - \mathbb{1}\{\psi(\tilde{Z}_i) > \hat{t}_{\text{samp}}(Z_i^{\text{obs}})\}) \right] \\
&= -\mathbb{E}_{Z, G_{1:N}} [D_f \mathcal{R}(\hat{t}_{\text{samp}})] + \mathbb{E}_{Z, G_{1:N}} \left[\frac{1}{N} \sum_{i \in A} (\alpha - s_i^*) f(Z_i^{\text{obs}}) \right].
\end{aligned} \tag{G.31}$$

Moreover, by the same calculation as in (G.5), we have

$$\begin{aligned}
\left| \mathbb{E}_{Z, G_{1:N}} \left[\frac{1}{N} \sum_{i \in A} (\alpha - s_i^*) f(Z_i^{\text{obs}}) \right] \right| &\leq \mathbb{E}_{Z, G_{1:N}} \left[\frac{1}{N} \sum_{i \in A} |f(Z_i^{\text{obs}})| \right] \\
&= \mathbb{E}_{Z, G_{1:N}} \left[\frac{1}{N} \sum_{i=1}^N |f(Z_i^{\text{obs}})| \mathbb{1}\{\psi(\tilde{Z}_i) = \hat{t}_{\text{samp}}(Z_i^{\text{obs}})\} \right] \\
&= \mathbb{E}_{Z, G_{1:N}} [|f(Z_{\text{obs}})| \mathbb{1}\{\psi(\tilde{Z}) = \hat{t}_{\text{samp}}(Z_{\text{obs}})\}].
\end{aligned} \tag{G.32}$$

Combining (G.31) and (G.32) completes the proof. \square

G.8 Proof of Proposition F.1

Recall that the primal problem is

$$\text{minimize } \sum_{i=1}^n w_i \cdot \ell_\alpha(t(x_i), s_i) + \mathcal{R}(t),$$

where $\ell_\alpha(t(x_i), s_i) = (1 - \alpha) [s_i - t(x_i)]_+ + \alpha [t(x_i) - s_i]_+$. Define $p_i = [s_i - t(x_i)]_+$ and $q_i = [t(x_i) - s_i]_+$, which satisfy $p_i, q_i \geq 0$ and the equality $s_i - t(x_i) - p_i + q_i = 0$. Let $p = [p_i]_{1 \leq i \leq n}$ and $q = [q_i]_{1 \leq i \leq n}$. With these decision variables $p, q \in \mathbb{R}^n$ and $t \in \{\mathcal{X} \rightarrow \mathbb{R}\}$, the optimization problem can be reformulated as follows:

$$\begin{aligned}
& \text{minimize } \sum_{i=1}^n w_i \cdot ((1 - \alpha)p_i + \alpha q_i) + \mathcal{R}(t), \\
& \text{subject to } s_i - t(x_i) - p_i + q_i = 0, \quad i = 1, \dots, n, \\
& \quad p_i, q_i \geq 0, \quad i = 1, \dots, n.
\end{aligned} \tag{G.33}$$

The Lagrangian of this problem is given by

$$\begin{aligned}
L(p, q, t, \lambda, \mu, \nu) &= \sum_{i=1}^n w_i \cdot ((1 - \alpha)p_i + \alpha q_i) + \mathcal{R}(t) \\
&\quad + \sum_{i=1}^n w_i \cdot \lambda_i (s_i - t(x_i) - p_i + q_i) - \sum_{i=1}^n w_i \cdot \mu_i p_i - \sum_{i=1}^n w_i \cdot \nu_i q_i \\
&= \sum_{i=1}^n w_i \cdot ((1 - \alpha) - \lambda_i - \mu_i) p_i + \sum_{i=1}^n w_i \cdot (\alpha + \lambda_i - \nu_i) q_i
\end{aligned}$$

$$+ \sum_{i=1}^n w_i \cdot \lambda_i s_i + \mathcal{R}(t) - \sum_{i=1}^n w_i \cdot \lambda_i t(x_i).$$

where $\lambda_i \in \mathbb{R}$ and $\mu_i, \nu_i \geq 0$ for $i = 1, \dots, n$. Therefore, the dual function is given by

$$\begin{aligned} g(\lambda, \mu, \nu) &= \inf_{p, q, t} L(p, q, t, \lambda, \mu, \nu) \\ &= \underbrace{\inf_{p \in \mathbb{R}^n} \left\{ \sum_{i=1}^n w_i \cdot ((1 - \alpha) - \lambda_i - \mu_i) p_i \right\}}_{\text{(I)}} + \underbrace{\inf_{q \in \mathbb{R}^n} \left\{ \sum_{i=1}^n w_i \cdot (\alpha + \lambda_i - \nu_i) q_i \right\}}_{\text{(II)}} \\ &\quad + \sum_{i=1}^n w_i \cdot \lambda_i s_i + \underbrace{\inf_{t \in \{\mathcal{X} \rightarrow \mathbb{R}\}} \left\{ \mathcal{R}(t) - \sum_{i=1}^n w_i \cdot \lambda_i t(x_i) \right\}}_{\text{(III)}}. \end{aligned}$$

For term (I), it is easy to see that

$$\inf_{p \in \mathbb{R}^n} \left\{ \sum_{i=1}^n w_i \cdot ((1 - \alpha) - \lambda_i - \mu_i) p_i \right\} = \begin{cases} 0, & \text{if } (1 - \alpha) - \lambda_i - \mu_i = 0, \text{ for all } i = 1, \dots, n, \\ -\infty, & \text{otherwise.} \end{cases}$$

Since $\mu_i \geq 0$, the condition $(1 - \alpha) - \lambda_i - \mu_i = 0$ simplifies to $\lambda_i \leq 1 - \alpha$ for all $i = 1, \dots, n$. Similarly, for term (II), we have

$$\inf_{q \in \mathbb{R}^n} \left\{ \sum_{i=1}^n w_i \cdot (\alpha + \lambda_i - \nu_i) q_i \right\} = \begin{cases} 0, & \text{if } \lambda_i \geq -\alpha, \text{ for all } i = 1, \dots, n, \\ -\infty, & \text{otherwise.} \end{cases}$$

For term (III), notice that

$$\inf_{t \in \{\mathcal{X} \rightarrow \mathbb{R}\}} \left\{ \mathcal{R}(t) - \sum_{i=1}^n w_i \cdot \lambda_i t(x_i) \right\} = -\mathcal{R}^*(w \odot \lambda),$$

where $\mathcal{R}^*(\alpha) := \sup_t \{ \sum_{i=1}^n \alpha_i t(x_i) - \mathcal{R}(t) \}$ is the Fenchel conjugate of \mathcal{R} , and $w \odot \lambda := [w_i \lambda_i]_{1 \leq i \leq n}$ denotes the Hadamard product of vectors $w, \lambda \in \mathbb{R}^n$. Combining these results, the dual function simplifies to

$$g(\lambda, \mu, \nu) = \begin{cases} \sum_{i=1}^n w_i \cdot \lambda_i s_i - \mathcal{R}^*(w \odot \lambda), & \text{if } -\alpha \leq \lambda_i \leq 1 - \alpha, \text{ for all } i = 1, \dots, n, \\ -\infty, & \text{otherwise.} \end{cases}$$

Therefore, the dual problem is to maximize the dual function subject to the derived constraints. We can express the dual problem in the following compact vector form:

$$\begin{aligned} &\text{maximize} && (w \odot \lambda)^\top s - \mathcal{R}^*(w \odot \lambda) \\ &\text{subject to} && -\alpha \mathbf{1} \preceq \lambda \preceq (1 - \alpha) \mathbf{1}, \end{aligned}$$

where $s = [s_i]_{1 \leq i \leq n}$ is the vector of scores, and “ \preceq ” denotes element-wise inequality. This completes the proof. \square

G.9 Proof of Proposition F.2

For the reformulated primal problem (G.33), we denote an optimal primal solution as $(\hat{p}, \hat{q}, \hat{t}_z)$, where $\hat{p} = [\hat{p}_i]_{1 \leq i \leq n}$ and $\hat{q} = [\hat{q}_i]_{1 \leq i \leq n}$. Let $\hat{\lambda} = [\hat{\lambda}_i]_{1 \leq i \leq n}$, $\hat{\mu} = [\hat{\mu}_i]_{1 \leq i \leq n}$, and $\hat{\nu} = [\hat{\nu}_i]_{1 \leq i \leq n}$ be the corresponding optimal dual solutions.²⁷

Recall the definition $\hat{p}_n = [s_n - \hat{t}_z(x_n)]_+$ and $\hat{q}_n = [\hat{t}_z(x_n) - s_n]_+$. Therefore,

²⁷For notational simplicity, we keep the dependence of the optimal solutions on s_n implicit.

- (i) $\widehat{p}_n = 0$ and $\widehat{q}_n > 0$ if and only if $s_n < \widehat{t}_z(x_n)$;
- (ii) $\widehat{p}_n = 0$ and $\widehat{q}_n = 0$ if and only if $s_n = \widehat{t}_z(x_n)$;
- (iii) $\widehat{p}_n > 0$ and $\widehat{q}_n = 0$ if and only if $s_n > \widehat{t}_z(x_n)$.

By the complementary slackness conditions, we have $\widehat{\mu}_n \widehat{p}_n = ((1-\alpha) - \widehat{\lambda}_n) \widehat{p}_n = 0$ and $\widehat{\nu}_n \widehat{q}_n = (\alpha + \widehat{\lambda}_n) \widehat{q}_n = 0$. Therefore, we have the following three cases:

- (i) if $\widehat{p}_n = 0$ and $\widehat{q}_n > 0$, then $\widehat{\lambda}_n = -\alpha$;
- (ii) if $\widehat{p}_n = 0$ and $\widehat{q}_n = 0$, then $\widehat{\lambda}_n$ can take any value in the feasible region $[-\alpha, 1 - \alpha]$;
- (iii) if $\widehat{p}_n > 0$ and $\widehat{q}_n = 0$, then $\widehat{\lambda}_n = 1 - \alpha$.

Combining these three cases with the previous characterization of \widehat{p}_n and \widehat{q}_n yields

$$\widehat{\lambda}_n \in \begin{cases} -\alpha, & \text{if } s_n < \widehat{t}_z(x_n), \\ [-\alpha, 1 - \alpha], & \text{if } s_n = \widehat{t}_z(x_n), \\ 1 - \alpha, & \text{if } s_n > \widehat{t}_z(x_n). \end{cases}$$

This completes the proof. □

G.10 Proof of Proposition F.3

Recall that $s_1 \dots, s_{n-1}$ are fixed, while s_n is treated as a parameter. Consider the dual problem (F.2) in scalar form:

$$\begin{aligned} \text{maximize} \quad & F(\lambda; s_n) := \sum_{i=1}^n w_i \cdot \lambda_i s_i - \mathcal{R}^*(w \odot \lambda), \\ \text{subject to} \quad & -\alpha \leq \lambda_i \leq 1 - \alpha, \quad i = 1, \dots, n. \end{aligned}$$

In the objective function F , the decision variable is $\lambda = [\lambda_i]_{1 \leq i \leq n} \in \mathbb{R}^n$, and the parameter is $s_n \in \mathbb{R}$. Let $\widehat{\lambda}(s_n) = [\widehat{\lambda}_i(s_n)]_{1 \leq i \leq n}$ denote an optimal solution to this dual problem.

We prove the monotonicity of $\widehat{\lambda}_n(\cdot)$ by contradiction. Suppose that $\widehat{\lambda}_n(\cdot)$ is not monotonically increasing, i.e., there exists $s_n, s'_n \in \mathbb{R}$ such that

$$(s'_n - s_n) (\widehat{\lambda}_n(s'_n) - \widehat{\lambda}_n(s_n)) < 0,$$

or equivalently,

$$s'_n (\widehat{\lambda}_n(s'_n) - \widehat{\lambda}_n(s_n)) < s_n (\widehat{\lambda}_n(s'_n) - \widehat{\lambda}_n(s_n)). \quad (\text{G.34})$$

By the optimality of $\widehat{\lambda}(s'_n)$ for the parameter value s'_n , we have $F(\widehat{\lambda}(s'_n); s'_n) \geq F(\widehat{\lambda}(s_n); s'_n)$, or equivalently,

$$\sum_{i=1}^{n-1} w_i \cdot \widehat{\lambda}_i(s'_n) s_i + w_n \cdot \widehat{\lambda}_n(s'_n) s'_n - \mathcal{R}^*(w \odot \widehat{\lambda}(s'_n)) \geq \sum_{i=1}^{n-1} w_i \cdot \widehat{\lambda}_i(s_n) s_i + w_n \cdot \widehat{\lambda}_n(s_n) s'_n - \mathcal{R}^*(w \odot \widehat{\lambda}(s_n)).$$

Rearranging terms yields

$$w_n \cdot s'_n (\widehat{\lambda}_n(s'_n) - \widehat{\lambda}_n(s_n)) \geq \sum_{i=1}^{n-1} w_i \cdot s_i (\widehat{\lambda}_i(s_n) - \widehat{\lambda}_i(s'_n)) - \left(\mathcal{R}^*(w \odot \widehat{\lambda}(s_n)) - \mathcal{R}^*(w \odot \widehat{\lambda}(s'_n)) \right). \quad (\text{G.35})$$

Combining (G.34) and (G.35), we obtain

$$w_n \cdot s_n (\widehat{\lambda}_n(s'_n) - \widehat{\lambda}_n(s_n)) > w_n \cdot s'_n (\widehat{\lambda}_n(s'_n) - \widehat{\lambda}_n(s_n))$$

$$\geq \sum_{i=1}^{n-1} w_i \cdot s_i (\widehat{\lambda}_i(s_n) - \widehat{\lambda}_i(s'_n)) - \left(\mathcal{R}^*(w \odot \widehat{\lambda}(s_n)) - \mathcal{R}^*(w \odot \widehat{\lambda}(s'_n)) \right).$$

Rearranging further gives

$$\sum_{i=1}^n w_i \cdot \widehat{\lambda}_i(s'_n) s_i - \mathcal{R}^*(w \odot \widehat{\lambda}(s'_n)) > \sum_{i=1}^n w_i \cdot \widehat{\lambda}_i(s_n) s_i - \mathcal{R}^*(w \odot \widehat{\lambda}(s_n)).$$

This implies $F(\widehat{\lambda}(s'_n); s_n) > F(\widehat{\lambda}(s_n); s_n)$, which contradicts the optimality of $\widehat{\lambda}(s_n)$ for the parameter value s_n . Hence $\widehat{\lambda}_n(\cdot)$ must be monotonically increasing. \square